U.PORTO
FACULDADE DE CIÊNCIAS
UNIVERSIDADE DO PORTO

MSc

LRP1B-Knockout Human Cancer Cell Line Model with a CRISPR/Cas9 Approach

Catarina Príncipe Ferreira dos Santos

Dissertação de Mestrado apresentada à
Faculdade de Ciências da Universidade do Porto em
Biologia Celular e Molecular

2020

MSc
2.º CICLO
FCUP
2020

U.PORTO

Establishment of a LRP1B-Knockout Human Cancer Cell Line Model with a CRISPR/Cas9 Approach

Catarina Príncipe Ferreira dos Santos

FC

Establishment of a *LRP1B*-Knockout Human Cancer Cell Line Model with a CRISPR/Cas9 Approach

Catarina Príncipe Ferreira dos Santos
Mestrado em Biologia Celular e Molecular
Departamento de Biologia
2020

Supervisor
Raquel Maria Torres Lima, PhD
Junior Researcher at the Cancer Signaling and Metabolism Group of the Institute of Molecular Pathology and Immunology of the University of Porto / Institute of Research and Innovation in Health of the University of Porto (IPATIMUP/i3S)
Affiliated Professor at the Faculty of Medicine of the University of Porto (FMUP)

Co-supervisor
Ana Paula Soares Dias Ferreira, PhD
Leader of the Cancer Signaling and Metabolism Group of the Institute of Molecular Pathology and Immunology of the University of Porto / Institute of Research and Innovation in Health of the University of Porto (IPATIMUP/i3S)
Assistant Professor at the Faculty of Medicine of the University of Porto (FMUP)

Todas as correções determinadas pelo júri, e só essas, foram efetuadas.

O Presidente do Júri,

Porto, _____/_____/_____

This work was part of a research project financed by FEDER – Fundo Europeu de Desenvolvimento Regional – funds through the COMPETE 2020 – Operational Programme for Competitiveness and Internationalisation (POCI); project NORTE-01-0145-FEDER-000029 – Advancing Cancer Research: From Basic Knowledge to Application, supported by Norte Portugal Regional Operational Programme (NORTE 2020), under the PORTUGAL 2020 Partnership Agreement; and by Portuguese funds through FCT – Fundação para a Ciência e a Tecnologia / Ministério da Ciência, Tecnologia e Ensino Superior in the framework of the project – "Predicting Patients' Response to Liposomal Anticancer Drugs: Focusing on LRP1B Endocytic Activity" (PTDC/MEC-ONC/31520/2017).

Part of the data obtained during this master's dissertation research project was presented in the following scientific communication:

Príncipe, C., Pestana, A., Soares, P., Lima, R. T. **Generation of an *LRP1B*-Knockout Glioblastoma Cell Line Model via CRISPR/Cas9**. IJUP 2020 – 13th Meeting of Young Researchers of the University of Porto (Book of Abstracts). No. 16985, Feb 12-14, 2020, Porto, Portugal. ISBN: 978-989-746-253-5. Appendix, Page 83.

“Nothing in life is to be feared, it is only to be understood. Now is the time to understand more, so that we may fear less.”

Marie Curie (1867-1934)

Agradecimentos

Na realização desta dissertação, contei com o contributo de várias pessoas que, de uma forma ou de outra, permitiram que este pequeno, mas importante, projeto pessoal se concretizasse, às quais desejo expressar a minha profunda e sincera gratidão:

À minha orientadora, a Professora Doutora Raquel Lima, por me ter ajudado e orientado exemplarmente, por ter partilhado os seus conhecimentos e experiências e por ter acreditado em mim e confiado nas minhas competências. Por todas as palavras sábias e gentis.

À minha coorientadora, a Professora Doutora Paula Soares, por me ter acolhido e integrado no grupo de investigação que lidera, por me ter proporcionado todas as condições materiais para a realização deste projeto e por me ter acompanhado atentamente. Por todas as palavras de encorajamento e motivação.

A todos os membros do grupo de investigação *Cancer Signaling and Metabolism* pelo espírito de equipa, entreajuda, respeito e amizade. Um agradecimento especial à Doutora Ana Pestana por todo o apoio e disponibilidade prestada.

Às minhas colegas de trabalho e amigas, Ana Gonçalves e Carolina Dias, pelo companheirismo, apoio e carinho. Por todos os risos e choros. Por todas as conversas sérias, mas também por todas as conversas sem nexo.

Aos meus colegas de faculdade e amigos, Ana Gomes, Marta Ramos, Nádia Silva, Francisco Moreira e Luís Póvoas, por estarem sempre presentes (mesmo quando fisicamente ausentes) e por me terem proporcionado momentos maravilhosos que jamais serão esquecidos.

À minha mãe por todos os sacrifícios que fez por mim e por todos os obstáculos e dificuldades que superou corajosamente para me proporcionar uma vida melhor, por me ter encorajado a alcançar todos os meus objetivos e por ter festejado orgulhosamente todas as minhas conquistas. Por ser um exemplo de resiliência e superação.

À minha irmã, melhor amiga, confidente e companheira de vida, por todo o incansável apoio e amor incondicional, por toda a generosidade, compreensão e dedicação, por todas as conversas, risos e lágrimas partilhadas. Por me inspirar todos os dias a ser a melhor versão de mim mesma.

À minha avó por me ter acolhido de braços abertos na sua casa, por me ter acompanhado de perto ao longo destes últimos cinco anos, por me ter emocionado com as suas palavras meigas, os olhares ternurentos e os abraços reconfortantes. Por ser um exemplo de força e coragem.

Ao meu namorado de longa data, e atual noivo, por ser o meu porto de abrigo e companheiro de todas as horas. Por acreditar mais em mim que eu. Por apoiar os meus sonhos e torná-los nossos. Por ter caminhado ao meu lado, por ter dividido os fardos comigo e por nunca ter desistido de mim. Por toda a paciência, compreensão e ajuda. Por todas as palavras ditas em silêncio e por todos os olhares. A ti te dedico este trabalho.

Aos pais e irmão do meu namorado, por terem feito da vossa família a minha família e por me terem presenteado amor, carinho, dedicação, lealdade e respeito. Em particular, à Ana Maria, pela generosidade desigual, pelas palavras amigas, pelos conselhos preciosos, pelos gestos carinhosos e maternais, pelos sorrisos e gargalhadas que só ela me consegue arrancar. Ao José pelo companheirismo, pelas histórias partilhadas, pelos momentos hilariantes, pelos gestos bondosos e pelos olhares, que sem nada dizerem, dizem tudo. Ao Francisco pela amizade, pela simplicidade, pela bondade, pela gentileza, pela delicadeza e pelos abraços de grupo maravilhosos e aconchegantes.

Por fim, agradeço, com todo o respeito e admiração, a alguns professores, absolutamente inspiradores, que marcaram a minha vida, em termos académicos e pessoais: à Professora Doutora Susana Pereira, à Professora Doutora Ana Séneca, à Professora Doutora Paula Tamagnini, à Professora Doutora Conceição Santos, ao Professor Doutor José Pissarra, ao Professor Doutor José Américo Sousa, ao Professor Doutor Fernando Tavares, ao Professor Doutor Luís Gustavo Pereira e ao Professor Doutor Paulo Talhadas.

Resumo

A proteína 1B relacionada com o recetor da lipoproteína de baixa densidade (LRP1B) é um membro gigante da família de proteínas do recetor da lipoproteína de baixa densidade (LDLR), uma grande classe de recetores de superfície celular com uma ampla gama de funções, que vão desde o papel clássico na endocitose mediada por recetores a papéis na transdução de sinais. O gene invulgarmente grande *LRP1B* (aproximadamente 1,90 Mbp) foi identificado pela primeira vez como estando frequentemente inativado em linhas celulares de cancro de pulmão de não pequenas células. Desde então, a sua inativação através de mecanismos genéticos e epigenéticos foi descrita em vários tipos de cancro. A inativação frequente do *LRP1B* em cancros humanos sugere que este tem um papel essencial na supressão tumoral. A sua reexpressão através da transfeção de minirecetores LRP1B em várias linhas celulares cancerígenas deficientes nesta proteína reduziu a proliferação celular, a migração, a invasão, o crescimento dependente e independente de ancoragem e o crescimento tumoral *in vivo*. Por outro lado, o silenciamento do *LRP1B*, por meio de interferência por RNA (RNAi), em várias linhas celulares cancerígenas que expressam *LRP1B*, aumentou a proliferação celular, a migração, a invasão e o crescimento dependente e independente de ancoragem. A LRP1B pode atuar como um supressor tumoral por meio da modulação do secretoma celular, da expressão génica ou de vias de sinalização. Além disso, a sua atividade endocítica pode influenciar a internalização de fármacos lipossomais e assim resposta à terapia. A perda do *LRP1B* em cancro de ovário (seroso de alto grau) foi associada à resistência à doxorrubicina lipossomal. Embora muito úteis, estas abordagens podem subestimar o potencial total das funções da LRP1B. O minirecetor LRP1B pode não mimetizar todas as funções biológicas que o recetor de comprimento total e a supressão da função da LRP1B através de RNAi pode ser incompleta. Estas limitações podem ser superadas pela criação de um modelo *knockout* para o *LRP1B*. A ferramenta de edição de genoma CRISPR/Cas9 tem sido amplamente utilizada para a criação de modelos *knockout* de gene *in vitro* e *in vivo*. Neste sentido, o objetivo deste estudo foi estabelecer, um modelo *knockout* para o *LRP1B*, numa linha celular cancerígena humana, usando CRISPR/Cas9. Para este efeito, os exões mais a montante compartilhados pela maioria dos transcritos codificadores de proteína previstos do *LRP1B* humano foram identificados como alvos para deleções disruptivas mediadas por CRISPR/Cas9. Tendo como alvo estes exões, quatro sgRNAs foram desenhados e clonados com sucesso no plasmídeo pSpCas9(BB)-2A-Puro (PX459) V2.0. Os vetores de expressão sgRNA/Cas9, verificados por sequenciação de Sanger, foram co-transfetados eficazmente em células

de glioblastoma U87 usando um reagente de transfeção à base de lípidos catiónicos. Após a seleção com puromicina, os clones derivados de uma única célula foram isolados usando diluição limitante. Deleções mediadas por CRISPR/Cas9 foram alcançadas com sucesso e potenciais clones *knockout* foram avaliados posteriormente ao nível da expressão de mRNA. Um clone foi validado como um verdadeiro knockout. O modelo *knockout* desenvolvido para o *LRP1B* pode ser extremamente útil, em estudos futuros, para decifrar os mecanismos exatos através dos quais o *LRP1B* funciona como um supressor tumoral e para obter mais informações sobre o valor do *LRP1B* como um novo biomarcador preditivo de resposta a fármacos anticancerígenos lipossomais.

Palavras-Chave: Cancro, CRISPR/Cas9, Deleção disruptiva, Gene supressor de tumor, Modelo *knockout*

Abstract

The low-density lipoprotein (LDL) receptor (LDLR)-related protein 1B (LRP1B) is a giant member of the LDLR protein family, an evolutionarily ancient large class of cell-surface receptors with a diverse range of functions, ranging from the classical role in receptor-mediated endocytosis to roles in signal transduction. The unusually large *LRP1B* gene (approximately 1.90 Mbp) was first identified as frequently inactivated in non-small-cell lung cancer cell lines. Thenceforward, *LRP1B* inactivation via genetic and epigenetic mechanisms has been reported in multiple cancer types. The frequent inactivation of *LRP1B* in human cancers suggests that it must have an essential role in tumor suppression. The re-establishment of *LRP1B* expression through transfection of LRP1B minireceptors into several LRP1B-deficient cancer cell lines reduced cell proliferation, migration, invasion, anchorage-dependent, and independent growth, and *in vivo* tumor growth. On the other hand, the downregulation of *LRP1B* expression through RNA interference (RNAi)-based approaches in several *LRP1B*-expressing cancer cell lines increased cell proliferation, migration, invasion, and anchorage-dependent and independent growth. LRP1B may act as a tumor suppressor through the modulation of cell secretome, gene expression, or signaling pathways. Also, LRP1B endocytic activity may influence the uptake of liposomal drugs and therapy response. *LRP1B* loss in high-grade serous ovarian cancer has been associated with resistance to liposomal doxorubicin. Although extremely useful, these approaches may underestimate the full potential of LRP1B functions. The LRP1B minireceptor may not share all biological functions with the full-length receptor, and RNAi-based suppression of *LRP1B* function (knockdown) may be incomplete. These limitations may be overcome by the generation of an *LRP1B* gene knockout model. The CRISPR/Cas9 genome-editing tool has been extensively used for the generation of *in vitro* and *in vivo* gene knockout models. In light of the foregoing, the objective of this study was to establish an *LRP1B*-knockout human cancer cell line model using CRISPR/Cas9. To achieve this, the most upstream exons shared by the majority of the predicted protein-coding transcripts of the human *LRP1B* were identified as targets for specific CRISPR/Cas9-mediated disrupting deletions. For exon targeting, four single guide RNAs (sgRNAs) were designed and successfully cloned into the pSpCas9(BB)-2A-Puro (PX459) V2.0 plasmid. Sanger sequencing-verified sgRNA/Cas9 expression vectors were effectively co-transfected into U87 glioblastoma cells using a cationic lipid-based transfection reagent. Following puromycin selection, single cell-derived clones were isolated using limiting dilution. CRISPR/Cas9-mediated deletions were successfully achieved, and potential knockout clones were further

evaluated for their mRNA expression. One clone was successfully validated as a true knockout. The developed *LRP1B*-knockout model can be extremely useful for deciphering the exact mechanisms through which LRP1B functions as a tumor suppressor and gain further insights into the value of *LRP1B* as a putative novel predictive biomarker for response to liposomal anticancer drugs.

Keywords: Cancer, CRISPR/Cas9, LRP1B, Disrupting deletion, Knockout model, Tumor suppressor gene

Table of Contents

List of Tables

List of Figures

List of Abbreviations, Acronyms, and Units

A2MR	alpha-2-macroglobulin receptor
A-beta	amyloid beta-peptide
AIP	aryl hydrocarbon receptor-interacting protein
ApoER	apolipoprotein E receptor
APP	amyloid precursor protein
bGH pA	bovine growth hormone polyadenylation signal
bp	base pair(s)
BSA	bovine serum albumin
cas	CRISPR-associated genes
Cas	CRISPR-associated proteins
cDNA	complementary DNA
CDS	coding sequence
CMV	cytomegalovirus
CRISPR	clustered regularly interspaced short palindromic repeats
crRNA	CRISPR RNA
C-terminus	carboxy terminus
CTF-alpha	carboxyl-terminal alpha fragment
CTF-beta	carboxyl-terminal beta fragment
CUB	complement C1r/C1s, Uegf, Bmp1
DMEM	Dulbecco’s modified eagle medium
DNA	deoxyribonucleic acid
DNase	deoxyribonuclease
dNTP	deoxynucleotide triphosphate
DSB(s)	double-stranded break(s)

ECM	extracellular matrix
EDTA	ethylenediaminetetraacetic acid
EGF	epidermal growth factor
EJC	exon junction complex
f1 ori	f1 bacteriophage origin of replication
FBS	fetal bovine serum
FN3	fibronectin type-III
g	gram(s)
g	g-force
G2SNT	gamma-2-syntrophin
gDNA	genomic DNA
gp330	glycoprotein 330
GRB7	growth factor receptor-bound protein 7
h	hour(s)
HBV	hepatitis B virus
HDL	high-density lipoprotein
HDR	homology-directed repair
HPV	human papillomavirus
HRG	histidine-rich glycoprotein
HRP	horseradish peroxidase
IgG	immunoglobulin G
IGHA1	immunoglobulin heavy constant alpha 1
IGKV 1-5	immunoglobulin kappa variable 1-5
Indel	insertion/deletion
JIP	C-Jun N-terminal kinase (JNK)-interacting protein
kbp	kilobase pair(s)

kDa	kilodalton(s)
L	liter(s)
LB	Luria-Bertani
LDL	low-density lipoprotein
LDLR	low-density lipoprotein receptor
LDS	lithium dodecyl sulfate
lncRNA	long non-coding RNA
LR11	LDLR relative with eleven ligand-binding repeats
LRP	low-density lipoprotein receptor-related protein
LRP-DIT	low-density lipoprotein receptor-related protein-deleted in tumors
MANEC	motif at the N-terminus with eight cysteines
Mbp	megabase pair(s)
MEGF7	multiple epidermal growth factor-like domains protein 7
mg	milligrams(s)
min	minute(s)
miRNA	microRNA
mL	milliliter(s)
mLRP1B4	LRP1B minireceptor
mLRP4	LRP1 minireceptor
mM	millimolar
MMP	matrix metalloproteinase
mRNA	messenger RNA
NA	non-applicable
ng	nanogram(s)
NHEJ	nonhomologous end-joining
nm	nanometer(s)

NMD	nonsense-mediated mRNA decay
NP-40	nonidet P-40
nt	nucleotide(s)
N-terminus	amino terminus
ON	overnight
ORF(s)	open reading frame(s)
Ori	origin of replication
PAI-1	plasminogen activator inhibitor 1
PAM	protospacer adjacent motif
PBS	phosphate-buffered saline
PCR	polymerase chain reaction
PFS	protospacer flanking sequence
pH	potential of hydrogen
PICK1	protein interacting with C kinase 1
PKC-alpha	protein kinase C alpha
PKD	polycystic kidney disease
pre-crRNA	precursor crRNA
pre-mRNA	precursor mRNA
PSD-95	postsynaptic density protein 95
PTC(s)	premature termination codon(s)
PVDF	polyvinylidene difluoride
qPCR	quantitative PCR
RanBP9	ran-binding protein 9
RAP	receptor-associated protein
RIP	regulated intramembrane proteolysis
RIPA	radioimmunoprecipitation assay

RNA	ribonucleic acid
RNAP	RNA polymerase
RNase	ribonuclease
RNP	ribonucleoprotein
rpm	revolutions per minute
RT	room temperature
RT-qPCR	reverse transcription quantitative real-time PCR
s	second(s)
SAP	serum amyloid P component
sAPP-alpha	soluble alpha-cleaved APP fragment
sAPP-beta	soluble beta-cleaved APP fragment
SDS	sodium dodecyl sulfate
sgRNA(s)	single guide RNA(s)
shRNA(s)	short hairpin RNA(s)
siRNA(s)	small interfering RNA(s)
sncRNA	small non-coding RNA
snRNA	small nuclear RNA
SNV	single-nucleotide variant
SorLA	sorting protein-related receptor containing LDLR class A
ssDNA	single-stranded DNA
ST7	suppressor of tumorigenicity seven protein
STR	short tandem repeat
SYT1	synaptotagmin-1
TALENs	transcription-activator-like effector nucleases
TBP	TATA-box-binding protein
TBS	tris-buffered saline

TIS	translation initiation site
tPA	tissue-type plasminogen activator
tracrRNA	trans-activating crRNA
U	unit(s)
uPA	urokinase-type plasminogen activator
uPAR	urokinase-type plasminogen activator receptor
UTR	untranslated region
UV	ultra-violet
V	volt(s)
VLDL	very low-density lipoprotein
VLDLR	very low-density lipoprotein receptor
VPS10P	vacuolar protein sorting 10 protein
ZFNs	zinc-finger nucleases
µg	microgram(s)
µL	microliter(s)
µm	micrometer(s)
µM	micromolar

1 Introduction

1.1 Low-Density Lipoprotein (LDL) Receptor (LDLR)-Related Protein (LRP) 1B (LRP1B)

1.1.1 LRP1B As a Member of the LDLR Protein Family

The low-density lipoprotein receptor-related protein 1B, originally named LRP-deleted in tumors (LRP-DIT) since its gene was found frequently inactivated in human non-small-cell lung cancer cell lines (Liu *et al.*, 2000a) but now referred to as LRP1B, is a gigantic member of the LDLR protein family that is broadly expressed in multiple normal human tissues [such as, brain, pituitary gland, salivary gland, thyroid gland, adrenal gland, skeletal muscle, smooth muscle, soft tissue, adipose tissue, breast, ovary, testis, prostate, lung, kidney, and liver; Liu *et al.* (2001), Tanaga *et al.* (2004), Li *et al.* (2005), Uhlén *et al.* (2015)]. This evolutionarily ancient protein family represents a large class of cell-surface receptors that fulfill a diverse range of functions from cargo transportation to cellular signaling [extensively reviewed in Strickland *et al.* (2002), May *et al.* (2007), Dieckmann *et al.* (2010)]. The human LDLR family is comprised of seven core members and seven distant-related members.

The core members of the LDLR family include LDLR itself (Yamamoto *et al.*, 1984), LRP1 [alternatively named as alpha-2-macroglobulin receptor (A2MR) or apolipo-protein E receptor (ApoER); Herz *et al.* (1988)], very-LDLR (VLDLR; Takahashi *et al.* (1992)], LRP2 [alternatively named as glycoprotein 330 (gp330) or megalin; Saito *et al.* (1994)], LRP8 [alternatively named as apolipoprotein E receptor 2 (ApoER2); Kim *et al.* (1996), Novak *et al.* (1996)], LRP4 [alternatively named as multiple epidermal growth factor-like domains protein 7 (MEGF7); Nakayama *et al.* (1998)] and LRP1B (Liu *et al.*, 2000a). These members share five structurally and functionally distinct domains: (i) LDLR class A domain, an approximately forty-amino acid sequence with six conserved cysteines and a highly conserved cluster of negatively-charged amino acids between the fourth and sixth cysteines (Südhof *et al.*, 1985, Bieri *et al.*, 1995, Daly *et al.*, 1995); (ii) epidermal growth factor (EGF)-like domain, a thirty to forty-amino acid sequence also with six conserved cysteines; (iii) YWTD β-propeller domain, with six contiguous repeats containing the conserved Tyr-Trp-Thr-Asp (YWTD) motif (Springer, 1998, Jeon *et al.*, 2001); (iv) transmembrane domain and (v) intracellular domain (endodomain) with one or more conserved Asn-Pro-x-Tyr (NPXY, where X designates any amino acid) motifs (Chen *et al.*, 1990, Li *et al.*, 2000). Their extracellular domains (ectodomains) are built

from a minimal central unit of an amino-terminus (N-terminus) cluster of LDLR class A domains (also known as the ligand-binding domain) followed by a carboxy-terminus (C-terminus) cluster of EGF-like and YWTD beta-propeller domains (Willnow *et al.*, 2007, Willnow *et al.*, 2012). The number of each extracellular domain and its clusters varies greatly among the core LDLR family members. Some of these receptors contain an additional extracellular O-glycosylated domain adjacent to the transmembrane domain (Willnow *et al.*, 1999). In comparison to the extracellular domains, the intracellular domains are less conserved between the receptors, except for the NPXY motif (Willnow *et al.*, 1999).

Besides the referred core members, the LDLR family also includes more distant related members, which are structurally and functionally highly diversified, such as LDLR relative with eleven ligand-binding repeats [LR11; alternatively named sorting protein-related receptor containing LDLR class A repeats (SorLA); Jacobsen *et al.* (1996), Yamazaki *et al.* (1996), Morwald *et al.* (1997)], LRP3 (Ishii *et al.*, 1998), LRP5 [alternatively named as LRP7; Dong *et al.* (1998), Hey *et al.* (1998), Kim *et al.* (1998)], LRP6 (Brown *et al.*, 1998), LRP10 [alternatively named as LRP9; Sugiyama *et al.* (2000)], LRP12 [alternatively named as suppressor of tumorigenicity seven protein (ST7); Qing *et al.* (1999), Battle *et al.* (2003)] and LRP11 (O'Leary *et al.*, 2016). The LRP5 and LRP6 still contain all three extracellular domains, but their arrangement is distinct to that of the core members: with the cluster of EGF-like and YWTD beta-propeller domains preceding the cluster of LDLR class A domains. Still, both LRP5 and LRP6 lack intracellular NPXY motifs (Brown *et al.*, 1998). In addition to the typical LDLR extracellular domains, LR11 (SorLA) has an additional vacuolar protein sorting ten protein (VPS10P) domain and a cluster of fibronectin type-III domains (Jacobsen *et al.*, 1996). Furthermore, LR11 contains one NPXY-related motif (FANSHY, Phe-Ala-Asn-Ser-His-Tyr) within its C-terminus endodomain (Fjorback *et al.*, 2012). The LRP3, LRP10, LRP11, and LRP12 only have the LDLR class A domain in common with the core members. The domain organization of the human LDLR family members is depicted in **Figure 1**.

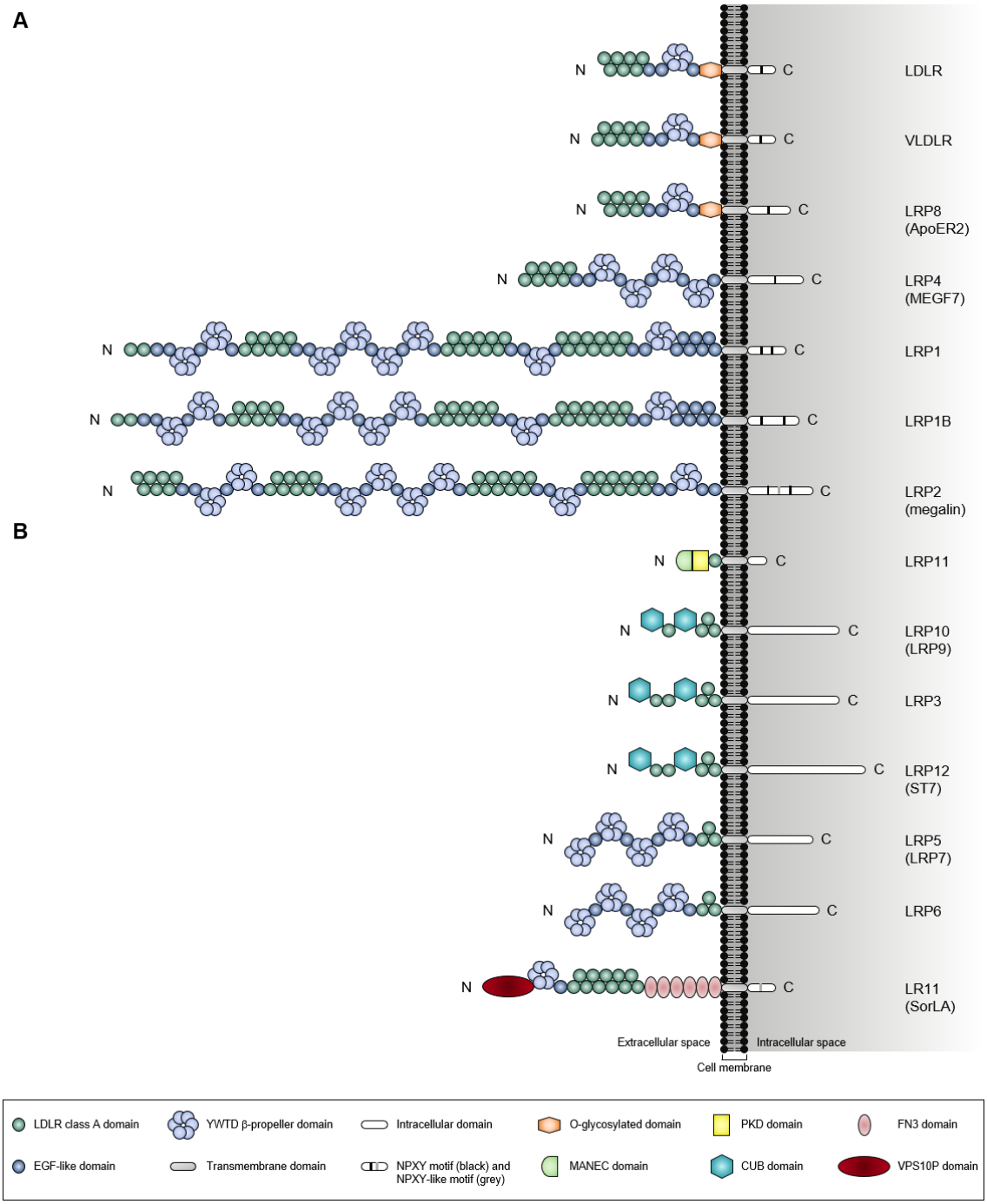

Figure 1. **The human LDLR family**. Schematic representation depicting the domain organization of core (**A**) and distant-related (**B**) members of the human LDLR family. All members are anchored to the cell membrane by a single membrane-spanning domain and contain an intracellular domain ranging from 50 to 346 amino acids. These are type I membrane proteins (i.e., extracellular N-terminus and intracellular C-terminus; the presence of an N-terminus signal peptide). The core members (**A**) contain an extracellular domain built from a minimal central unit of an N-terminus cluster of LDLR class A domains followed by a carboxy-terminus cluster of EGF-like and YWTD beta-propeller domains. LDLR, VLDLR, and LRP8 contain an additional extracellular O-glycosylated domain adjacent to the transmembrane domain. The core members also have an intracellular domain with at least one NPXY motif. The distant-related members (**B**) contain at least one of the extracellular domains of the core members. In addition, these also include other domains that are not present in the core members. Abbreviations: MANEC, motif at the N-terminus with eight cysteines; PKD, polycystic kidney disease; CUB, complement C1r/C1s, Uegf, Bmp1; FN3, fibronectin type-III; VPS10P, vacuolar protein sorting ten protein.

1.1.2 LRP1B Structure

LRP1B, along with LRP1 and LRP2, is one of the largest members of the LDLR family with a molecular weight of approximately 610 kilodaltons [kDa; Liu *et al.* (2001), Li *et al.* (2005)]. It shows a high degree of amino acid sequence similarity to LRP1 [59% amino acid sequence identity; Altschul *et al.* (1997)]. Interestingly, these two cell-surface receptors exhibit a nearly identical overall structure (Liu *et al.*, 2000a, Liu *et al.*, 2000b, Liu *et al.*, 2001, Marzolo & Bu, 2009). LRP1B has four putative extracellular ligand-binding domains (I, II, III, and IV from the N-terminus) that consist of two, eight, ten, and twelve LDLR class A domains, respectively. As in LRP1, these ligand-binding domains are interspaced by three clusters of EGF-like and YWTD beta-propeller domains. Moreover, both contain a furin cleavage site between the fourth ligand-binding domain and the transmembrane domain (Liu *et al.*, 2001). Like LRP1, the human LRP1B undergoes a furin-mediated proteolytic cleavage event (in the trans-Golgi network) to form the mature receptor as a noncovalently associated heterodimer composed of an N-terminus large subunit and a carboxy-terminal smaller subunit (Herz *et al.*, 1990, Liu *et al.*, 2001, Cam *et al.*, 2004, Li *et al.*, 2005). Still, both receptors have a cluster of six EGF-like domains adjacent to the transmembrane domain and an intracellular domain with two NPXY, one YXXØ (where X designates any amino acid and Ø an amino acid with a bulky hydrophobic group), and two dileucine (LL) motifs (Liu *et al.*, 2000a, Knisely *et al.*, 2007). Nevertheless, LRP1 and LRP1B have two structural differences: (i) an extra LDLR class A domain in the fourth ligand-binding domain (encoded by exon 68) of LRP1B and (ii) a unique 33 amino acid sequence (encoded by exon 90) between the two NPXY motifs in the intracellular domain of LRP1B (Liu *et al.*, 2001). The domain organization comparison between both receptors is depicted in **Figure 2**.

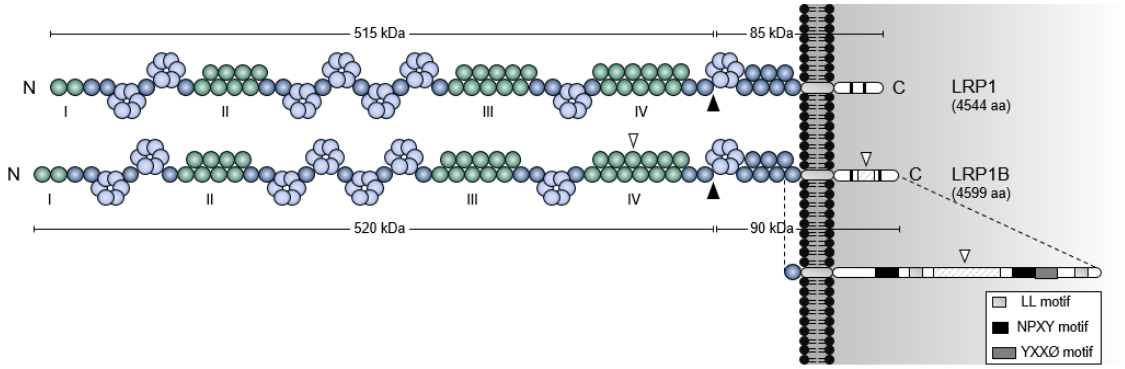

Figure 2. **Domain organization comparison between human LRP1 and LRP1B proteins**. The four extracellular ligand-binding domains (I to IV) are shown. The two structural differences between LRP1 and LRP1B are indicated with white arrowheads: (i) an extra LDLR class A domain in the fourth ligand-binding domain of LRP1B and (ii) a unique 33 amino acid sequence between the two NPXY motifs in the intracellular domain of LRP1B. The locations of the furin cleavage sites in the receptors are pointed out by black arrowheads. The intracellular domain of LRP1B is shown in more detail.

1.1.3 LRP1B Function

In-light-of the high degree of amino acid sequence similarity between LRP1 and LRP1B (and their nearly identical overall structure), it was early speculated that these two cell-surface receptors might exhibit overlapping ligand specificity and functions (Liu *et al.*, 2000a, Liu *et al.*, 2001). To identify potential extracellular ligands of LRP1B, two main approaches were used. The first approach, and the most commonly described in the literature, uses an LRP1B minireceptor (designated mLRP1B4; **Figure 3**) which comprises LRP1B fourth (IV) ligand-binding domain, transmembrane domain, and intracellular domain to assess its ability to bind and internalize ligands after its overexpression in cells (Liu *et al.*, 2001, Li *et al.*, 2002, Cam *et al.*, 2004, Pastrana *et al.*, 2005). The second approach uses soluble recombinant LRP1B ectodomains containing the first (I), the second (II), the third (III), or the fourth (IV) ligand-binding domains (designated LRP1B ectodomains I, II, III, and IV; **Figure 3**) to assess their ability to bind various ligands present in mouse brain tissue lysate (Marschang *et al.*, 2004) and human plasma (Haas *et al.*, 2011).

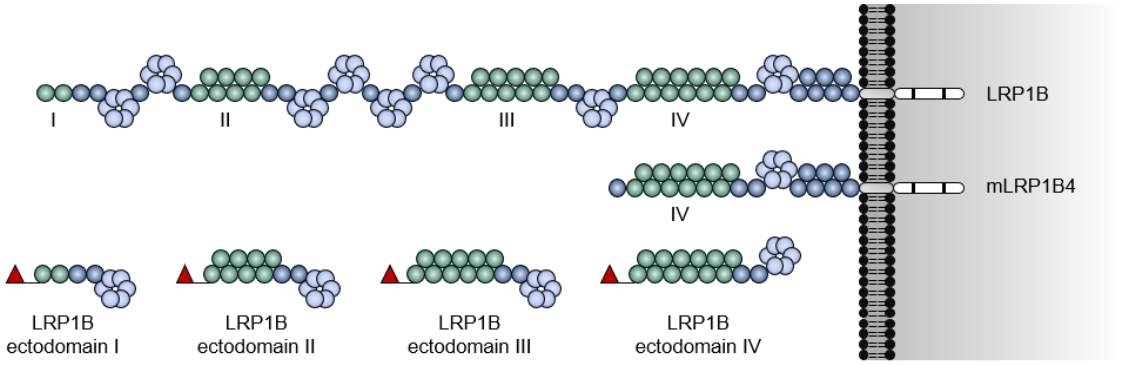

Figure 3. **Structure comparison between full-length LRP1B, LRP1B minireceptor (mLRP1B4), and N-terminal-tagged LRP1B ectodomains I, II, III, and IV**. The extracellular ligand-binding domains (I to IV) are identified. The red flag represents the N-terminal tag.

Together, these approaches have provided significant insights into the ligand specificity and recognition properties of LRP1B (**Table 1**). As expected, some of the extracellular ligands of LRP1B were already known to bind to the homologous LRP1, such as the receptor-associated protein (RAP), the components of the urokinase-type plasminogen activator (uPA) system [i.e., uPA, uPA receptor (uPAR), and plasminogen activator inhibitor-1 (PAI-1)], the tissue-type plasminogen activator (tPA), the amyloid precursor protein (APP), the *Pseudomonas aeruginosa* exotoxin A, and the apolipoprotein E-containing lipoproteins HDL and VLDL (Herz & Strickland, 2001). Additionally, several well-known chaperones and co-chaperones (sacsin, endoplasmin, DnaJ homolog subfamily A member 1, and clusterin), and other structurally and functionally diverse proteins

(synaptotagmin-1, glutathione S-transferase LANCL1, 40S ribosomal protein SA, fibrinogen, histidine-rich glycoprotein, vitronectin, serum amyloid P component, and two immunoglobulin components) were also identified as LRP1B ligands. These ligands are involved in a wide range of biological processes such as angiogenesis, blood coagulation, fibrinolysis, hemostasis, chemotaxis, cell proliferation, adhesion, spreading, migration, apoptosis, endocytosis, innate and adaptive immunity, host-virus interaction, and protein folding and trafficking (Bu, 1998, de Haas, 1999, Schvartz *et al.*, 1999, Mosesson, 2005, Xu *et al.*, 2009, Scheiman *et al.*, 2010, Schroeder & Cavacini, 2010, Poon *et al.*, 2011, Zheng & Koo, 2011, Marzec *et al.*, 2012, Aisina & Mukhametova, 2014, DiGiacomo & Meruelo, 2016, Matukumalli *et al.*, 2017). Almost all the identified LRP1B ligands were found to bind to either the second or the fourth ligand-binding domain (**Table 1**). Interestingly, these domains also appear to represent the major ligand-binding sites of LRP1 (Herz & Strickland, 2001). Also, some ligands, namely RAP, endoplasmin, 40S ribosomal protein SA, fibrinogen, and VLDL, were found to bind to more than one ligand-binding domain.

Using RAP, Liu *et al.* (2001) evaluated the internalization rates of both LRP1 and LRP1B minireceptors (designated by the authors as mLRP4 and mLRP1B4, respectively). mLRP1B4 showed a much slower rate of internalization ($t_{1/2}$ > 10 min) in comparison with mLRP4 ($t_{1/2}$ < 0.5 min). Another study showed that the rate and the extent of uPA/PAI-1 complexes internalization in mLRP1B4-expressing cells was much slower and incomplete than in mLRP4-expressing cells (Li *et al.*, 2002). This study also showed that mLRP1B4, like mLRP4, could bind uPA/PAI-1/uPAR complexes and internalize them (Li *et al.*, 2002). By then, it was known that after the internalization of the uPA/PAI-1/uPAR complexes mediated by LRP1, the uPA/PAI-1 complexes were trafficked to lysosomes for degradation, and the unoccupied (ligand-free and active) forms of LRP1 and uPAR were recycled back to the cell surface (Nykjaer *et al.*, 1992, Conese *et al.*, 1995, Nykjaer *et al.*, 1997, Czekay *et al.*, 2001). However, mLRP1B4-expressing cells, compared with mLRP4-expressing cells, showed a substantially reduced capacity to recycle unoccupied uPAR to the cell surface, which was consistent with the functional difference in the internalization rates of the LRP1 and LRP1B minireceptors (Li *et al.*, 2002), and to migrate. Li *et al.* (2002) showed that LRP1B could act as a negative regulator of uPAR regeneration and cell migration. Later, Cam *et al.* (2004) also showed that mLRP1B4-expressing cells, in contrast to mLRP4-expressing cells, exhibited a considerable accumulation of APP (another of the referred LRP1B extracellular ligands) at the cell surface, which was in accordance with a low internalization rate of APP mediated by mLRP1B4, and a concomitant decrease in amyloid beta-peptide (A-beta) production and

increase in soluble alpha-cleaved APP fragment (sAPP-alpha) secretion. Models depicting the differential functions of LRP1 and LRP1B in the endocytosis of uPAR and APP are shown in **Figure 4** and **Figure 5**, respectively. Overall, these studies suggest that LRP1B, when expressed in the same cells (or tissues) that LRP1, may antagonize LRP1 function by (i) competing for binding of common ligands and reducing their intracellular catabolism or (ii) modulating the function of other cell-surface receptors.

Table 1. Extracellular ligands and membrane-associated receptors of LRP1B.

Ligand	Description	Ligand-binding domain (I to IV)	Reference
Receptor-associated protein (RAP)	Chaperone	II, IV	Liu *et al.* (2001) Marschang *et al.* (2004)
Urokinase-type plasminogen activator (uPA)	Serine protease	IV	Liu *et al.* (2001)
Tissue-type plasminogen activator (tPA)	Serine protease	IV	Liu *et al.* (2001)
Plasminogen activator inhibitor-1 (PAI-1)	Serine protease inhibitor	IV	Liu *et al.* (2001)
Urokinase plasminogen activator surface receptor (uPAR)	Cell-surface receptor	IV	Li *et al.* (2002)
Amyloid precursor protein (APP)	Cell-surface receptor	IV	Cam *et al.* (2004)
Sacsin	Co-chaperone	IV	Marschang *et al.* (2004)
Endoplasmin (also known as GP96 homolog)	Chaperone	II, III	Marschang *et al.* (2004)
Synaptotagmin-1 (SYT1)	Calcium ion sensor	IV	Marschang *et al.* (2004)
DnaJ homolog subfamily A member 1	Co-chaperone	II	Marschang *et al.* (2004)
Glutathione S-transferase LANCL1 (also known as LanC-like protein 1)	Transferase	IV	Marschang *et al.* (2004)
40S ribosomal protein SA (also known as 37/67 kDa laminin receptor)	Host cell receptor for virus entry, cell-surface receptor for laminin, ribonucleoprotein	II, IV	Marschang *et al.* (2004)
Pseudomonas aeruginosa exotoxin A	*P. aeruginosa* toxin	IV	Pastrana *et al.* (2005)
Fibrinogen alpha-chain	Substrate for thrombin, plasmin, and fibrin stabilizing factor	II	Haas *et al.* (2011)
Fibrinogen beta-chain		IV	Haas *et al.* (2011)
Fibrinogen gamma-chain		IV	Haas *et al.* (2011)
Histidine-rich glycoprotein (HRG)	Plasma glycoprotein	II	Haas *et al.* (2011)
Clusterin	Chaperone	II	Haas *et al.* (2011)
Vitronectin	Glycoprotein found in blood and the extracellular matrix	II	Haas *et al.* (2011)
Serum amyloid P component (SAP)	Plasma protein	II	Haas *et al.* (2011)
Immunoglobulin kappa variable 1-5 (IGKV 1-5)	Variable domain of immunoglobulin light chains	II	Haas *et al.* (2011)
Immunoglobulin heavy constant alpha 1 (IGHA1)	Constant region of immunoglobulin heavy chains	II	Haas *et al.* (2011)
High-density lipoprotein (HDL)	Apolipoprotein E (apoE)-containing lipoprotein	II	Haas *et al.* (2011)
Very low-density lipoprotein (VLDL)	apoE-containing lipoprotein	II, IV	Haas *et al.* (2011)

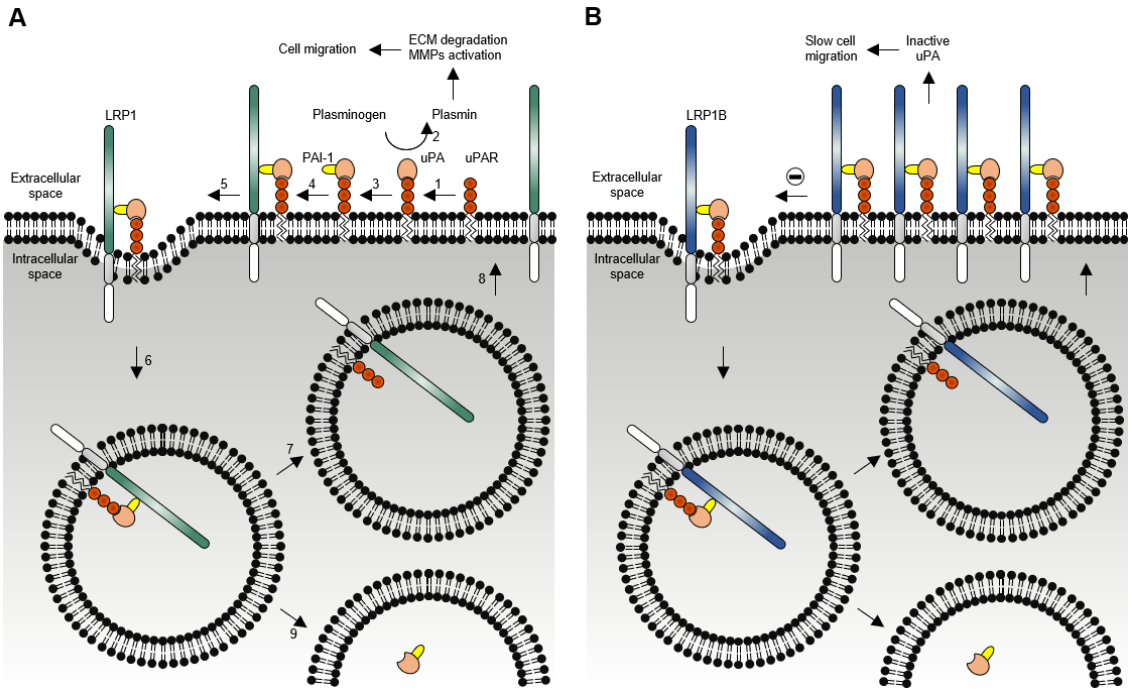

Figure 4. Model depicting the differential functions of LRP1 (A) and LRP1B (B) in endocytosis of uPAR. **A**, uPAR LRP1-mediated endocytosis: (1) uPA binds to uPAR; (2) active uPA catalyzes the conversion of plasminogen to plasmin, which cleaves and activates matrix metalloproteinases (MMPs); both plasmin and MMPs degrade many extracellular matrix (ECM) components; (3) PAI-1 binds to and inhibits uPA; (4) binding of PAI-1 promotes binding of LRP1; (5) fast distribution of the quaternary complexes (uPA/PAI-1/uPAR/LRP1) to clathrin-coated pits; (6) the quaternary complexes are internalized and delivered into early endosomes; (7) sorting of LRP1 and uPAR into recycling vesicles; (8) recycling of unoccupied forms of LRP1 and uPAR back to the cell surface; (9) uPA/PAI-1 complexes are trafficked through late endosomes to lysosomes for degradation. **B**, Like LRP1, LRP1B forms complexes with uPA/PAI-1/uPAR. However, slow endocytosis of LRP1B causes a slow elimination of occupied uPAR from the cell. As a result, occupied uPAR accumulates on the cell surface, functional uPAR is not regenerated effectively, uPA proteolytic activity is scarce, and cell migration is diminished.

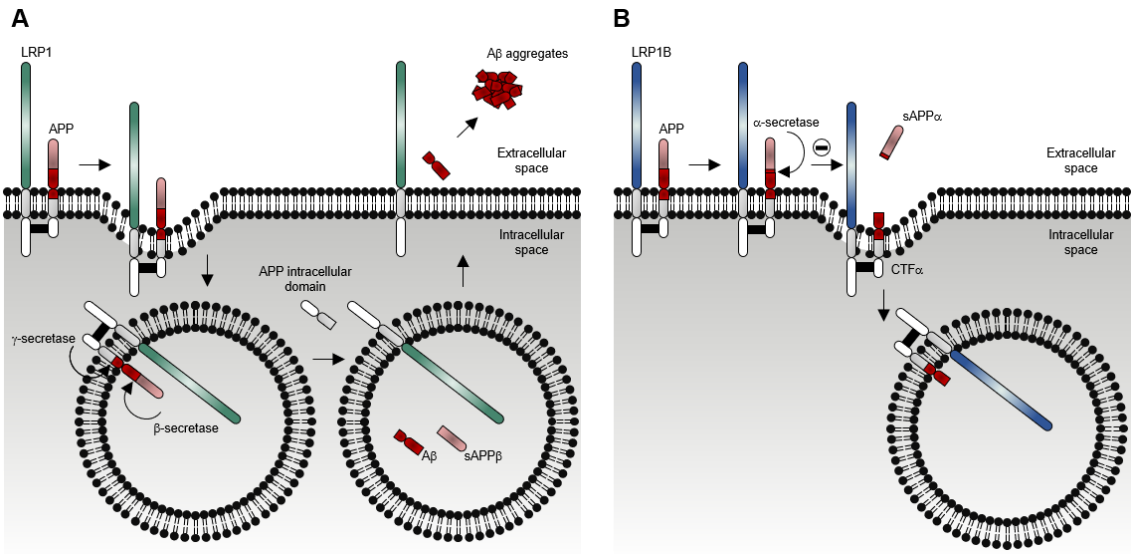

Figure 5. Model depicting the differential functions of LRP1 (A) and LRP1B (B) in endocytosis of APP. **A**, The fast endocytosis of LRP1 enhances APP endocytosis and, therefore, promotes the proteolytic processing of APP through the amyloidogenic pathway. Once delivered to the endosomes, APP is firstly cleaved by a beta-secretase, producing a soluble beta-cleaved APP fragment (sAPP-beta) and a carboxyl-terminal beta fragment (CTF-beta). This fragment is further cleaved by a gamma-secretase, producing the highly toxic amyloid beta-peptide (A-beta) and the APP intracellular domain. Most of the A-beta peptides are secreted to the extracellular space, where they can rapidly aggregate and form fibrils that deposit into the amyloid plaques (which are associated with the progression of Alzheimer's disease). **B**, The slow endocytosis of LRP1B decreases APP endocytosis and, therefore, promotes the proteolytic processing of APP through the non-amyloidogenic pathway. At the cell surface, APP is firstly cleaved by an alpha-secretase, producing a soluble alpha-cleaved APP fragment (sAPP-alpha) and a carboxyl-terminal alpha fragment (CTF-alpha). This fragment can be further cleaved by a gamma-secretase, producing the non-toxic peptide P3 and the APP intracellular domain.

Besides the classical role of LDLR family members in receptor-mediated endocytosis, over the last two decades, compelling evidence has shown that several LDLR family members play essential roles in signal transduction through the interaction of their intracellular domains with cytosolic adaptor and scaffold proteins (Gotthardt *et al.*, 2000, Herz, 2001, Herz & Bock, 2002, May *et al.*, 2003, Schneider & Nimpf, 2003, Herz *et al.*, 2009, Schneider, 2016). To date, eight interacting partners of the LRP1B intracellular domain have been identified [**Table 2**; Marschang *et al.* (2004), Shiroshima *et al.* (2009)]. These intracellular partners are involved in several biological processes such as signal transduction, synaptic transmission and plasticity, cell migration, tumorigenesis and tumor progression, and DNA damage response (Yasuda *et al.*, 1999, Han *et al.*, 2002, Terashima *et al.*, 2008, Chu *et al.*, 2010, Volk *et al.*, 2010, Palmieri *et al.*, 2016, Bhat *et al.*, 2019, Coley & Gao, 2019).

Table 2. Interacting partners of the intracellular domain of LRP1B.

Intracellular interacting partner	Description	Reference
Postsynaptic density protein 95 (PSD-95)	Scaffold protein	Marschang *et al.* (2004)
Aryl hydrocarbon receptor-interacting protein (AIP)	Co-chaperone	Marschang *et al.* (2004)
C-Jun N-terminal kinase (JNK)-interacting protein 1b (JIP-1b)	Scaffold protein	Shiroshima *et al.* (2009)
C-Jun N-terminal kinase (JNK)-interacting protein 2 (JIP-2)	Scaffold protein	Shiroshima *et al.* (2009)
Protein interacting with C kinase 1 (PICK1)	Scaffold protein	Shiroshima *et al.* (2009)
Ran-binding protein 9 (RanBP9)	Scaffold protein and adaptor protein	Shiroshima *et al.* (2009)
Growth factor receptor-bound protein 7 (GRB7)	Adaptor protein	Shiroshima *et al.* (2009)
Gamma-2-syntrophin (G2SNT)	Adaptor protein	Shiroshima *et al.* (2009)

One of the best-elucidated pathways was described by Shiroshima *et al.* (2009) that found the scaffold protein PICK1 (protein interacting with C kinase 1) was able to recognize the intracellular domain of LRP1B and inhibit its phosphorylation by protein kinase C alpha (PKC-alpha). Interestingly, although PICK1 was able to bound to the intracellular domain of LRP1, even more efficiently than to the intracellular domain of LRP1B, PICK1 did not affect its phosphorylation by PKC-alpha. A previous study indicated that the phosphorylation of the intracellular domain of LRP1 by PKC-alpha was responsible for the regulation of the endocytic and signaling activity of this cell-surface receptor by altering its association with its interacting partners (Ranganathan *et al.*, 2004). In regard to LRP1B, it appears that the phosphorylation by PKC-alpha and its regulation by PICK1 modulate the endocytic and signaling activity of LRP1B (Shiroshima *et al.*, 2009). Still, further studies are required to comprehend the biological significance

of the interactions between LRP1B and its intracellular partners.

Like other LDLR family members, LRP1B has also been shown to undergo regulated intramembrane proteolysis [RIP; Liu *et al.* (2007)]: a proteolytic process whereby a transmembrane protein undergoes two consecutive proteolytic cleavages by distinct proteases (Brown *et al.*, 2000). First, a membrane-anchored protease cleaves a transmembrane protein substrate close to its transmembrane domain, resulting in the release of the soluble extracellular domain into the extracellular space. After, the remaining membrane-bound carboxyl-terminal fragment is cleaved within its transmembrane domain by an intramembrane protease that results in the secretion of the small remaining peptide into the extracellular space and the liberation of the intracellular domain into the cytosol. The soluble intracellular domain can be rapidly degraded or translocated to the nucleus to regulate gene transcription (Lal & Caplan, 2011, McCarthy *et al.*, 2017, Kühnle *et al.*, 2019). Liu *et al.* (2007) showed that LRP1B was first cleaved by a metalloproteinase, which led to the release of its extracellular domain and then cleaved within the transmembrane domain by a gamma-secretase that led to the liberation of its intracellular domain (**Figure 6**). Furthermore, this study demonstrated that the soluble intracellular domain of LRP1B was translocated to the nucleus via a nuclear localization signal that is found within this domain (Liu *et al.*, 2007). The exact function(s) of the released intracellular domain of LRP1B in the nucleus remains unknown.

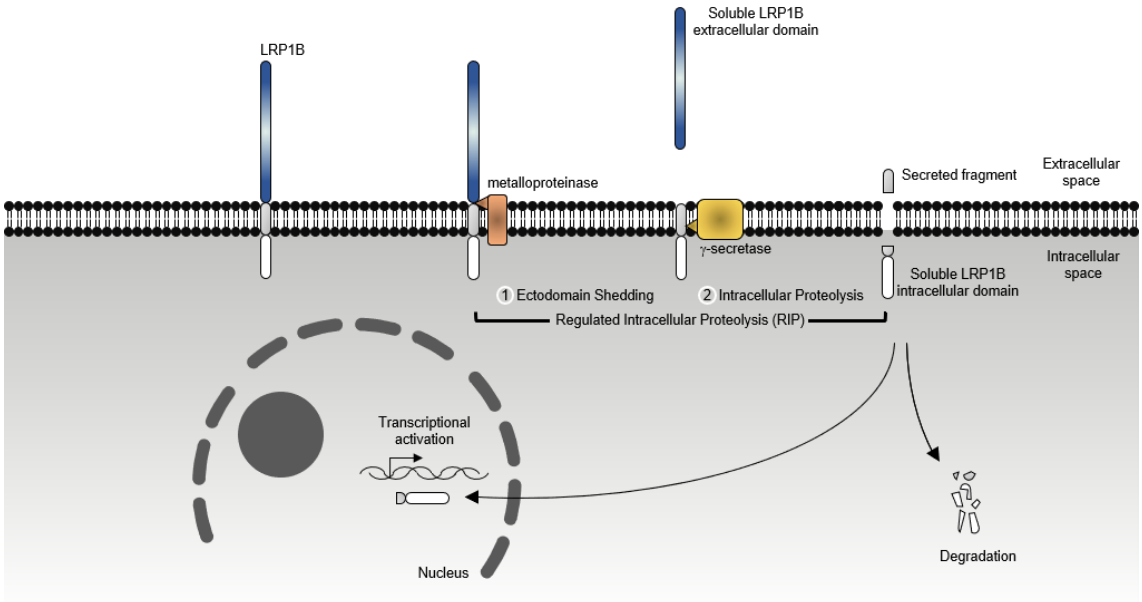

Figure 6. **Regulated intramembrane proteolysis (RIP) of LRP1B**. First, LRP1B undergoes proteolytic cleavage by a metalloproteinase (i.e., ADAM17) that results in the shedding of its extracellular domain. Then, the remaining 21 kDa membrane-bound carboxyl-terminal fragment undergoes a gamma-dependent intramembrane cleavage that results in the release of the LRP1B intracellular domain (18 kDa) into the cytosol, where it can be degraded or translocated to the nucleus to participate in the transcriptional activation of the target genes (yet, unknown).

1.1.4 Impairment of LRP1B Expression and Function in Cancer

As previously referred, the *LRP1B* gene was first identified to be frequently inactivated in non-small-cell lung cancer cell lines (Liu *et al.*, 2000a). It was therefore proposed as a novel candidate tumor suppressor gene (Liu *et al*., 2000a, Liu *et al*., 2000b). Thenceforward, *LRP1B* inactivation via genetic and epigenetic mechanisms (**Figure 7**) has been reported in multiple cancer types, including kidney (Langbein *et al.*, 2002, Karlsson *et al.*, 2011, Ni *et al.*, 2013), liver (Pineau *et al.*, 2003, Wang *et al.*, 2019), cervical (Hirai *et al.*, 2004, Choi *et al.*, 2007, Liu *et al.*, 2018), esophageal (Sonoda *et al.*, 2004, Brown *et al.*, 2011), brain (Roversi *et al.*, 2005, Yin *et al.*, 2009, Tabouret *et al.*, 2015), lymphoma (Rahmatpanah *et al.*, 2006, Taylor *et al.*, 2007a), oral (Nakagawa *et al.*, 2006, Cengiz *et al.*, 2007), leukemia (Taylor *et al.*, 2007a, Taylor *et al.*, 2007b), breast (Kadota *et al.*, 2010), gastric (Lu *et al.*, 2010), thyroid (Prazeres *et al.*, 2011), skin (Nikolaev *et al.*, 2011), ovarian (Cowin *et al.*, 2012), colon (Wang *et al.*, 2017), and prostate (Tucker *et al.*, 2019, Zhang *et al.*, 2019, Zheng & Bai, 2019).

Homozygous and hemizygous whole- and partial- *LRP1B* deletions were found in several cancers and cancer-derived cell lines (Liu *et al.*, 2000a, Langbein *et al.*, 2002, Pineau *et al.*, 2003, Hirai *et al.*, 2004, Sonoda *et al.*, 2004, Roversi *et al.*, 2005, Nakagawa *et al.*, 2006, Cengiz *et al.*, 2007, Choi *et al.*, 2007, Yin *et al.*, 2009, Kadota *et al.*, 2010, Kohno *et al.*, 2010, Brown *et al.*, 2011, Karlsson *et al.*, 2011, Prazeres *et al.*, 2011, Cowin *et al.*, 2012, Ni *et al.*, 2013, Tabouret *et al.*, 2015, Tucker *et al.*, 2019). Furthermore, point mutations (including missense, nonsense, and splice-site disrupting mutations) and frameshift mutations [derived from insertions and deletions (indels)] within this gene were also found (Liu *et al.*, 2000a, Ding *et al.*, 2008, Nikolaev *et al.*, 2011, Lee *et al.*, 2017, Maru *et al.*, 2017, Xiao *et al.*, 2017, Corre *et al.*, 2018, Konukiewitz *et al.*, 2018, Leung *et al.*, 2018, Wolff *et al.*, 2018, Chen *et al.*, 2019, Elgendy *et al.*, 2019, Hu *et al.*, 2019, Lan *et al.*, 2019, Li *et al.*, 2019, Tucker *et al.*, 2019, Zhao *et al.*, 2019, Ge *et al.*, 2020, Zhu *et al.*, 2020). Also, several epigenetic mechanisms including hypermethylation of the CpG island located in the *LRP1B* promoter region (Sonoda *et al.*, 2004, Nakagawa *et al.*, 2006, Rahmatpanah *et al.*, 2006, Taylor *et al.*, 2007a, Taylor *et al.*, 2007b, Lu *et al.*, 2010, Prazeres *et al.*, 2011, Ni *et al.*, 2013, Tabouret *et al.*, 2015), histone deacetylation of the *LRP1B* promoter region (Ni *et al.*, 2013), and microRNA (miRNA)-mediated post-transcriptional regulation of *LRP1B* expression (Prazeres *et al.*, 2011, Zhang *et al.*, 2019, Zheng & Bai, 2019) were shown to result in *LRP1B* inactivation. Moreover, *LRP1B* was identified as a common target gene for viral integration in hepatitis

B virus (HBV)-related liver cancer (Ding *et al.*, 2012) and in human papillomavirus (HPV)-positive cervical cancers (Hu *et al.*, 2015, Jiang *et al.*, 2019). Hu *et al.* (2015) reported that LRP1B expression was downregulated when HPV integrated into its introns. Overall, the prevalence of *LRP1B* inactivation in multiple cancer types strongly supports the tumor suppressor hypothesis.

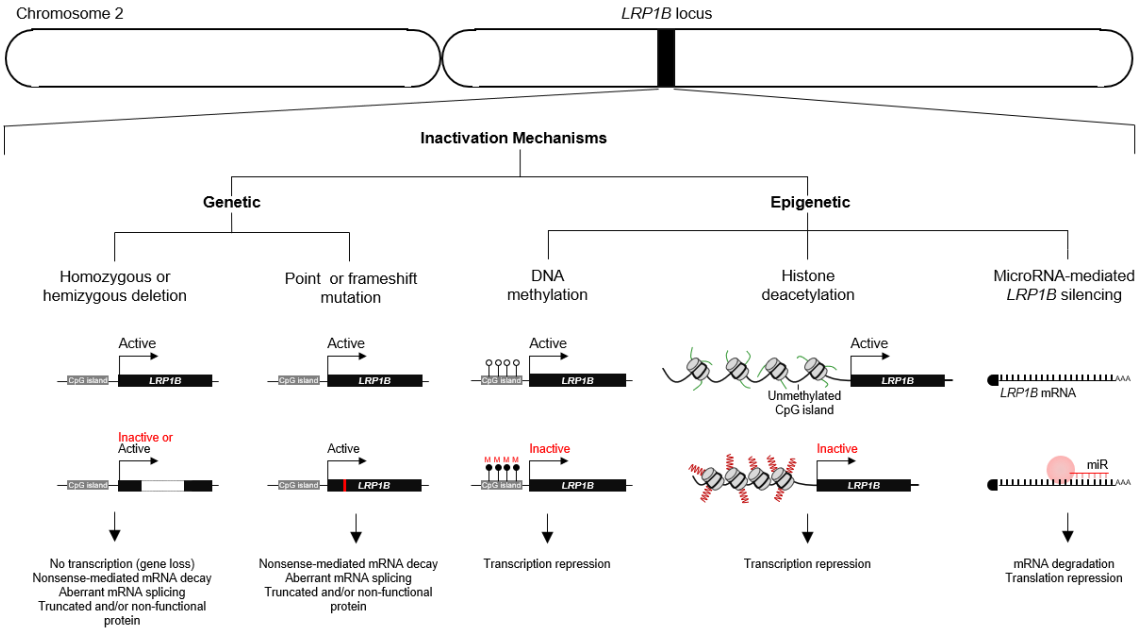

Figure 7. Mechanisms of genetic and epigenetic inactivation of the putative tumor suppressor gene *LRP1B*. The genetic mechanisms include (i) homozygous or hemizygous whole- and partial-deletions, and (ii) point mutations or frameshift mutations. The epigenetic mechanisms include (i) hypermethylation of the CpG island located in the *LRP1B* promoter region, (ii) histone deacetylation of the *LRP1B* promoter region, and (iii) *LRP1B* silencing by microRNAs, such as miR-548a-5p [thyroid cancer; Prazeres *et al.* (2011)], miR-500 [prostate cancer; Zhang *et al.* (2019)], and miR-301b-3p [prostate cancer; Zheng and Bai (2019)]. The genetic elements are shown in the correct order but not on the right scale.

Although the knowledge about the possible functional role of LRP1B in cancer is still limited. To date, several authors demonstrated that the re-establishment of *LRP1B* expression through the transfection of mLR1B4 into LRP1B-deficient cancer cells led to the suppression of anchorage-dependent growth [esophageal cancer, Sonoda *et al.* (2004); gastric cancer, Lu *et al.* (2010)] and anchorage-independent growth [brain cancer, Liu *et al.* (2007); gastric cancer, Lu *et al.* (2010); thyroid cancer, Prazeres *et al.* (2011); colon cancer, Wang *et al.* (2017)]. Interestingly, Liu *et al.* (2007) also found that cells transfected with a mutant mLRP1B4 (resistant to the extracellular domain release) were less able to suppress colony growth. To further determine whether this observation was linked to the regulated intramembrane proteolysis of LRP1B, the authors performed a soft agar assay with cells transfected with the intracellular domain of LRP1B, and discovered that the intracellular domain of LRP1B *per se* was able to suppress anchorage-independent growth like mLRP1B4 (Liu *et al.*, 2007); suggesting that LRP1B tumor suppressor activity requires its proteolytic processing. Still, further studies are needed to

identify target genes of the intracellular domain of LRP1B. This may provide other insights into its specific role. Moreover, the restoration of *LRP1B* expression through the transfection of mLRP1B4: (i) reduced cell proliferation in gastric cancer cell lines and tumorigenicity in nude mice (Lu *et al.*, 2010); (ii) decreased *in vivo* tumor development and growth, impaired cell invasion, and modulated cell secretome particularly reducing the levels of matrix metalloproteinase 2 (MMP-2; a proteolytic enzyme involved in the degradation of ECM) in the extracellular medium (Prazeres *et al.*, 2011) in thyroid cancer cell lines; (iii) suppressed cell proliferation in ovarian cancer cell lines (Cowin *et al.*, 2012); and (iv) inhibited cell proliferation and migration in colon cancer cell lines (Wang *et al.*, 2017).

On the other hand, the down-regulation of *LRP1B* expression through the action of small interfering RNAs (siRNAs) or short hairpin RNAs (shRNAs): (i) increased the anchorage-independent growth, cell migration, and invasion in renal cancer cell lines (Ni *et al.*, 2013); (ii) enhanced cell proliferation in lung cancer cell lines (Beer *et al.*, 2016); and (iii) promoted anchorage-independent growth, cell proliferation and migration in colon cancer cell lines (Wang *et al.*, 2017). Interestingly, Ni *et al.* (2013) found that the increased migration and invasion of *LRP1B*-silenced renal cancer cells were not due to the endocytic uptake of matrix metalloproteinases (such as MMP-2 and MMP-9), but possibly due to the actin cytoskeleton remodeling regulated by Rho/Cdc42 pathway, and the alteration of focal adhesions complex components. Zhang *et al.* (2019) showed that miR-500 promoted cell proliferation by directly targeting (downregulating) *LRP1B* mRNA in prostate cancer cells. Zheng and Bai (2019) also showed that the up-regulation of miR-301b-3p induced by hypoxia promoted cell proliferation, migration, and invasion of prostate cancer cells and enhanced tumorigenicity in nude mice through negative regulation of *LRP1B* expression. Altogether, these observations strongly suggest a suppressive role of LRP1B in tumorigenesis. However, the mechanisms through which LRP1B functions as a tumor suppressor may be distinct among the malignancies.

Also, *LRP1B* deletion or downregulation was associated with poor prognosis of high-grade ovarian cancer patients due to acquired chemotherapy resistance to liposomal doxorubicin (Cowin *et al.*, 2012). In fact, Cowin *et al.* (2012) showed that decreased expression of *LRP1B* increased the resistance of ovarian cancer cells to liposomal doxorubicin, whereas its overexpression increased the sensitivity of ovarian cancer cells to this drug. However, no studies are available regarding the value of *LRP1B* as a putative novel predictive biomarker for liposomal doxorubicin response, namely in ovarian cancer.

Overall, and as previously shown, the gathered knowledge on the potential tumor-suppressive role of LRP1B in cancer has mostly arisen from studies in which the *LRP1B* expression was re-established through transfection of LRP1B minireceptors into several LRP1B-deficient cancer cell lines (Sonoda *et al.*, 2004, Liu *et al.*, 2007, Lu *et al.*, 2010, Prazeres *et al.*, 2011, Wang *et al.*, 2017). The downregulation of *LRP1B* expression through RNA interference (RNAi)-based approaches in several *LRP1B*-expressing cancer cell lines has also been used to validate information (Beer *et al.*, 2016, Cowin *et al.*, 2012, Ni *et al.*, 2013, Wang *et al.*, 2017). Although extremely useful, both approaches may underestimate the full potential of LRP1B functions. The LRP1B minireceptor may not share all biological functions with the full-length receptor, and RNAi-based suppression of the *LRP1B* function may be incomplete. These limitations may be overcome by the generation of an *LRP1B* gene knockout.

1.2 CRISPR/Cas System

From the late 1980s through the 1990s, a series of repeat sequences [typically 25 to 50 base pairs (bp) in length] interspersed with similar-sized non-repetitive sequences were detected in several bacterial and archaeal species genomes (Ishino *et al.*, 1987, Nakata *et al.*, 1989, Hermans *et al.*, 1991, Mojica *et al.*, 1993, Mojica *et al.*, 1995, Bult *et al.*, 1996, Masepohl *et al.*, 1996, Smith *et al.*, 1997, Kawarabayasi *et al.*, 1998, Sensen *et al.*, 1998, She *et al.*, 1998, Kawarabayasi *et al.*, 1999, Nelson *et al.*, 1999). However, it was only in 2000 that these peculiar repetitive elements were brought to the attention of the scientific community when Mojica *et al.* (2000) stated that their prevalence among the prokaryotic genomes suggested a common and essential biological function. Later in 2002, Francisco Mojica, Rudd Jansen, and their colleagues proposed the acronym CRISPR (for clustered regularly interspaced short palindromic repeats) to unify the description of these repetitive microbial elements (Mojica *et al.*, 2000, Jansen *et al.*, 2002). Meanwhile, numerous genes initially hypothesized to encode uncharacterized DNA repair proteins specific for thermophilic archaea and bacteria (Makarova *et al.*, 2002) were identified as being closely associated with CRISPR and hence designated as CRISPR-associated (*cas*) genes by (Jansen *et al.*, 2002). However, the function of CRISPR and CRISPR-associated (Cas) proteins remained unknown until the mid-2000s. The similarities between the non-repetitive (currently known as spacer sequences) and sequences within foreign nucleic acids (later called protospacers) such as viral genomes and plasmids (Bolotin *et al.*, 2005, Mojica *et al.*, 2005, Pourcel *et al.*, 2005), together with the discovery that the CRISPR locus was transcribed (Tang *et al.*, 2002), and also the observation that *cas* genes encode proteins with putative nuclease and helicase domains

(Jansen *et al.*, 2002, Bolotin *et al.*, 2005, Haft *et al.*, 2005, Pourcel *et al.*, 2005) led to the hypothesis that the CRISPR/Cas was a prokaryotic adaptive and heritable immune system against invading bacteriophages, archaeal viruses, and conjugative plasmids (Makarova *et al.*, 2006). A fast series of studies with experimental evidence supporting this hypothesis followed soon after and helped to unravel details of the CRISPR/Cas-based defense mechanism (Barrangou *et al.*, 2007, Brouns *et al.*, 2008, Deveau *et al.*, 2008, Marraffini & Sontheimer, 2008, Hale *et al.*, 2009, Garneau *et al.*, 2010).

1.2.1 CRISPR/Cas As a Prokaryotic Defense System

A typical CRISPR/Cas system is composed of: (i) an array of short repeated sequences (repeats) interspersed by similar-sized non-repetitive (unique) sequences [spacers; Mojica *et al.* (2000), Jansen *et al.* (2002)] acquired from foreign nucleic acid sequences (protospacers) that can consist of hundreds of repeat-spacer units [CRISPR array; Bolotin *et al.* (2005), Mojica *et al.* (2005), Pourcel *et al.* (2005)]; (ii) an adenine- and thymine-rich (AT-rich) sequence (leader) located immediately upstream from the first repeat of the CRISPR array (Jansen *et al.*, 2002, Alkhnbashi *et al.*, 2016); and (iii) a highly diverse set of *cas* genes located adjacent to the CRISPR locus that encodes proteins involved in the different phases of CRISPR/Cas-based defense mechanisms (Jansen *et al.*, 2002, Haft *et al.*, 2005, Makarova *et al.*, 2006). Currently, the CRISPR/Cas systems can be classified into two classes, 1 and 2, based on the architectures of Cas effector complexes (multiprotein effector complex or a single-protein effector complex), which are further subdivided into six types, I to VI, based on presence of unique signature Cas proteins, and thirty-three subtypes based on additional signature genes and characteristic gene arrangements (Burstein *et al.*, 2017, Koonin *et al.*, 2017, Shmakov *et al.*, 2017, Koonin & Makarova, 2019, Makarova *et al.*, 2020).

The CRISPR/Cas-based defense mechanisms can be divided into three general phases [**Figure 8**; extensively reviewed in Sorek *et al.* (2013), van der Oost *et al.* (2014), Marraffini (2015), Amitai and Sorek (2016), Hille *et al.* (2018)]: (i) CRISPR adaptation (i.e., new spacer acquisition), where a unique sequence of the invading nucleic acid (DNA or RNA) is integrated into the CRISPR array (spacer sequence) for future recognition of the invader (Sternberg *et al.*, 2016); (ii) CRISPR RNA (crRNA) biogenesis, where the CRISPR array is transcribed into a long precursor crRNA (pre-crRNA) that is further processed into small mature crRNAs either by a single Cas protein, the effector Cas protein or the host RNase III with the help of the trans-activating crRNA (tracrRNA) – depending on the type of CRISPR/Cas system (Brouns *et al.*, 2008, Hale *et al.*, 2008,

Deltcheva *et al.*, 2011, East-Seletsky *et al.*, 2016, Fonfara *et al.*, 2016), and (iii) crRNA-guided interference, where the mature crRNAs and Cas effector complexes form ribonucleoprotein (RNP) complexes that recognize and cleave the invading nucleic acid (DNA or RNA) via base pairing of spacer-derived crRNA and the target protospacer (Gasiunas *et al.*, 2012, Plagens *et al.*, 2015, Nishimasu & Nureki, 2017).

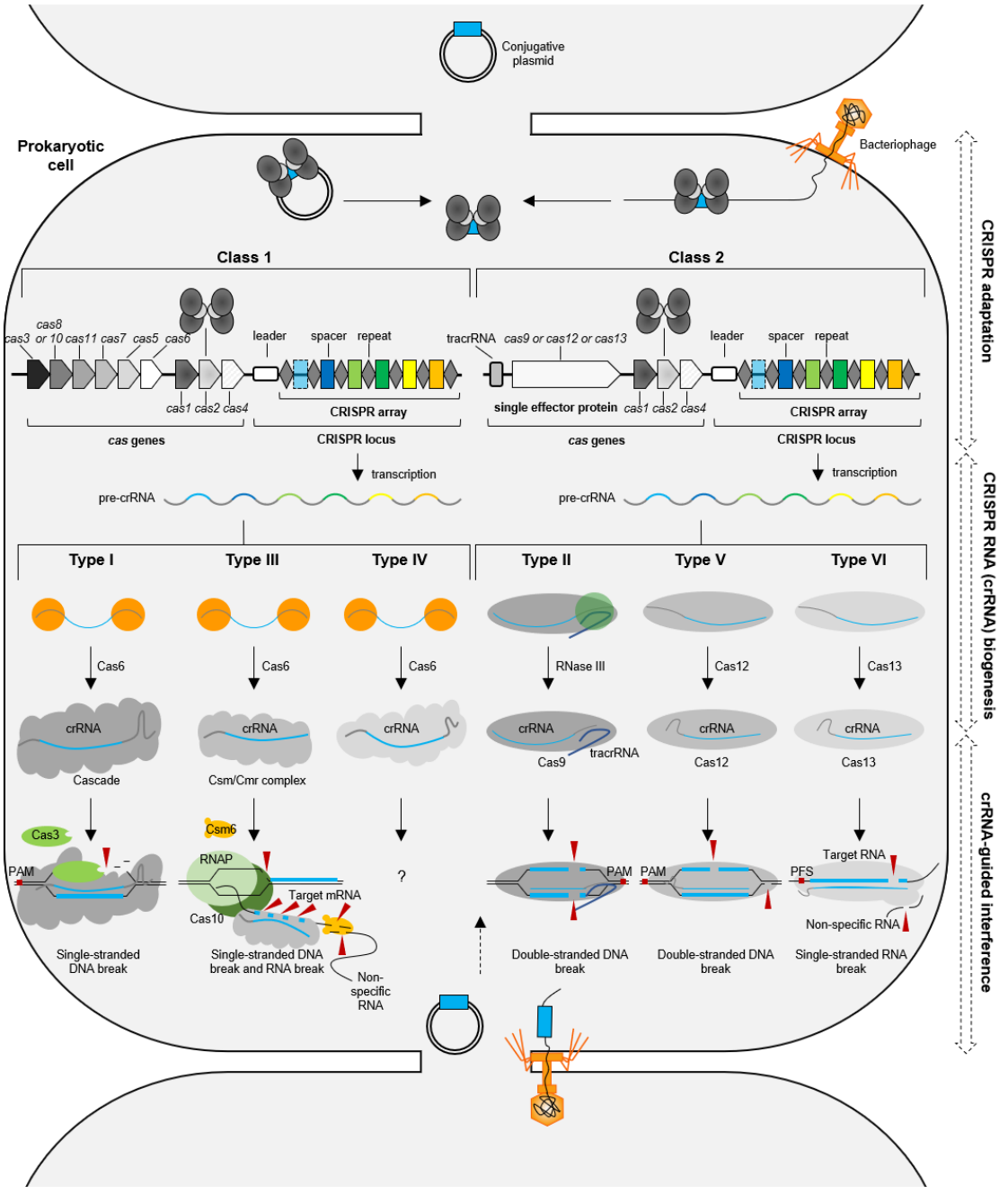

Figure 8. **Overview of the CRISPR/Cas-based defense mechanisms.** The CRISPR/Cas-based defense mechanisms can be divided into three general phases: (i) CRISPR adaptation, (ii) CRISPR crRNA biogenesis, and (iii) crRNA-guided interference. The generic organizations of class 1 and 2 CRISPR/Cas loci are illustrated. In the adaptation phase, a short fragment of an invading nucleic acid (bacteriophage or conjugative plasmid) is acquired as a new spacer (light blue) into the CRISPR array by the Cas1-Cas2-(Cas4) complex. In the crRNA biogenesis phase, the CRISPR array is transcribed into a long pre-crRNA that is further processed into small mature crRNAs either by a single Cas protein (Cas6 for type I, III and IV), the effector Cas protein (Cas12 for type V and Cas13 for type VI) or the host RNase III with the help of the tracrRNA (type II). In the crRNA-guided interference phase, the RNP complexes (mature crRNA Cas effector complexes) cleave invading nucleic acid via their respective mechanism. Abbreviations: PAM, protospacer adjacent motif; PFS, protospacer flanking sequence; RNAP, RNA polymerase.

1.2.2 CRISPR/Cas As a Genome-Editing Tool

Besides their natural function in prokaryotic adaptive immunity, the CRISPR/Cas-systems have been adapted to function as a programmable genome-editing tool that has enabled efficient targeting and precise modification of genomic sequences in either prokaryotes or eucaryotic cells and organisms.

The most noteworthy is the CRISPR/Cas9 system, which relies on the single protein, Cas9, to catalyze DNA cleavage (Sapranauskas *et al.*, 2011). This protein requires both the crRNA and tracrRNA, which is partially complementary to the crRNA, to recognize the DNA target and introduce a site-specific double-stranded break (DSB). DNA target recognition requires both base-pairing to the crRNA sequence and the presence of a protospacer adjacent motif (PAM) sequence adjacent to the crRNA-binding sequence within the DNA target (Deltcheva *et al.*, 2011, Gasiunas *et al.*, 2012, Jinek *et al.*, 2012). At sites complementary to the 20-nucleotide (nt) sequence of the crRNA, the Cas9 HNH domain cleaves the complementary DNA strand, whereas the Cas9 RuvC-like domain cleaves the non-complementary DNA strand (Gasiunas *et al.*, 2012, Jinek *et al.*, 2012). The native tracrRNA:crRNA duplex was then engineered as a single guide RNA (sgRNA) composed of: (i) a 20-nt sequence at the 5' end of the sgRNA that determines the DNA target site (known as sgRNA target sequence), and (ii) a non-variable scaffold sequence at the 3' end of the sgRNA target sequence that binds to Cas9 [known as sgRNA scaffold sequence; Jinek *et al.* (2012), Mali *et al.* (2013)]. By changing the 20-nt target sequence of the sgRNA, Cas9 can be re-targeted to any DNA sequence of interest, as long as it is near a PAM sequence, and introduce a DSB (Jinek *et al.*, 2012). In the type II CRISPR/Cas system derived from *Streptococcus pyogenes*, the DNA target sequence must precede a 5'-NGG-3' PAM sequence (Jinek *et al.*, 2012), whereas other Cas9 orthologs may have distinct PAM sequence requirements such as those of *S. thermophilus* [5'-NNAGAAW-3'; Garneau *et al.* (2010)], *Staphylococcus aureus* [5'-NNGRRT-3'; Ran *et al.* (2015)] and *Neisseria meningitidis* [5'-NNNNGATT-3'; Hou *et al.* (2013)].

Upon the CRISPR/Cas9-induced DSB within the target DNA, one of the two general DNA damage repair pathways might occur: (i) the efficient but error-prone nonhomologous end-joining (NHEJ) pathway or (ii) the less efficient but high-fidelity homology-directed repair (HDR) pathway [**Figure 9**; extensively reviewed in Jackson (2002), Lieber (2010), Deriano and Roth (2013), Ceccaldi *et al.* (2016)]. In the presence of a suitable, exogenously introduced repair template, the cell might use the HDR pathway to integrate a new or modified sequence at the target site. In its absence, the CRISPR/Cas9-induced

DSB ends are re-ligated via the NHEJ pathway, which can leave a scar in the form of an insertion/deletion (indel) mutation (at the repair junction site). This pathway can be used to mediate gene knockouts, as indels might result in frameshift mutations and lead to premature termination codons (PTCs) within the open reading frames (ORFs) of the targeted genes (Ran *et al.*, 2013, Hsu *et al.*, 2014). Consequently, the aberrant mRNA (harboring a PTC) can be translated into a truncated and/or non-functional protein or degraded through the nonsense-mediated mRNA decay (NMD) pathway (Santiago *et al.*, 2008).

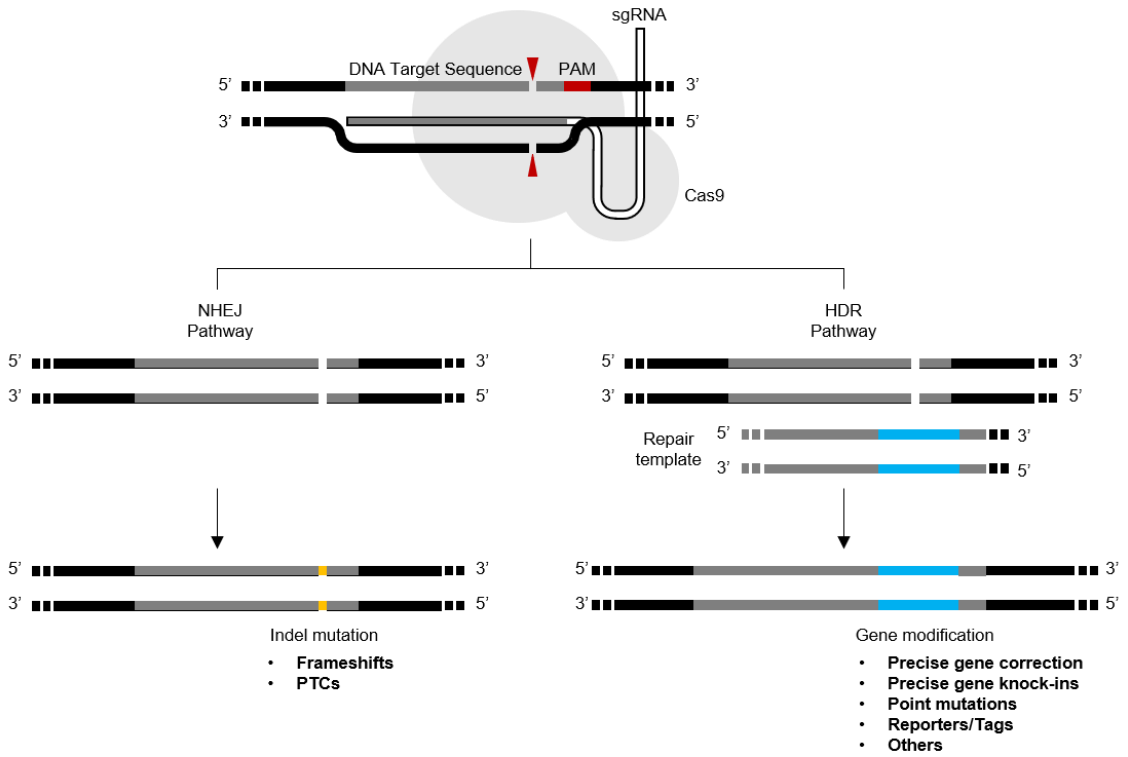

Figure 9. **Genome editing via the CRISPR/Cas9 system**. Upon the CRISPR/Cas9-induced DSB within the target DNA, one of the two general DNA damage repair pathways might occur: (i) the nonhomologous end-joining (NHEJ) pathway or (ii) the homology-directed repair (HDR) pathway. The NHEJ pathway is the most active repair mechanism and often introduces an indel mutation at the repair junction site. For the cell to use the HDR pathway, a DNA repair template in the form of a single-stranded donor oligonucleotide, a double-stranded donor oligonucleotide, or a double-stranded DNA plasmid must be delivered into the cell together with the CRISPR/Cas9 machinery. The repair template must contain the desired edit and two flanking homology arms.

In contrast to the previously used genome-editing tools such as the zinc-finger nucleases (ZFNs) and the transcription-activator-like effector nucleases (TALENs), which require substantial protein engineering for each DNA target site to be edited (Porteus & Baltimore, 2003, Miller *et al.*, 2007, Hockemeyer *et al.*, 2011, Wood *et al.*, 2011), CRISPR/Cas9 system only requires a modification in the sgRNA target sequence. Due to its comparative simplicity and adaptability, the CRISPR-Cas9 system quickly became the most popular and powerful tool for genome editing, honored by the 2020 Chemistry Nobel Prize to Emmanuelle Charpentier and Jennifer Doudna.

2 Objectives

LRP1B has been proposed as a tumor suppressor gene in several types of human cancer, although the exact molecular mechanisms underlying the suppressive function of LRP1B in cancer are still widely unexplored. Due to the enormous size of this gene (13,800 bp of coding sequence) and its encoding protein (approximately 610 kDa), there is a lack of *in vitro* and *in vivo* experimental models that can provide new insights about LRP1B functions, namely in cancer. The establishment of an *LRP1B* knockout model can be a better alternative (more predictable and reproducible) to the previously utilized overexpression and knockdown models. The CRISPR/Cas9 genome-editing tool has been extensively used to create knockout cell lines, in which the open reading frame (ORF) of a target gene can be permanently disrupted, leading to the complete ablation of the protein it encodes.

Therefore, the main objective of this study was to generate an *LRP1B*-knockout human cancer cell line model using the CRISPR/Cas9 genome-editing tool.

The specific objectives were:

1. To design sgRNAs for CRISPR/Cas9-mediated *LRP1B* knockout;
2. To generate sgRNA/Cas9 expression vectors for cell transfection;
3. To transfect the sgRNA/Cas9 expression constructs into human cancer cells;
4. To screen single cell-derived clones for CRISPR/Cas9-mediated deletions;
5. To validate potential knockout clones at mRNA and protein expression levels.

3 Materials and Methods

3.1 sgRNA Selection

The Benchling's CRISPR Guide RNA Design Software was used to identify all 5'-NGG-3' PAM sequences within the chosen target exons (exon 1 and 85) of the human *LRP1B* and list possible sgRNA target sequences. The human *LRP1B* gene sequence (Ensembl ID: ENS00000168702) was used as the "input sequence" for analysis. Four sgRNA target sequences were selected based on their predicted target specificity [off-target score; Hsu *et al.* (2013b)] and cleavage efficiency [on-target score; Doench *et al.* (2016)]. Potential off-target sequences within the human genome [GRCh38; Schneider *et al.* (2017)] were identified using the same software. The sgRNA target sequences used in this study are listed in **Table 3**.

Table 3. sgRNA target sequences used in this study.

Target exon	Position within the gene (bp)[a]	Strand	sgRNA target sequence (5' → 3')	PAM sequence
1	6720	Minus	GACATTGTGGTCGCCCGGTA	AGG
	6800	Plus	CGTGGGAGCCGACCGAGGTA	AGG
85	1 862 943	Minus	TTTGGTCCTTCATAGCGCGT	TGG
	1 862 993	Minus	TTATAATGCAGTGCCCCCCA	TGG

[a] Human *LRP1B* RefSegGene; NCBI reference sequence: NG_051023.1; O'Leary *et al.* (2016).

3.2 sgRNA/Cas9 Expression Vector Generation

3.2.1 Cas9 Expression Vector Preparation

The pSpCas9(BB)-2A-Puro (PX459) V2.0 vector (Addgene Plasmid #62988), a gift from Professor Feng Zhang (Massachusetts Institute of Technology, Cambridge, MA, USA), was used as a backbone for the construction of the sgRNA/Cas9 expression vectors. This vector contains an ampicillin resistance gene that allows the selection of vector-containing bacteria and a puromycin marker that confers antibiotic resistance to transfected mammalian cells (Ran *et al.*, 2013). Preceding sgRNA cloning, the stab culture of PX459-containing *Escherichia coli* (Addgene, Watertown, MA, USA) was used to streak bacteria onto an LB-ampicillin agar plate (10 g/L tryptone, 5 g/L yeast extract, 10 g/L NaCl, 15 g/L agar, 100 μg/mL ampicillin). After overnight incubation at 37ºC, a single colony was picked to inoculate a 5 mL starter culture of LB selective medium (10 g/L

tryptone, 5 g/L yeast extract, 10 g/L NaCl, 100 μg/mL ampicillin). This starter culture was incubated for 8 h at 37ºC on an orbital shaker (250 rpm) and then used (1 mL) to inoculate a 100 mL culture of LB selective medium and incubated overnight (37ºC, 250 rpm). *E. coli* cells were harvested by centrifugation (6,000 *g*, 15 min, 4ºC), and plasmid DNA was extracted from the pellets using the NZYMidiprep Kit (NZYTech, Lisbon, Portugal). The kit included all reagents, except for the isopropanol, ethanol, and nuclease-free distilled water. Plasmid DNA was extracted as follows. Bacterial pellets were resuspended entirely in 8 mL of buffer M1, and then an equal volume of buffer M2 was added to the bacterial suspensions. Samples were mixed by gentle inversion and incubated for 5 min at room temperature (RT). Bacterial lysates were gently mixed with 8 mL of prechilled buffer M3 and incubated on ice for 15 min before centrifugation (20,000 *g*, 30 min, 4ºC). Supernatants were carefully loaded onto gravity-flow columns pre-equilibrated with buffer MEQ (2.5 mL). After discarding the flowthroughs, the columns were washed with 10 mL of buffer MW and transferred to new sterile collection tubes. Plasmid DNA was eluted from the columns with 5.0 mL of pre-heated (50ºC) buffer ME, mixed with 3.5 mL of isopropanol [99.8% (v/v); Thermo Fisher Scientific, Waltham, MA, USA] and incubated for 2 min at RT. Samples were centrifuged at 15,000 *g* for 30 min at 4ºC and washed with 2 mL of 70% (v/v) ethanol solution. The ethanol solution was prepared using absolute ethanol [99.8% (v/v); PanReac AppliChem, Barcelona, Spain] and UltraPure™ DNase/RNase-free distilled water (Thermo Fisher Scientific, Waltham, MA, USA). Following centrifugation at 15,000 *g* for 5 min at RT, plasmid DNA pellets were air-dried for 15 min, resuspended in 100 μL of nuclease-free distilled water, and stored until use at -20ºC. Plasmid DNA (5 μg) was digested with 25 U of BbsI in the presence of 1 × buffer G (with BSA) for 6 h at 37ºC (both from Thermo Fisher Scientific, Waltham, MA, USA). The digested plasmid DNA was then separated by electrophoresis on a 0.8% (w/v) preparative agarose gel and further isolated using the Cut & Spin Gel Extraction Columns (GRiSP, Oporto, Portugal) according to the manufacturer's instructions.

3.2.2 sgRNA Oligonucleotide Duplex Preparation

The oligonucleotide pairs used for sgRNA cloning are listed in **Table 4**. To improve the efficiency of U6-driven transcription, an extra guanine (highlighted in gray, **Table 4**) was appended at the 5' ends of the sgRNA target sequences [underlined, **Table 4**; Guschin *et al.* (2010)]. Also, an extra cytosine was appended at the 3' ends of the reverse-complement sgRNA target sequences. The overhang sequences 5'–CACC–3' and 5'–AAAC–3' (bold, **Table 4**) were added to the 5' ends of the sgRNA target sequences and the reverse-complement sgRNA target sequences, respectively, for ligation

into the pair of BbsI sites in PX459. Prior to sgRNA cloning, the oligonucleotide pairs (Integrated DNA Technologies, Leuven, Belgium) were phosphorylated and annealed. Each 10 μL reaction contained 10 μM of each oligonucleotide, 1 × T4 DNA ligase buffer (Thermo Fisher Scientific, Waltham, MA, USA) and 1.5 U of T4 polynucleotide kinase (NZYTech, Lisbon, Portugal). All reactions were carried out in a MyCycler™ thermal cycler (Bio-Rad Laboratories, Hercules, CA, USA) with the following profile: 37ºC for 30 min, 95ºC for 5 min, 70 cycles of 95ºC for 30 s (-0.5ºC per cycle) and 70 cycles of 60ºC for 30 s (-0.5ºC per cycle).

Table 4. Oligonucleotides used for sgRNA cloning.

Oligonucleotide duplex name	Oligonucleotide name	Sequence (5' → 3')
Duplex-1	1-sense	**CACC**GACATTGTGGTCGCCCGGTA
	1-antisense	**AAAC**TACCGGGCGACCACAATGTC
Duplex-2	2-sense	**CACC**GCGTGGGAGCCGACCGAGGTA
	2-antisense	**AAAC**TACCTCGGTCGGCTCCCACGC
Duplex-3	3-sense	**CACC**GTTTGGTCCTTCATAGCGCGT
	3-antisense	**AAAC**ACGCGCTATGAAGGACCAAAC
Duplex-4	4-sense	**CACC**GTTATAATGCAGTGCCCCCCA
	4-antisense	**AAAC**TGGGGGGCACTGCATTATAAC

3.2.3 sgRNA Cloning Into Cas9 Expression Vector

Each sgRNA-encoding oligonucleotide duplex (1 μL) was ligated into the BbsI-digested PX459 vector (50 ng) using 5 U of T4 DNA ligase in the presence of 1 × T4 DNA ligase buffer (both from Thermo Fisher Scientific, Waltham, MA, USA). Ligation reactions (10 μL) were incubated for 1 h at 22ºC. Ligation products were transformed into chemically competent *E. coli* DH5α cells. Briefly, 1 μL of the ligation reaction was gently mixed with 50 μL of ice-cold competent cells. After 30 min of incubation on ice, cells were heat-shocked at 42ºC for 90 s, placed back on ice for 2 min, and allowed to recover for 60 min (37ºC, 200 rpm) after addition of 945 μL of LB medium (10 g/L tryptone, 5 g/L yeast extract, 10 g/L NaCl). After incubation, cells were pelleted by centrifugation for 1 min at 14,000 *g*, resuspended in 100 μL of remaining supernatant, and plated onto LB-ampicillin agar plates. After overnight incubation at 37ºC, two colonies of each plate were randomly picked to be screened for the correct insertion of the sgRNA target sequences. Negative (*E. coli* DH5α cells only, and *E. coli* DH5α cells transformed with

digested plasmid DNA) and positive (DH5α cells transformed with non-digested DNA plasmid) controls were included. Plasmid DNA was recovered from 100 mL cultures, as mentioned before (see **Page 20**, **3.2.1**). All sgRNA/Cas9 expression vectors generated (**Table 5**) were verified by Sanger sequencing using the U6 promoter forward primer: 5'–GAGGGCCTATTTCCCATGATTCC–3' at the Genomics Core Facility, i3S, Oporto, Portugal.

Table 5. sgRNA/Cas9 expression vectors generated in this study.

Vector ID	Features[a]
PX459-sgRNA1 (9198 bp)	ori – U6 promoter – sgRNA target sequence 1 – sgRNA scaffold sequence – CBh promoter – 3×FLAG – SV40 NLS – *SpCas9* – NP NLS – T2A – *PuroR* – bGH pA – f1 ori – AmpR promoter – *AmpR*
PX459-sgRNA2 (9199 bp)	ori – U6 promoter – sgRNA target sequence 2 – sgRNA scaffold sequence – CBh promoter – 3×FLAG – SV40 NLS – *SpCas9* –NP NLS – T2A – *PuroR* – bGH pA – f1 ori – AmpR promoter – *AmpR*
PX459-sgRNA3 (9199 bp)	ori – U6 promoter – sgRNA target sequence 3 – sgRNA scaffold sequence – CBh promoter – 3×FLAG – SV40 NLS – *SpCas9* –NP NLS – T2A – *PuroR* – bGH pA – f1 ori – AmpR promoter – *AmpR*
PX459-sgRNA4 (9199 bp)	ori – U6 promoter – sgRNA target sequence 4 – sgRNA scaffold sequence – CBh promoter – 3×FLAG – SV40 NLS – *SpCas9* –NP NLS – T2A – *PuroR* – bGH pA – f1 ori – AmpR promoter – *AmpR*

[a] Abbreviations: ori, origin of replication; U6 promoter, RNA polymerase III promoter for human U6 small nuclear RNA (snRNA); CBh promoter, human cytomegalovirus (CMV) immediate early enhancer fused to modified chicken β-actin promoter; bGH pA, bovine growth hormone polyadenylation signal; f1 ori, f1 bacteriophage origin of replication. Products: 3×FLAG, three tandem FLAG epitopes; SV40 NLS, nuclear localization signal (NLS) of simian virus 40 (SV40) large T antigen; SpCas9, Cas9 endonuclease from the *S. pyogenes*; NP NLS, bipartite nuclear localization signal (NLS) from nucleoplasmin; T2A, 2A peptides from *Thosea asigna virus* capsid protein; PuroR, puromycin N-acetyltransferase; AmpR, β-lactamase.

3.3 Cell Culture

The U87 human glioblastoma cell line was kindly provided to the group by Doctor Bruno Costa (ICVS, School of Medicine, University of Minho, Braga, Portugal). The cell line was screened for mycoplasma contamination at the Cell Culture and Genotyping (CCGen) Core Facility (i3S, Oporto, Portugal). The mycoplasma-free cells were cultured as a monolayer in Dulbecco's Modified Eagle Medium (DMEM) high glucose (4.5 g/L) with stable glutamine and sodium pyruvate (Capricorn Scientific, Hessen, Germany) supplemented with 10% (v/v) Gibco™ heat-inactivated fetal bovine serum (FBS; Thermo Fisher Scientific, Waltham, MA, USA), 1% (v/v) penicillin-streptomycin (Biowest, Nuaille,

France) and 0.5% (v/v) Corning™ amphotericin B (Thermo Fisher Scientific, Waltham, MA, USA); hereafter, named complete medium. Cells were routinely maintained at 37ºC in a humidified atmosphere containing 5% carbon dioxide (CO_2) and monitored using a CK2 inverted-phase contrast microscope (Olympus, Tokyo, Japan). Whenever required, cell concentration (cells/mL) was determined using a Z2™ Coulter particle count and size analyzer (Beckman Coulter, Brea, CA, USA).

3.4 Cell Transfection and Selection

Before cell transfection, the optimal puromycin concentration for selection after transfection was determined through a dose-response curve assessment. Briefly, 7.5×10^4 cells were seeded in 0.5 mL of complete medium per well in a 24-well plate and allowed to adhere for 24 h. Cells were then treated with increasing concentrations of puromycin (0.00, 0.10, 0.25, 0.50, 1.00, 1.50, 2.00, 2.50, 3.00, 5.00, 7.50, 10.00 μg/mL; InvivoGen, San Diego, CA, USA), and the medium replaced every two or three days. Treated cells were monitored daily (for a week) by microscopy to assess puromycin induced cell death. The lowest puromycin concentration that decreased viability of U87 cells by at least 90% within a 3-day period (and killed all cells within a week) was chosen as the optimal antibiotic concentration to be used for the selection of U87 transfected cells.

Prior to transfection, U87 cells were seeded at a density of 7.5×10^4 cells per well of a 24-well plate in 0.5 mL of complete medium and further incubated to allow adhesion. After 24 h of incubation, cells (at 70-80% confluency) were co-transfected with two or four sgRNA/Cas9 expression vectors (see **Page 23**, **Table 5**) using the cationic lipid-based Lipofectamine™ 3000 transfection reagent (Thermo Fisher Scientific, Waltham, MA, USA) according to the manufacturer's protocol. Briefly, 1 h before transfection, the cell culture medium was replaced with Opti-MEM™ I reduced serum medium (Thermo Fisher Scientific, Waltham, MA, USA), and cells placed back in the incubator. Meanwhile, 1 μL of Lipofectamine™ 3000 reagent was diluted in 24 μL of Opti-MEM™ medium and incubated for 5 min at RT. sgRNA/Cas9 expression vectors (500 ng or 1000 ng) were mixed in equimolar ratios with Opti-MEM™ to a total volume of 24 μL before adding 1 μL of P3000™ reagent. The diluted plasmid DNA was mixed with the diluted Lipofectamine™ 3000 reagent (1:1 ratio), incubated for 15 min at RT to allow DNA-lipid complexes formation, and added dropwise to the cells. The empty Cas9 expression vector was used as a negative control. After 6 h of incubation, the transfection medium was replaced with complete medium, and cells were further incubated. Following 24 h of

incubation, the cell culture medium was changed with fresh medium containing 1 μg/mL of puromycin and cells selected for three days. Cells were monitored daily by microscopy and compared to untreated cells. Once removed the antibiotic (72 h post-selection), the antibiotic-selected cell pools were expanded into 6-well-plates and then T25 flasks.

3.5 Single-Cell (Clonal) Isolation

The antibiotic-selected cell pools were dissociated into single cells through trypsinization and resuspended in complete medium. Cells were diluted to a final concentration of 5 cells/mL and then transferred into a 96-well plate (at 0.5 cells/well in 100 μL of culture medium). One 96-well plate was seeded for each heterogeneous cell population. Plates were observed daily by microscopy to assess the establishment of single-cell colonies, and the medium was replaced every three or four days. Once colonies were grown to 70-80% confluency, cells were scaled up into 12-well plates and then T25 flasks. Cells were collected for cryopreservation and DNA and RNA extraction (as described on **Page 25**, **3.6.1,** and **Page 26**, **3.6.2**, respectively).

3.6 Nucleic Acid Extraction

3.6.1 Genomic DNA Extraction

Cells were pelleted by centrifugation at 1,500 *g* for 5 min at 4ºC, washed once with prechilled sterile PBS (1 ×, pH 7.4), re-centrifuged as previously described, and pellets stored at -20ºC until DNA extraction. Genomic DNA (gDNA) was extracted using the GRS Genomic DNA Kit - Blood and Cultured Cells (GRiSP, Oporto, Portugal). The kit included all reagents, except for the ethanol and nuclease-free distilled water. Frozen cell pellets were thawed on ice and lysed in 150 μL of lysis buffer. After adding 200 μL of buffer BC1 to the lysed samples, these were shaken vigorously for 5 s and incubated for 10 min at 70ºC with constant agitation (500 rpm). After cooled to RT, 5 μL of 10 mg/mL RNase A was added to the lysates, and then further incubated for 5 min at RT. Then, 200 μL of absolute ethanol [99.8% (v/v); PanReac AppliChem, Barcelona, Spain] was added to the samples that were shaken vigorously for 10 s, transferred to spin columns, and centrifuged at 16,000 *g* for 2 min. After discarding the flowthroughs, the spin columns were washed first with 400 μL of wash buffer 1 and then with 600 μL of wash buffer 2 through serial centrifugations at 16,000 *g* for 1 min, and dried by an additional 3 min centrifugation. gDNA was eluted from the spin columns by adding 100 μL of pre-heated (70ºC) nuclease-free water to the center of the columns membranes, incubation for 5

min at RT, and centrifugation (16,000 g, 1 min). gDNA was kept at -20ºC.

3.6.2 Total RNA Extraction

Cell pellets (previously were collected by centrifugation at 1,500 *g* for 5 min at 4ºC and frozen at -80ºC) were thawed on ice and then disrupted in 500 μL of TripleXtractor (GRiSP, Oporto, Portugal) for 5 min at RT. Lysates were then vigorously mixed with 100 μL of chloroform (Carlo Erba Reagents, Milan, Italy), incubated for 5 min at RT, and centrifuged at 12,000 *g* for 15 min at 4ºC. The colorless upper aqueous phase of each sample was transferred to a new RNase-free microcentrifuge tube and further mixed with 250 μL of isopropanol [99.8% (v/v); Thermo Fisher Scientific, Waltham, MA, USA]. Following incubation for 10 min at RT, samples were centrifuged at 12,000 *g* for 15 min at 4ºC. RNA pellets were washed with 500 μL of 75% (v/v) ethanol (prepared using absolute ethanol [99.8% (v/v); PanReac AppliChem, Barcelona, Spain] and nuclease-free distilled water), centrifuged at 7,500 *g* for 5 min at 4ºC, and air-dried for 10 min. RNA pellets were resuspended in 25 μL of nuclease-free distilled water and stored until use at -80ºC.

3.7 Nucleic Acid Quantification

DNA/RNA concentration was determined by measuring the absorbance at 260 nm using a Nanodrop™ 1000 spectrophotometer (Thermo Fisher Scientific, Waltham, MA, USA). Nucleic acid purity was also assessed by determining the ratios of the absorbance values of 260 nm versus 280 nm (A_{260}/A_{280}) and the 260 nm versus 230 nm (A_{260}/A_{230}).

3.8 Agarose Gel Electrophoresis

Nucleic acid electrophoresis was performed in 0.8-1.0% (w/v) agarose (GRiSP, Oporto, Portugal) gels with 0.5 × SGTB buffer (GRiSP, Oporto, Portugal). DNA ladder and samples were prepared with a loading buffer containing glycerol (as a density agent; PanReac AppliChem, Barcelona, Spain), bromophenol blue (as tracking dye; Sigma-Aldrich, St. Louis, MO, USA), and GelRed (as fluorescent nucleic acid stain; Biotium, Fremont, CA, USA). DNA bands were visualized under ultra-violet (UV) light with a ChemiDoc™ XRS + System with Image Lab™ Software (Bio-Rad Laboratories, Hercules, CA, USA). The 1 kb plus DNA ladder (Thermo Fisher Scientific, Waltham, MA, USA)

was used as a molecular-weight size marker.

3.9 Polymerase Chain Reaction (PCR)

CRISPR/Cas9-mediated genomic deletions were screened by PCR using gDNA as template and the primers indicated in **Table 6**. The PCR primers were designed using Primer-BLAST (Ye *et al.*, 2012), available at https://www.ncbi.nlm.nih.gov/tools/primer-blast/, and purchased from Integrated DNA Technologies (Leuven, Belgium). Each PCR reaction (10 μL) contained 50 ng of gDNA, 0.25 μM of each primer, and 1 × MyTaq™ HS mix (Bioline, London, UK). PCRs were carried out in a MyCycler™ thermal cycler with the following profile: 2 min at 95ºC for initial denaturation, followed by 10 cycles of 30 s at 95ºC for denaturation, 30 s at 68ºC (-1ºC per cycle) for annealing, and 30 s at 72ºC for extension, and 30 cycles at 30 s at 95ºC for denaturation, 30 s at 58ºC for annealing and 30 s at 72ºC for extension, and 1 min at 72ºC for the final extension. All PCRs included a negative control (no template) and a positive control (wild-type U87 gDNA). The PCR products (amplicons) were resolved through 1.0% (w/v) agarose gels, and their sizes estimated by comparison with the DNA molecular-weight size marker.

Table 6. Oligonucleotide primers used in this study for PCR amplification.

Oligonucleotide name	Position within the gene (bp)[a]	Strand	Sequence (5' → 3')
LRP1B-01-Fw	6574	Plus	GCTGACTGGCTGGACTCATT
LRP1B-01-Rv	6869	Minus	TTATCTGCAAGCATCGCCCA
LRP1B-01-In	6774	Minus	ACCCTGGCAATCGGCAATAA
LRP1B-85-Fw	1 862 483	Plus	AGGTGTGAAGGAGGCAACAA
LRP1B-85-Rv	1 862 145	Minus	GCAATGGGCACAATACGGAA
LRP1B-85-In	1 862 966	Minus	ACCTTACACACTTGTCAACCTCA

[a] Human *LRP1B* RefSegGene; NCBI reference sequence: NG_051023.1; O'Leary *et al.* (2016).

3.10 Sanger Sequencing

CRISPR/Cas9-mediated genomic deletions of each potential knockout clone were further characterized by Sanger sequencing. All reagents were purchased from Thermo Fisher Scientific (Waltham, MA, USA) except otherwise specified. PCR amplicons (7.5 μL) were subjected to a post-reaction clean-up with 10 U of exonuclease I and 1 U of FastAP™ thermosensitive alkaline phosphatase for 30 min at 37ºC. After enzymes inactivation (85ºC for 15 min), cycle sequencing reactions were performed using the

BigDye™ Terminator v3.1 Cycle Sequencing Kit. Each reaction contained 0.50 μL of purified PCR amplicon, 0.25 μL of the selected PCR primer (10 μM), 0.25 μL of BigDye™ terminator, 3.50 μL of sequencing buffer (5 ×) and 3.50 μL of nuclease-free distilled water. Sequencing reactions were carried out in a MyCycler™ thermal cycler using the following conditions: 2 min at 95º for initial denaturation, followed by 35 cycles of 15 s at 95ºC for denaturation, 15 s at 55ºC for annealing, and 2 min at 60ºC for extension, and 10 min at 60ºC for the final extension. After the purification of the sequencing reactions by gel filtration through Sephadex™ G-50 fine (GE Healthcare, Chicago, IL, USA) spin columns (1,100 *g*, 4 min, RT), these were mixed with 15 μL of Hi-Di™ formamide and subjected to capillary electrophoresis on a 3130/3130*xl* Genetic Analyzer (Thermo Fisher Scientific, Waltham, MA, USA) at the Genomics Core (GenCore) Facility (i3S, Oporto, Portugal).

3.11 Reverse Transcription Quantitative Real-Time PCR (RT-qPCR)

LRP1B gene expression was evaluated by RT-qPCR. Prior to cDNA synthesis, 1 μg of total RNA from each sample was treated with 1 U of DNase I in the presence of the 1 × reaction buffer (with $MgCl_2$) for 30 min at 37ºC. ETDA was then added to a final concentration of 5 mM before heating at 65ºC for 10 min. cDNA was then reverse transcribed from 1 μg of DNase-treated RNA using 100 μM of random hexamer primer, 5 × reaction buffer, 20 U of RiboLock™ RNase inhibitor, 20 mM of dNTP Mix, and 200 U of RevertAid™ reverse transcriptase in a 20 μL reaction volume. Reverse transcription reactions were carried out in a MyCycler™ thermal cycler using the following conditions: 10 min at 25ºC for primer annealing, 60 min at 42ºC for DNA polymerization, and 10 min at 70ºC for enzyme deactivation. A no-template control (NTC) and minus reverse transcriptase control (MRTC) were included in all RT-qPCR experiments. The RT-qPCRs were performed on MicroAmp™ optical 96-well reaction plates covered with MicroAmp™ optical adhesive films. Each reaction contained 1.0 μL of cDNA template, 0.5 μL of PrimeTime™ qPCR probe assay (20 ×; **Table 7**), 5.0 μL of TaqMan™ universal PCR master mix no AmpErase™ UNG (5 ×), and 3.50 μL of nuclease-free distilled water. All the above-mentioned reagents were purchased from Thermo Fisher Scientific (Waltham, MA, USA). RT-qPCRs were carried out in a QuantStudio™ 5 Real-Time PCR System (Thermo Fisher Scientific, Waltham, MA, USA) using the following thermocycling parameters: 10 min at 95ºC for polymerase activation followed by 40 cycles of 15 s at 95ºC for denaturation and 1 min at 60ºC for annealing and extension. All samples were amplified

in triplicate, and each RT-qPCR experiment was repeated three times. The human *TBP* (TATA-box binding protein) was used as an endogenous control to normalize gene expression. *LRP1B* mRNA expression levels were determined in U87 parental (wild-type), U87 mock (empty vector), and potential *LRP1B*-knockout cell lines and analyzed using the following formula: $2^{-\Delta CT}$ [CT strands for cycle threshold; ΔCT = CT(LRP1B) – CT(TBP)].

Table 7. Gene expression assays used in this study for qPCR.

Gene expression assay name[a]	Target gene	Target region
Hs.PT.58.21358572	*LRP1B*	Exon 1-2
Hs.PT.58.19387941	*LRP1B*	Exon 3-4
Hs.PT.58.14536045	*LRP1B*	Exon 85-86
Hs.PT.39a.22214825	*TBP*	Exon 5-6

[a] Purchased from Integrated DNA Technologies (Leuven, Belgium)

3.12 Protein Extraction

Cells were collected by centrifugation at 1,500 *g* for 5 min at 4ºC, rinsed twice in ice-cold sterile PBS (1 ×, pH 7.4), and stored at -20ºC. Cell pellets were lysed for in 30 μL of ice-cold radioimmunoprecipitation assay (RIPA) buffer [50 mM Tris-HCl, 1.0% (v/v) NP-40, 150 mM NaCl, 2 mM EDTA; pH 7.5] supplemented with 1 × cOmplete™ protease inhibitor cocktail (Roche, Basel, Switzerland) and 1 × phosphate inhibitor cocktail 3 (Sigma-Aldrich, St. Louis, MO, USA) for 45 min on ice with occasional vortexing. Cell debris were centrifugated at 14,000 *g* for 15 min at 4ºC, and the protein cell lysates (supernatants) were quantified (as described on **Page 29**, **3.13**) and stored until use at -20ºC.

3.13 Protein Quantification

Protein quantification was performed using the DC™ protein assay (Bio-Rad Laboratories, Hercules, CA, USA). Seven protein standards (Bovine Serum Albumin, BSA: 0.25, 0.50, 0.75, 1.00, 1.25, 1.50, 3.00 mg/mL) were used to generate a standard curve. The absorbances were measured at 650 nm using a Synergy™ Mx microplate reader (BioTek Instruments, Winooski, VT, USA). For each protein assay, a standard curve was created by plotting normalized absorbance (Y-axis) versus BSA concentration (X-axis); being the normalized absorbance of each standard calculated by subtracting the background absorbance (the average value of the blanks). The resulting regression equation

was used to determine the concentration of the unknown proteins based on their absorbance. A coefficient of determination (r^2) greater than 0.97 (5% error) was used as the acceptability threshold.

3.14 Western Blot

LRP1B protein expression was assessed by western blot. Prior to gel loading, the protein samples were prepared by adding NuPAGE™ LDS sample buffer (4 ×) and NuPAGE™ reducing agent (10 ×) to a final concentration of 1 ×, and then heated at 70ºC for 10 min. The heated protein samples (50 μg per lane) were separated by denaturing gel electrophoresis on NuPAGE™ 3-8% tris-acetate protein gels for 1 h at 150 V. The electrophoresed proteins were electrotransferred to Amersham™ Hybond™ PVDF membranes (pore size, 0.45 μm; GE Healthcare, Chicago, IL, USA), previously soaked in 100% (v/v) methanol and equilibrated in the transfer buffer [20% (v/v) methanol, 0.1% (v/v) NuPAGE™ antioxidant], for 1 h at 100 V. The HiMark™ pre-stained protein standard was used to monitor protein separation and transfer, and estimate the molecular weight of sample proteins. After transfer, PVDF membranes were reversibly stained with Ponceau S staining solution to evaluate transfer efficiency and loading uniformity. Then, the unoccupied protein-binding sites on the membranes were blocked with 5% (w/v) non-fat dried-milk in TBS-T [1 × Tris-Buffered Saline (TBS) with 0.1% (v/v) Tween™ 20 detergent] for at least 1 h at RT or overnight (ON) at 4ºC. Membranes were incubated with primary antibodies in blocking buffer and rinsed with TBS-T three times for 10 min each. Detailed information about the primary antibodies and their usage is represented in **Table 8**. Membranes were further incubated for 1h at RT with appropriate horseradish peroxidase (HRP)-labeled secondary antibodies in blocking buffer [Amersham™ ECL™ anti-mouse IgG, HRP-linked species-specific whole antibody from sheep (1:3000) or Amersham™ ECL™ anti-rabbit IgG, HRP-linked species-specific whole antibody from donkey (1:3000); both from GE Healthcare, Chicago, IL, USA]. Membranes were rinsed with TBS-T as aforementioned and, posteriorly, incubated with Western Lightning™ chemiluminescence reagent plus (PerkinElmer, Waltham, MA, USA) for 1 min. Finally, the membranes were exposed to Amersham™ Hyperfilm™ ECL films (GE Healthcare, Chicago, IL, USA) for the optimum exposure time. After exposure, the membranes were rinsed with TBS-T, as mentioned earlier, and incubated for 30 min in stripping buffer [25 mM glycine pH 2.5, 1% (w/v) SDS]. Membranes were rinsed again in TBS-T (6 times; 5 min each) and reused (starting at the blocking step). Unless otherwise stated, all reagents were purchased from Thermo Fisher Scientific (Waltham, MA, USA). The cytoskeleton protein alpha-tubulin was served as the loading control.

Table 8. Primary antibodies used for western blot analysis.

Product name (commercialized by)	Immunogen	Biological source	Dilution ratio	Incubation conditions
LRP1B Polyclonal Antibody (Thermo Fisher Scientific, Waltham, MA, USA)	Synthetic peptide corresponding to amino acids 4526 to 4589 of human LRP1B	Rabbit	1:1000	ON at 4ºC
Anti-LRP1B (Sigma-Aldrich, St. Louis, MO, USA)	Synthetic peptide corresponding to a sequence near the C-terminus of human LRP1B	Rabbit	1:1000	ON at 4ºC
LRP1B polyclonal antibody (Abnova, Taipei, Taiwan)	Synthetic peptide corresponding to amino acids 111 to 200 of human LRP1B	Mouse	1:1000	ON at 4ºC
Monoclonal Anti-Alpha-Tubulin (Sigma-Aldrich, St. Louis, MO, USA)	Sarkosyl-resistant filaments from sea urchin sperm axonemes	Mouse	1:8000	1 h at RT

4 Results and Discussion

4.1 CRISPR/Cas9-Mediated Knockout Strategy Targeting the *LRP1B* Locus

4.1.1 Target Site Selection

According to the literature, to generate the complete and permanent loss of gene expression or function (knockout), the target region should be chosen within the most upstream exon that is common to all the predicted transcripts of that gene (Campenhout *et al.*, 2019, Spiegel *et al.*, 2019). Taking this into consideration, this study was initiated by conducting a comparative analysis of the putative alternatively spliced protein-coding transcripts of the human *LRP1B* using EMBL-EBI's Ensembl/GENCODE database (Frankish *et al.*, 2018). Briefly, the human *LRP1B* is located on the long arm of chromosome 2 at the position 2q22.1-2q22.2 (**Figure 10**, **A**). It spans from 140,231,423 to 142,131,016 bp, according to the human genome assembly GRCh38.p13 from the Genome Reference Consortium (Schneider *et al.*, 2017); being approximately 1.90 megabase pairs (Mbp) long and composed of 91 exons that comprise 13.80 kilobase pairs (kbp) of coding sequence (CDS). The exon-intron structure of *LRP1B* is depicted in **Figure 10**, **B**. The human *LRP1B* (ID: ENSG00000168702) has four putative protein-coding transcripts [**Figure 10**, **C**; Frankish *et al.* (2018)]: (i) full-length *LRP1B* transcript (hereafter referred to as *LRP1B* transcript 1; ID: ENST00000389484.8), which includes all 91 annotated exons that together encode a 4599-amino acid membrane-bound protein (LRP1B) and, (ii) three other predicted alternatively spliced *LRP1B* transcripts (*LRP1B* transcripts 2, 3, and 4) that have their CDS incomplete on the 3' end, 5' end, or both ends. Specifically, *LRP1B* transcript 2 contains 14 exons (1,2, 18-29; ID: ENST00000434794.1), which encode a putative 781-amino acid soluble LRP1B isoform. *LRP1B* transcripts 3 and 4 encode two putative membrane-bound LRP1B isoforms of 789 and 280 amino acids, respectively. *LRP1B* transcript 3 contains 17 exons (74-89, 91; ID: ENST0000043-7977.5), whereas *LRP1B* transcript 4 contains 7 exons (84-89, including an extra 114 bp exon between exons 86 and 87; ID: ENST00000442974.1).

As outlined above, four protein-coding transcripts have been bioinformatically-predicted for the human *LRP1B* (Frankish *et al.*, 2018). However, there is not a single exon that is conserved across all its protein-coding transcripts. Considering this, we decided to target simultaneously two distinct exons, 1 and 85, which constitute the most upstream exons shared by most of the *LRP1B* predicted transcripts (signaled with red

flags, **Figure 10**, **C**). For this, we decided to use a paired sgRNA CRISPR/Cas9 deletion strategy to maximize the likelihood of knocking out *LRP1B*. This strategy uses a sgRNA pair to direct the Cas9 activity to the sites flanking the target region and simultaneously induce two DSBs, which are frequently repaired through the NHEJ pathway (**Figure 10**, **D**). In fact, this strategy has been used successfully for knocking out protein-coding genes (Chen *et al.*, 2014, Zheng *et al.*, 2014, Brandl *et al.*, 2015, Treuren & Vishwanatha, 2018, Grotz *et al.*, 2019), small non-coding RNA (sncRNA) genes (Ho *et al.*, 2015, Hannafon *et al.*, 2019), long non-coding RNA (lncRNA) genes (Chen *et al.*, 2014, Han *et al.*, 2014, Aparicio-Prat *et al.*, 2015, Zare *et al.*, 2018) and enhancers (Li *et al.*, 2014).

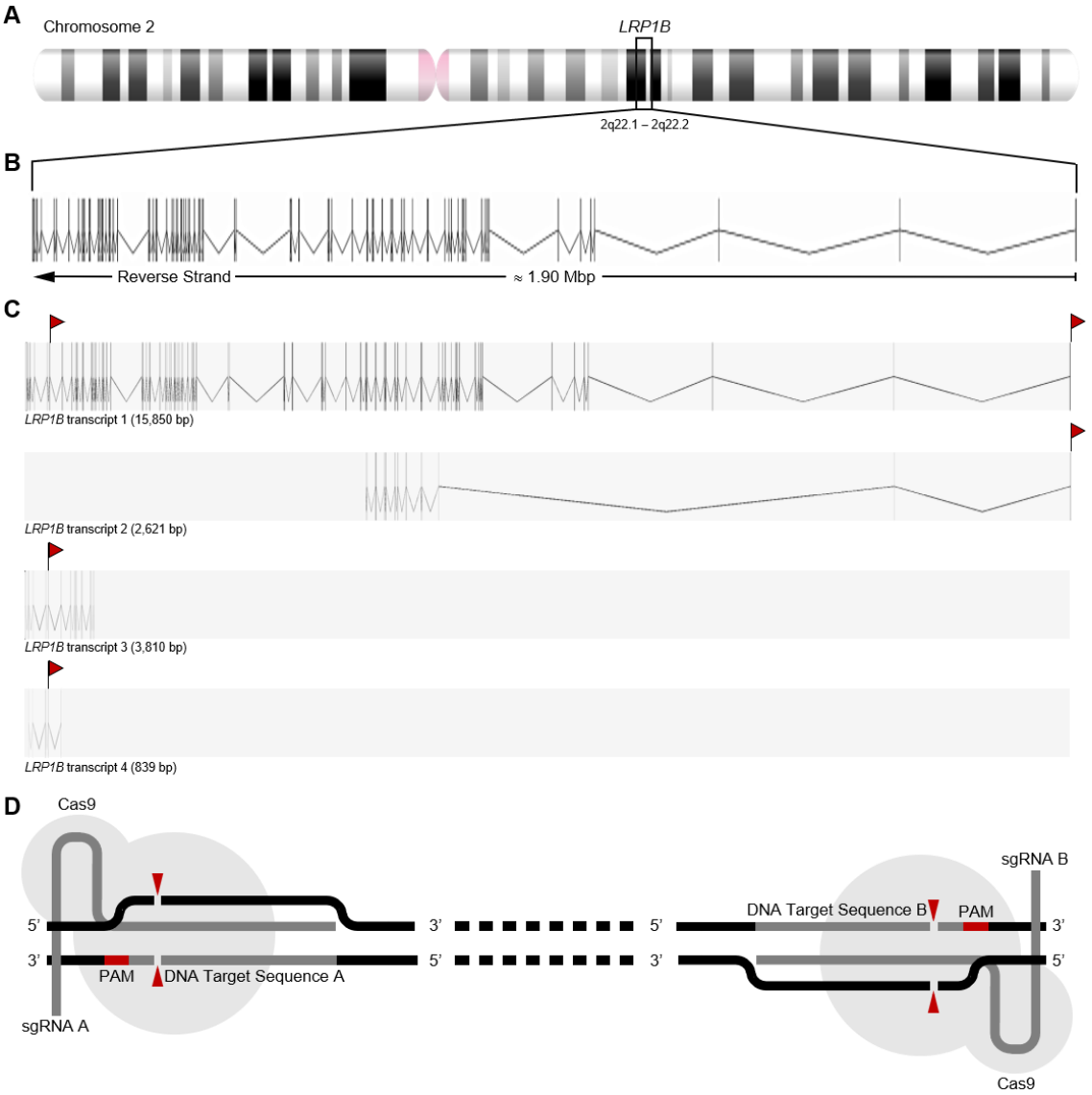

Figure 10. **Paired sgRNA CRISPR/Cas9 deletion strategy for the ablation of human *LRP1B* gene**. **A**, Chromosomal location of the *LRP1B* locus. The chromosome ideogram was obtained from the NCBI online tool, Genome Decoration Page. **B**, Schematic representation of *LRP1B* gene structure. **C**, Comparison between the structure of the full-length LRP1B transcript and the predicted alternatively spliced LRP1B transcripts. The gene and transcripts schemes were obtained from Ensembl release 100. The most upstream exons shared by the majority of the LRP1B predicted transcripts are signaled with red flags. **D**, Schematic representation of the paired sgRNA CRISPR/Cas9 deletion strategy. The Cas9 nuclease (gray) complexed with a sgRNA (dark gray) recognizes and binds to the PAM sequence (red). PAM binding enables local DNA strand separation and subsequent base pairing between the sgRNA target sequence and its complementary DNA strand. Successful base-pairing induces Cas9 activation and leads to a DBS. The red arrowheads indicate

the predicted Cas9 cleavage sites [3 bp upstream (5') of the PAM sequence] within the target DNA. Simultaneous cleavage of both target sites, followed by NHEJ repair, often results in the deletion of the intervening DNA through the re-ligation of the Cas9-induced distal blunt ends.

4.1.2 sgRNA Selection

To select the optimal sgRNA pair for each *LRP1B* target exon (1 and 85), the CRISPR Guide RNA design software (available online at https://www.benchling.com/crispr/) was used. First, the sequence of each target exon was screened for all possible 20-nt sequences that immediately precede a canonical *S. pyogenes* Cas9 (SpCas9) PAM sequence [5'-NGG-3'; which occurs on average every 8-12 bp within the human genome (Cong *et al.*, 2013, Hsu *et al.*, 2013a)]. The potential sgRNA target sequences retrieved of each target exon were ranked according to their predicted off-target score [from the highest to the lowest; Hsu *et al.* (2013b)], which represents the overall on-target specificity of each potential sgRNA in the reference genome. Then, sgRNA pairs (one for each target exon) were manually selected according to the following criteria: (i) to minimize the Cas9 off-target cleavage activity (and potential related off-target effects) to provide reliable genotype-phenotype correlations, and (ii) to generate disrupting deletions easily detectable by conventional PCR. Since SpCas9 creates blunt-ended DSBs 3 bp upstream (5') of the PAM sequences (Jinek *et al.*, 2012), and the NHEJ pathway often leads to the accurate repair of two, close and concurrent, Cas9-induced DSBs [direct ligation of the distal ends of the two DBSs; Geisinger *et al.* (2016), Guo *et al.* (2018)], it is possible to predict deletions accurately. The sgRNA target sequences chosen for the present study, as well as their respective off- and on-target scores, are shown in **Table 9**. sgRNA1 and sgRNA2 were selected to target *LRP1B* exon 1, whereas sgRNA3 and sgRNA4 were chosen to target *LRP1B* exon 85, as depicted in **Figure 11**.

Table 9. Off- and on-target scores for the sgRNA target sequences used in this study.

Target exon	sgRNA ID	sgRNA target sequence (5' → 3')	PAM	Off-target score[a]	On-target score[b]
Exon 1	sgRNA1	GACATTGTGGTCGCCCGGTA	AGG	96.6	51.9
	sgRNA2	CGTGGGAGCCGACCGAGGTA	AGG	90.2	50.3
Exon 85	sgRNA3	TTTGGTCCTTCATAGCGCGT	TGG	94.8	32.1
	sgRNA4	TTATAATGCAGTGCCCCCCA	TGG	80.5	44.2

[a] Hsu *et al.* (2013b); [b] Doench *et al.* (2016). Off- and on-target scores range from 0 to 100, with higher scores indicating lower off-target potential and higher predicted Cas9 activity at the target site, respectively.

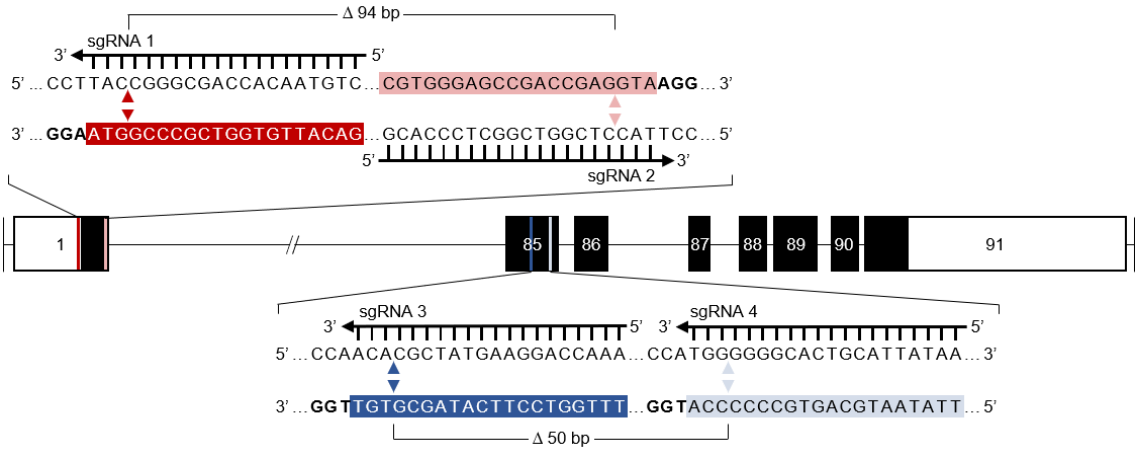

Figure 11. **Schematic representation of the four sgRNAs targeting the human *LRP1B* gene**. Boxes on the horizontal connecting black line (introns) represent exons. Filled black boxes (or portion of boxes) represent coding-sequence, and the unfilled (white) portions of boxes represent non-coding sequence (i.e., untranslated region). Exons and introns are not drawn at a precise scale. The CRISPR/Cas9 target sites are shown as colorful bars. The sgRNA target sequences (highlighted in color) and their respective PAM sequences (bold) are also represented. The predicted CRISPR/Cas9-mediated deletions (Δ) are also indicated.

4.2 sgRNA/Cas9 Expression Vector Generation

To use the CRISPR/Cas9 system for genome editing, both Cas9 and target-specific sgRNA(s) must be delivered to the target cells. In this study, the pSpCas9(BB)-2A-Puro (PX459) V2.0 vector (Ran *et al.*, 2013) was chosen for the delivery and expression of the CRISPR/Cas9 machinery in cells. To assemble (clone) the chosen sgRNA target sequences into the PX459 vector and improve their expression, the appropriate sgRNA-encoding oligonucleotides and their reverse complements were designed. Since this vector uses the human U6 promoter to drive sgRNA expression and this promoter prefers a guanine at the transcription start site (+1) (Guschin *et al.*, 2010), an extra guanine was added to the 5' ends of the sgRNA target sequences 2, 3, and 4 (which do not start with one). An additional cytosine was also added to the 3' ends of the reverse-complement sgRNA target sequences 2, 3, and 4. Moreover, the overhang sequences 5'–CACC–3' and 5'–AAAC–3' were added to the 5' ends of the sgRNA target sequences and the reverse-complement sgRNA target sequences, respectively, for cloning into the BbsI-digested PX459 vector. The presence of two, asymmetrically arranged, non-palindromic BbsI recognition sites (in the cloning site of the PX459 vector) not only allows directional cloning but also prevents self-ligation of the empty vector and tandem ligation of multiple oligonucleotide duplexes. The designed single-stranded DNA (ssDNA) oligonucleotides were synthesized and commercially obtained from Integrated DNA Technologies. Following the annealing of the ssDNA oligonucleotide pairs, these were independently cloned into the PX459 vector (**Figure 12**, **A**). All sgRNA/Cas9 expression vectors (named PX459-sgRNA1, PX459-sgRNA2, PX459-sgRNA3, and PX459-sgRNA4) were

transformed into competent DH5α *E. coli* cells, which were plated onto LB-ampicillin agar plates for overnight growth. To check for the correct insertion of the sgRNA-encoding oligonucleotide duplexes, two ampicillin-resistant colonies of each plate (from each transformation) were picked for plasmid DNA isolation (**Figure 12**, **B**) and Sanger sequencing validation. As expected, all colonies tested (8 out of 8) contained correctly assembled sgRNA/Cas9 expression vectors (**Figure 12**, **C**).

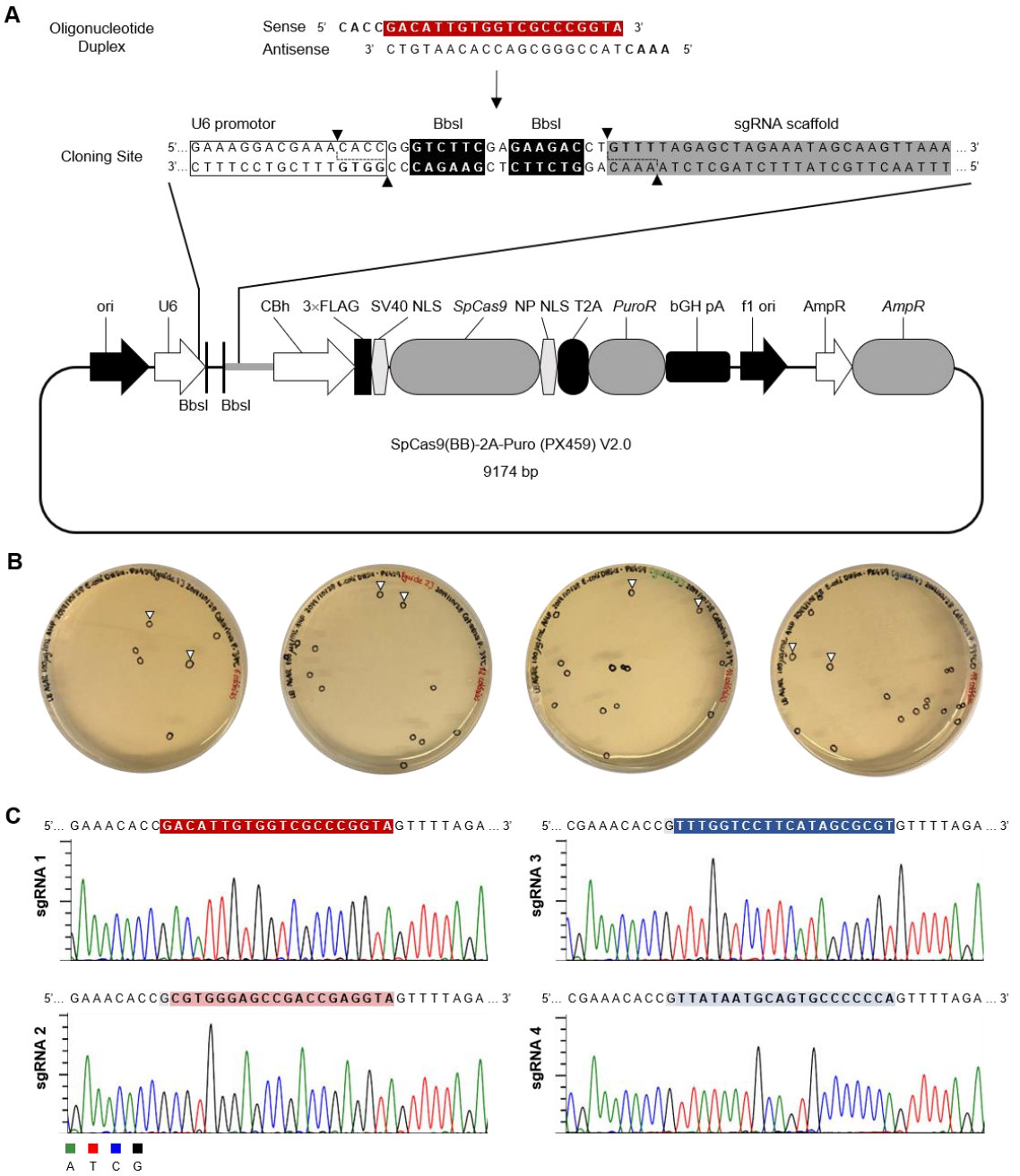

Figure 12. **Generation of sgRNA/Cas9 expression vectors**. **A**, Schematic representation for the scarless cloning of the sgRNA-encoding oligonucleotide duplexes into the pSpCas9(BB)-2A-Puro (PX459) V2.0 vector. The sgRNA-encoding oligonucleotide duplex contains BbsI-compatible to vector overhangs (bold). The sense oligonucleotide encodes the sgRNA target sequence (highlighted in red). Digestion of PX459 with BbsI allows direct insertion of the oligonucleotide duplex. The partial DNA sequence was retrieved from https://www.addgene.org/62988/sequences/. The genetic elements of the PX459 vector are shown in the correct order but are not at a precise scale. **B**, *E. coli* colonies from each transformation plate. The colonies picked for plasmid DNA isolation and Sanger sequencing validation are pointed out by white arrowheads. **C**, Representative DNA-sequencing electropherograms of the four sgRNA/Cas9 expression vectors containing correctly cloned sgRNA target sequences (highlighted in colors).

4.3 Transfection and Clonal Selection

The established sgRNA/Cas9 vectors were then used to transfect the U87 human glioblastoma cell line. This was chosen for the establishment of a CRISPR/Cas9-induced *LRP1B*-knockout *in vitro* model since it is described as being among the few cancer cell lines reported to express *LRP1B* (Uhlen *et al.*, 2017). Specifically, parental U87 cells were transfected with (i) the empty vector PX459 (no sgRNA), (ii) PX459-sgRNA1 and PX459-sgRNA2 (designed to target *LRP1B* exon 1), (iii) PX459-sgRNA3 and PX459-sgRNA4 (designed to target *LRP1B* exon 85), and (iv) all four sgRNA/Cas9 expression vectors (targeting both exons). Transfections were performed using the cationic lipid-based Lipofectamine™ 3000 transfection reagent and a total amount of plasmid DNA of 500 ng (manufacturer's recommended DNA amount per well of a 24-well plate). For cells transfected with all sgRNA/Cas9 expression vectors, a higher amount of DNA (1000 ng) was also used.

After transfection, cells were selected with 1 μg/mL puromycin for 72 h: a concentration that killed non-transfected cells (non-resistant) while selecting those expressing the puromycin resistance gene (transfected cells). As expected, 72-h puromycin treatment resulted in the death of all non-transfected control cells. On the other hand, in wells with cells transfected with either the empty vector or the PX459-sgRNA1 and PX459-sgRNA2 (experimental group 1) or PX459-sgRNA3 and PX459-sgRNA4 (experimental group 2), although the levels of cell death were high, some viable cells were still observed (about 20% compared to untreated control cells). Interestingly, in wells with cells transfected with all four sgRNA/Cas9 expression vectors (experimental group 3A and 3B, with 500 and 1000 ng, respectively), cell death levels were even lower (about 50% of cells survived compared to untreated control cells). These results suggest that the transfection efficiency (indirectly observed through the estimated cell survival) was higher in cells transfected with all sgRNA/Cas9 expression vectors and independent of the total amount of transfected plasmid DNA.

After selection, cell pools (derived from each experimental group) were plated at a very low cell density (<1 cell per well in 96-well plate) for the isolation of potential *LRP1B*-knockout monoclonal cell lines. Only wells with one colony were considered monoclonal and expanded for characterization. Six single-cell clones were derived from experimental group 1, seven from experimental group 2, seven from experimental group 3A, and six from experimental group 3B. Interestingly, the clones showed profound differences in their phenotypes (**Figure 13**). The main differences were in their (i) cell morphology, between epithelial-like cells (unpolarized, polygonal shape; **Figure 13**, **A** and

F) and fibroblastic-like cells (polarized, elongated shape; **Figure 13**, **B**, **C**, **D**, **E**, **G**, **H** and **I**); (ii) cell distribution, between well-distributed cells (**Figure 13**, **A**, **C**, **E**, and **F**) and cells forming branch-like (**Figure 13**, **D**, **G**, and **I**) or sphere-like structures (**Figure 13**, **B** and **H**); (iii) cell organization, between cells monolayers (**Figure 13**, **A**, **E**, and **F**), and multi-layers (**Figure 13**, **C**, **D**, **G**, and **I**).

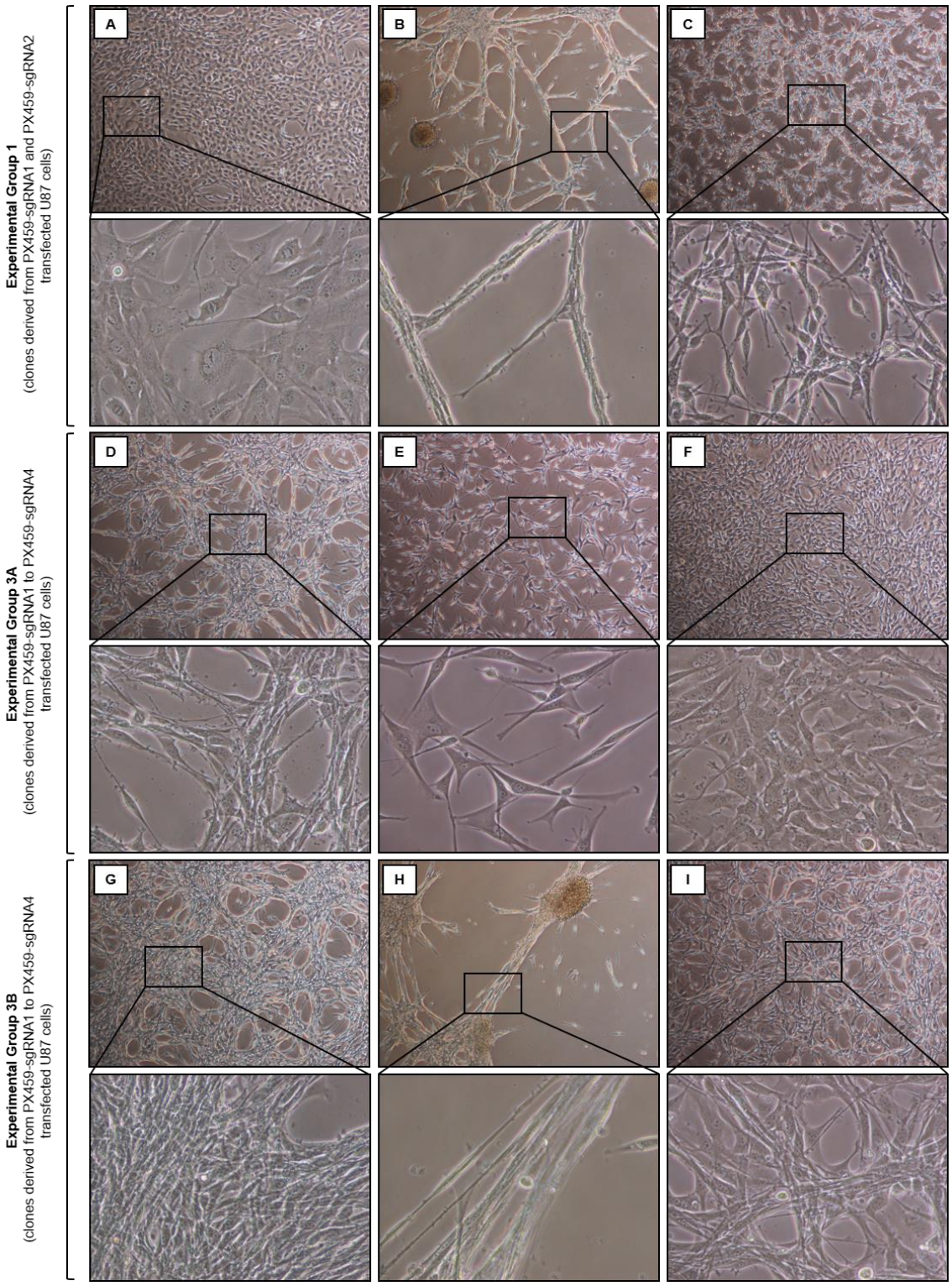

Figure 13. **Representative phase-contrast images of nine potential *LRP1B*-knockout clones**. Images were captured using 4× and 20× objectives (upper and lower panels, respectively) 3 days after seeding.

Regardless of the passage number, the clones maintained their phenotypic traits. Since several clones derived from different combinations of the sgRNA/Cas9 expression vectors transfected U87 cells were found to have similar phenotypes, we hypothesized that the phenotypic differences observed within the single-cell clones could represent the heterogeneity of the parental U87 human glioblastoma cell line (**Figure 14**). Actually, several studies have found that single cell-derived clones, established from the same parental cells (from different tissue origins), often exhibit distinct and heritable phenotypes (Solimene *et al.*, 2001, Wangsa *et al.*, 2018, Wu *et al.*, 2020).

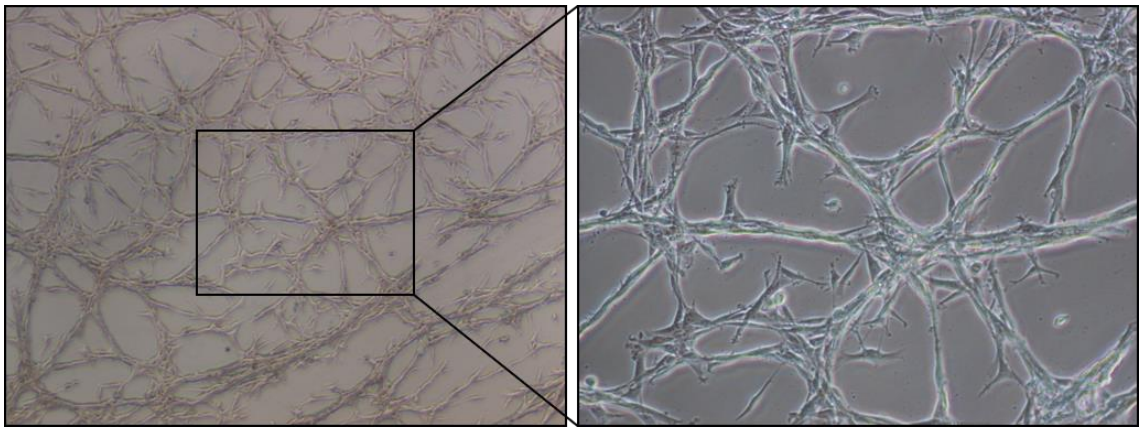

Figure 14. **Representative phase-contrast images of parental U87 human glioblastoma cell line**. Images were captured using 4× and 10× objectives (*left* and *right side*, respectively) 3 days after seeding.

However, the hypothesis that some of the phenotypic traits found in the clones could reflect the consequences of the CRISPR/Cas9-induced alterations was not ruled out. Interestingly, the epithelial-like morphology (**Figure 13**, **A** and **F**) and sphere-like structures (**Figure 13**, **B** and **H**) were exclusive of clones derived from PX459-sgRNA1 and PX459-sgRNA2 transfected U87 cells (experimental group 1) or PX459-sgRNA1, PX459-sgRNA2, PX459-sgRNA3, and PX459-sgRNA4 transfected U87 cells (experimental group 3A and 3B).

4.4 Screening Single Cell-Derived Clones for CRISPR/Cas9-Mediated Deletions and Clone Selection

To screen single cell-derived clones for CRISPR/Cas9-mediated deletions and evaluate their allelic status (as non-deleted, monoallelic-deleted, or biallelic-deleted alleles), genomic DNA was amplified by PCR using different primer sets. The first PCR was performed using two primers outside the predicted deleted region(s) of the target exon(s) (**Figure 15**; Fw and Rv) designed to amplify either non-deleted or deleted DNA fragments (**Figure 15**; *upper and lower panels*). The second PCR was performed using

one primer outside the predicted deleted region(s) of the target exon(s) and another one within the region(s) to be deleted (**Figure 15**; Fw and In). Only clones with at least one non-deleted allele (non-deletion or monoallelic deletion clones) should present DNA amplification (**Figure 15**; *upper panel*). Before genotyping PCR, all primer sets were tested against the genomic DNA from the parental U87 human glioblastoma cell line to assess non-specific primer binding. All of these produced a single amplicon of the expected size (data not shown).

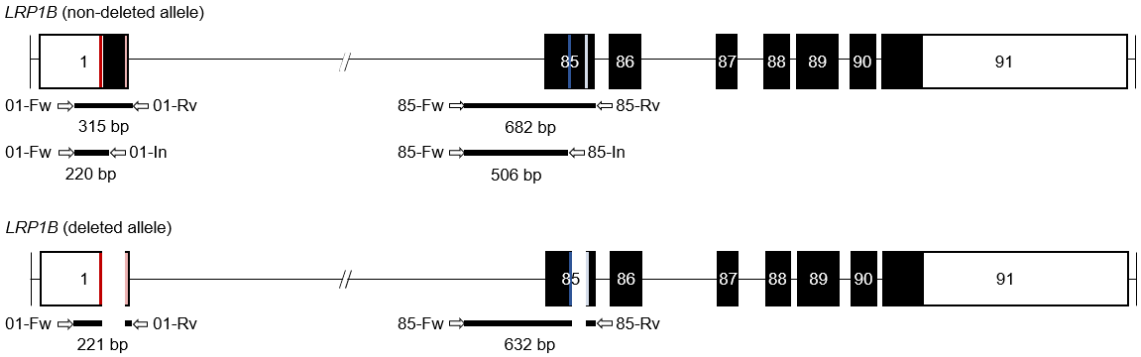

Figure 15. **Schematic representation of possible PCR amplicons according to *LRP1B* allelic status**. *Upper panel*, Schematic representation of *LRP1B* non-deleted allele. *Lower panel*, Schematic representation of *LRP1B* deleted allele. Boxes on the horizontal connecting black line (introns) represent exons (white: non-coding region; black: coding region). The CRISPR/Cas9 target sites are shown as colorful bars. Arrows indicate the positions and orientations of PCR primers. The expected sizes of the PCR amplicons for *LRP1B* non-deleted and deleted alleles are also indicated.

The results presented in the following sub-sections (**4.4.1** to **4.4.3**) are representative of two independent DNA extractions followed by separate PCR amplifications.

4.4.1 Analysis of Clones derived from PX459-sgRNA1 and PX459-sgRNA2 Transfected U87 Cells

The PCR genotyping analysis of the six clones derived from PX459-sgRNA1 and PX459-sgRNA2 (designed to target *LRP1B* exon 1) transfected U87 cells (experimental group 1) is depicted in **Figure 16**, **A**. Results from the first PCR (**Figure 16**, **A**, *upper panel*) showed that three clones (C11, D6, and F8) were monoallelic deletion clones exhibiting both non-deletion and deletion size amplicons (315 and 221 bp, respectively), and two clones (D8 and H6) were biallelic deletion clones showing only a single deletion size amplicon (221 bp). These results were further corroborated by the second PCR (**Figure 16**, **A**, *lower panel*), where only the monoallelic deletion clones showed amplification (220-bp size band). Interestingly, one clone (G1) yielded two unexpected PCR bands of a larger size than the band expected from non-deleted alleles (**Figure 16**, **A**, *upper and lower panels*). This may be due to the integration of random DNA fragments into the CRISPR/Cas9 target sites within *LRP1B* exon 1.

To characterize the CRISPR/Cas9-induced deletions of the biallelic deletion clones (as homozygous or heterozygous), the deletion amplicons from clones D8 and H6 were subjected to Sanger sequencing. In both clones, three sets of overlapping peaks, downstream the predicted deletion junction in *LRP1B* exon 1, were observed (**Figure 16**, **B**, highlighted with asterisks). These results suggest that these clones (D8 and H6) were actually derived from at least two biallelic-deleted cells [i.e., their origin is not monoclonal; Dehairs *et al.* (2016)]. Therefore, these clones were not further studied. However, this hurdle could be overcome by further subcloning these false-positive monoclones. Overall, these results demonstrate that the SpCas9, together with the pair sgRNA1 and sgRNA2, can efficiently excise the targeted region of *LRP1B* exon 1.

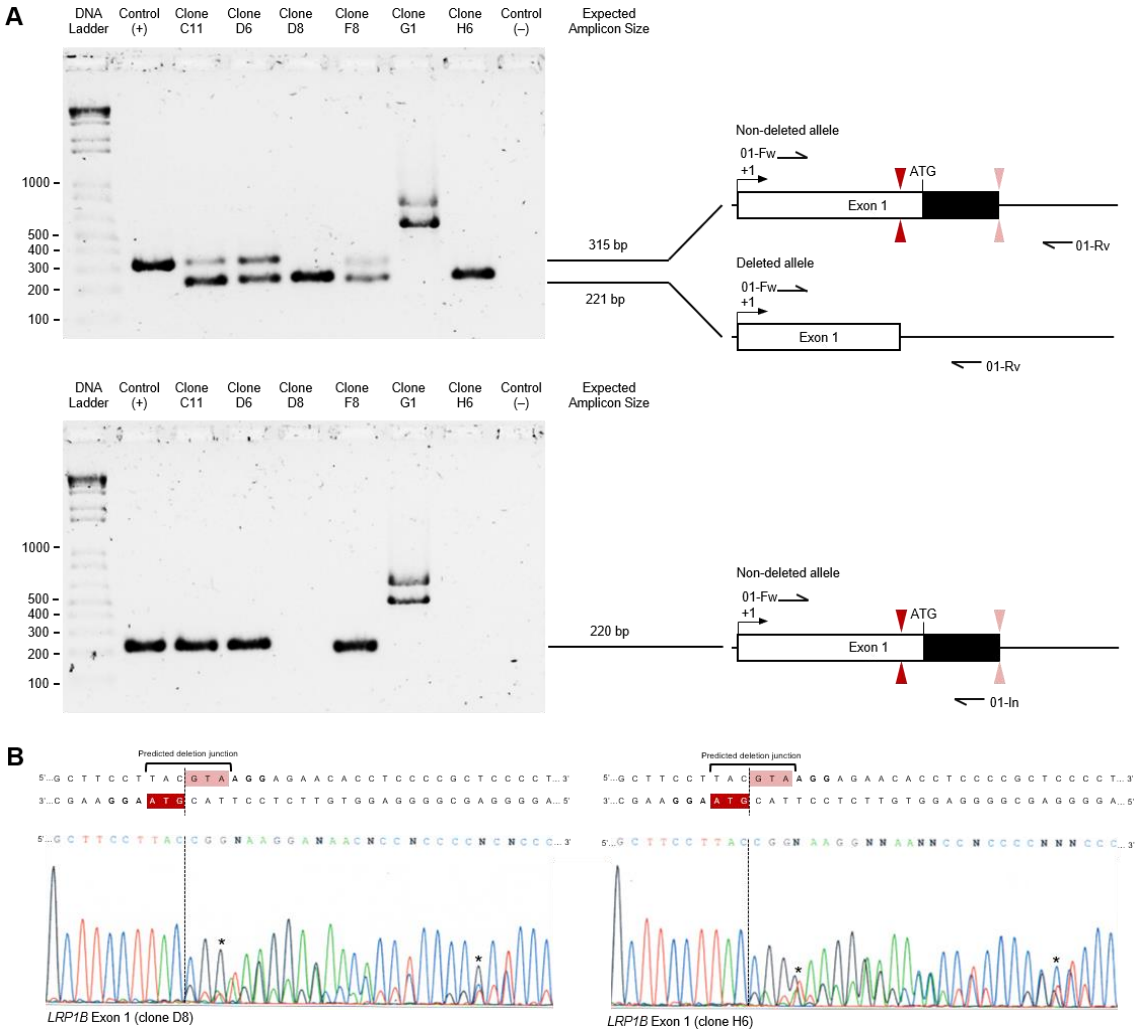

Figure 16. **Genotyping analysis of the clones derived from PX459-sgRNA1 and PX459-sgRNA2 transfected U87 cells**. **A**, *Upper panel*, the CRISPR/Cas9-targeted exon 1 was amplified from genomic DNA using the primers forward (01-Fw) and reverse (01-Rv). The expected sizes of the PCR amplicons for *LRP1B* non-deleted and deleted alleles are 315 bp and 221 bp, respectively. **A**, *Lower panel*, the CRISPR/Cas9-targeted exon 1 was amplified from genomic DNA using the primers forward (01-Fw) and reverse internal (01-In). The expected size of the PCR amplicon for the *LRP1B* non-deleted allele is 220 bp. Control (+), positive control using genomic DNA from the parental U87 human glioblastoma cell line and the appropriate primer set for each PCR; Control (-), negative control for each primer set (no DNA template); DNA Ladder, 1 kbp DNA ladder. Schematic representation of the *LRP1B* non-deleted and deleted alleles is depicted on the right side of the panels. Labeled black arrows indicate the positions and orientations of PCR primers. The arrowheads indicate the CRISPR/Cas9 target sites within *LRP1B* exon 1. **B**, Representative DNA-sequencing electropherograms are displaying the deletion junctions of the biallelic deletion clones. The nucleotide positions with three overlapping peaks are indicated with an asterisk (*).

4.4.2 Analysis of Clones Derived from PX459-sgRNA3 and PX459-sgRNA4 Transfected U87 Cells

The PCR genotyping analysis of the seven clones derived from PX459-sgRNA3 and PX459-sgRNA4 (designed to target *LRP1B* exon 85) transfected U87 cells (experimental group 2) is depicted in **Figure 17**. Results from the first PCR (**Figure 17**, *upper panel*) showed that all clones were non-deletion clones, exhibiting only a single non-deletion size amplicon (682 bp). These results were further validated by the second PCR (**Figure 17**, *lower panel*), where all clones showed amplification (506-bp size band). These results suggest that the SpCas9, together with the pair sgRNA3 and sgRNA4, cannot excise the targeted region of *LRP1B* exon 85 (at least efficiently). The absence of CRISPR/Cas9-mediated deletions might be explained by the individual low on-target score of the sgRNA3 (32.1 out of 100) and sgRNA4 (44.2 out of 100), which represents the efficiency of sgRNA binding and Cas9 cleavage at the target site (Doench *et al.*, 2016). However, these on-target scores were between the best on-target scores for all the possible sgRNA target sequences within *LRP1B* exon 85.

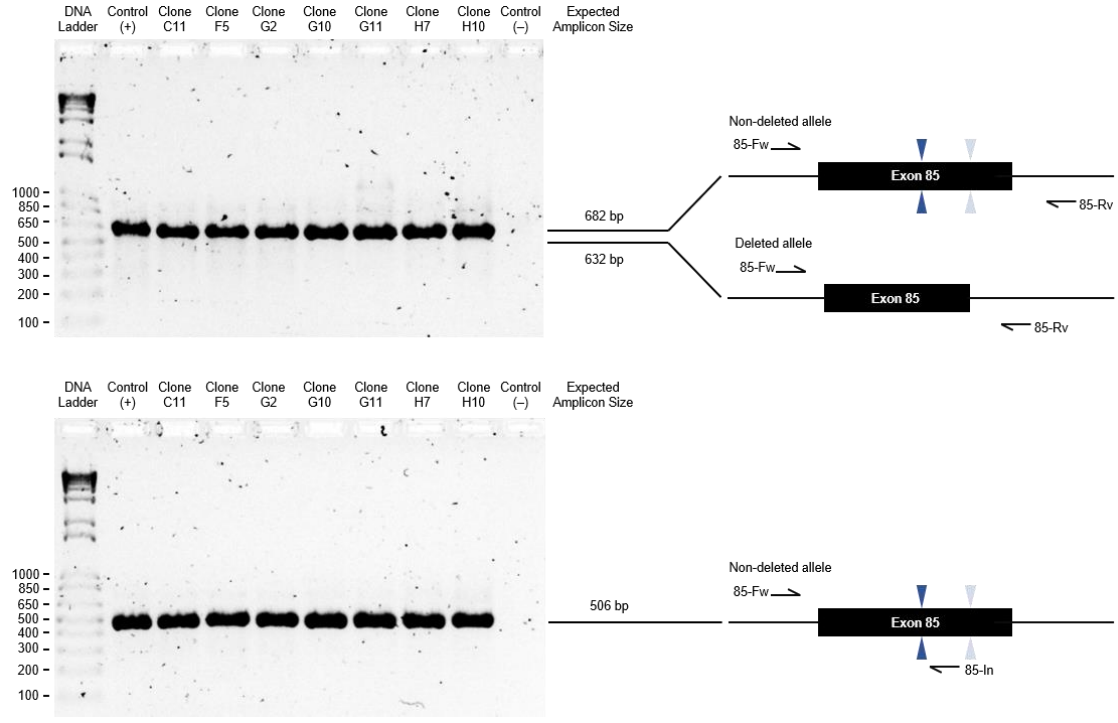

Figure 17. **Genotyping analysis of the clones derived from PX459-sgRNA3 and PX459-sgRNA4 transfected U87 cells**. *Upper panel*, the CRISPR/Cas9-targeted exon 85 was amplified from genomic DNA using the primers forward (01-Fw) and reverse (01-Rv). The expected sizes of the PCR amplicons for *LRP1B* non-deleted and deleted alleles are 682 bp and 632 bp, respectively. *Lower panel*, the CRISPR/Cas9-targeted exon 85 was amplified from genomic DNA using the primers forward (01-Fw) and reverse internal (01-In). The expected size of the PCR amplicon for the *LRP1B* non-deleted allele is 506 bp. Control (+), positive control using genomic DNA from the parental U87 human glioblastoma cell line and the appropriate primer set for each PCR; Control (-), negative control for each primer set (no DNA template); DNA Ladder, 1 kbp DNA ladder. Schematic representation of the *LRP1B* non-deleted and deleted alleles is depicted on the right side of the panels. Labeled black arrows indicate the positions and orientations of PCR primers. The arrowheads indicate the CRISPR/Cas9 target sites within *LRP1B* exon 85.

4.4.3 Analysis of Clones Derived from PX459-sgRNA1 to PX459-sgRNA4 Transfected U87 Cells

Regarding the genotyping analysis of the clones derived from PX459-sgRNA1, PX459-sgRNA2, PX459-sgRNA3, and PX459-sgRNA4 transfected U87 cells (experimental group 3A and 3B), the *LRP1B* target exons (1 and 85) were analyzed separately.

Regarding exon 1, the results from the first PCR (**Figure 18**, **A**, *left side*) showed that: one clone (E6) was a non-deletion clone exhibiting only a single non-deletion size amplicon (315 bp), one clone (C4) was monoallelic deletion clone showing both non-deletion and deletion size amplicons (315 and 221 bp, respectively) and nine clones (A5, B9, C2, C9, D4, D11, F5, G5, and H7) were biallelic deletion clones exhibiting only a single deletion size amplicon (221 bp). Besides the expected non-deletion and/or deletion size amplicons, two clones (H3 and H9) yielded other unexpected amplicons; therefore, these were excluded for further analysis. Intriguingly, among the nine clones (A5, B9, C2, C9, D4, D11, F5, G5, and H7), initially identified as biallelic deletion clones, only three clones (A5, B9, and H7) were confirmed as such due to the lack of amplification with the gene-specific primer set, 01-Fw and 01-In (**Figure 18**, **A**, *right side*). The other six clones (C2, C9, D4, D11, F5, and G5) presented amplicons of the same size as the expected amplicons for *LRP1B* non-deleted alleles (220 bp; **Figure *18***, **A**, *right side*). These results cannot be explained by sample cross-contamination or PCR reagents contamination (with exogenous DNA) since identical results were obtained from two independent DNA extractions followed by separate PCR amplifications, and the negative control lacked amplification. Moreover, the hypothesis that these clones could be, in fact, monoallelic deletions clones seemed rather unlikely since no non-deletion size amplicons (315 bp) were generated with the first set of primers (01-Fw and 01-Rv; **Figure 18**, **A**, *left side*). Since it was not possible to confirm the biallelic-deleted status of C2, C9, D4, D11, F5, and G5 by the PCR genotyping analysis, and there was no obvious explanation for these non-concordant PCR results, these were not further studied.

To characterize the CRISPR/Cas9-induced deletions of the biallelic deletion clones (as homozygous or heterozygous), the deletion amplicons of clones A5, B9, and H7 were subjected to Sanger sequencing. Clone A5 turned out to be a false-positive monoclone (i.e., its origin is not monoclonal), and therefore it was excluded from further analysis. Clones B9 and H7 were found as heterozygous for the deletion. The manual alignment of the sequences of each deleted allele with the wild-type sequence (from the parental U87 human glioblastoma cell line) revealed that (**Figure 18**, **B**): (i) clone B9

harbored one allele with a precise 94-bp deletion (mediated by accurate NHEJ) and another with a 1-bp insertion at the vicinity of the predicted deletion junction (93-bp deletion), and (ii) clone H7 harbored two alleles with distinct insertions close to predicted deletion junction (2-bp and 20-bp insertions that corresponds to 92-bp and 84-bp deletions, respectively). The insertions had homology to the sequence within the predicted CRISPR/Cas9-mediated deletion (**Figure 18**, **B**). Since only two biallelic deletion clones were examined, no conclusions can be drawn regarding whether this sgRNA pair can generate precise deletions (of defined length) mediated by accurate NHEJ repair of the Cas9-induced DSBs.

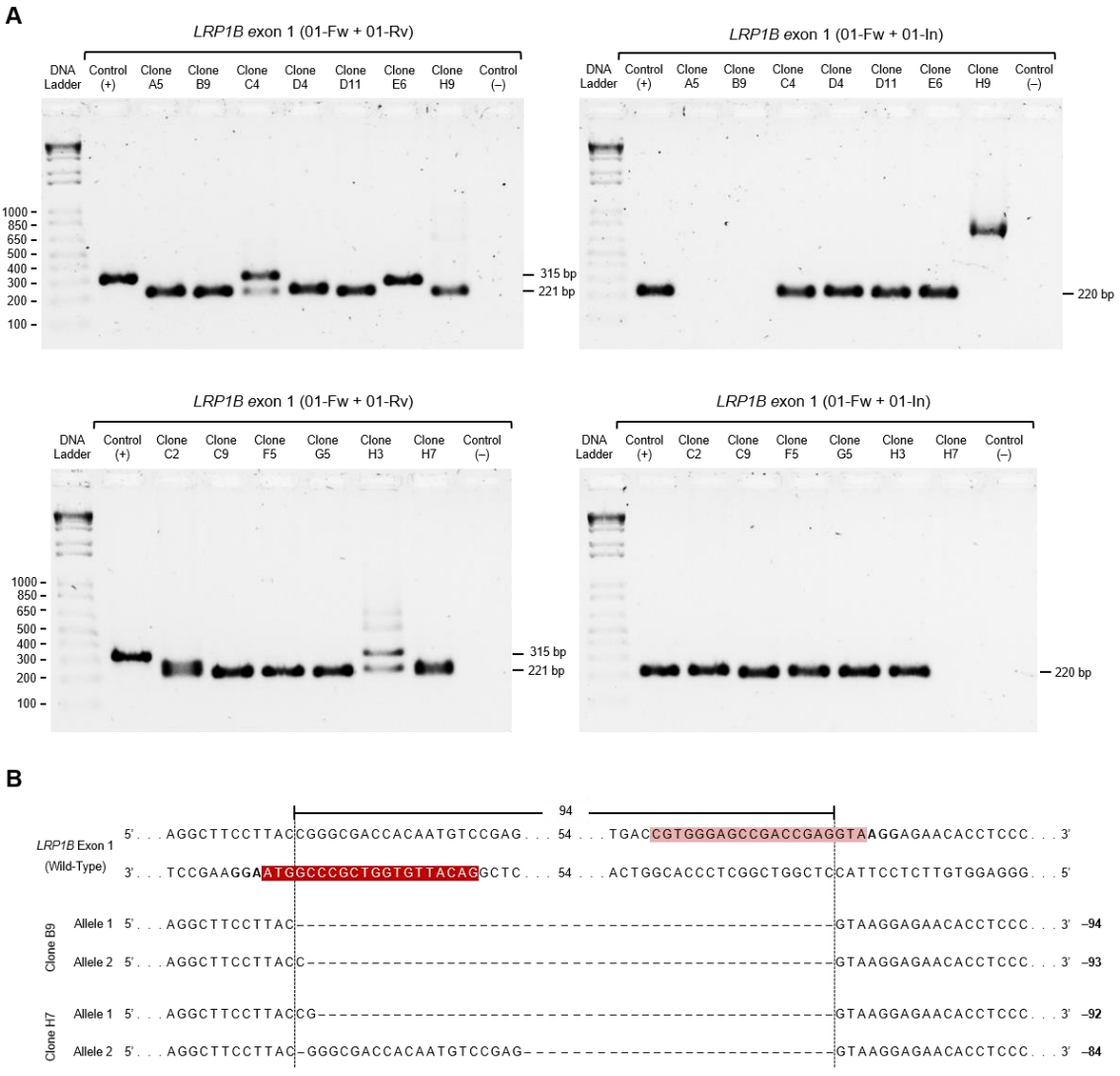

Figure 18. **Genotyping analysis of the clones derived from PX459-sgRNA1, PX459-sgRNA2, PX459-sgRNA3, and PX459-sgRNA4 transfected U87 cells**. **A**, *Left side*, the CRISPR/Cas9-targeted exon 1 was amplified from genomic DNA using the primers forward (01-Fw) and reverse (01-Rv). The expected sizes of the PCR amplicons for *LRP1B* non-deleted and deleted alleles are 315 bp and 221 bp, respectively. **A**, *Right side*, the CRISPR/Cas9-targeted exon 1 was amplified from genomic DNA using the primers forward (01-Fw) and reverse internal (01-In). The expected size of the PCR amplicon for the *LRP1B* non-deleted allele is 220 bp. Control (+), positive control using genomic DNA from the parental U87 human glioblastoma cell line and the appropriate primer set for each PCR; Control (-), negative control for each primer set (no DNA template); DNA Ladder, 1 kbp DNA ladder. **B**, Sequencing analysis of the deletion junctions of the biallelic deletion clones identified by PCR. The deleted amplicon sequences are aligned with the *LRP1B* wild-type sequence. The PAM (bold) and DNA target (highlighted in color) sequences within *LRP1B* exon 1 are depicted in the wild-type sequence. The number within the *LRP1B* wild-type alleles represents the number of nucleotides not shown. The

vertical dashed lines indicate the predicted Cas9 cleavage site, 3-nt upstream (5') of the PAM sequence (5'-NGG-3'). The deleted nucleotides are shown as dashes (–). The number of deleted nucleotides is displayed on the right side of the deleted amplicon sequences.

A recent study showed that the frequency of accurate NHEJ in the repair of two close and concurrent Cas9-induced DSBs (distances ranging from 23 to 148 bp) was high (Guo *et al.*, 2018). Interestingly, a former study showed that the distance between the CRISPR/Cas9 target sites negatively correlated with the frequency of the deletion and the accuracy of the NHEJ repair pathway [for distances greater than 1 kbp up to 1 Mbp; Canver *et al.* (2014)]. Hence, the NHEJ repair pathway can be exploited to improve CRISPR/Cas9-mediated genome editing that requires out-of-frame or in-frame precise deletions. Interestingly, Guo *et al.* (2018) indicated that the frequency of accurate NHEJ in repairing two (close and concurrent) Cas9-induced DSBs was hampered by frequent 1-bp and 2-bp insertions at the predicted deletion junctions. As a matter of fact, several studies have shown that Cas9 generates predominantly blunt DNA ends but occasionally DNA ends with 5' overhangs, particularly 1-nt and 2-nt 5' overhangs, that often result in template-dependent insertions [**Figure 19**; Jinek *et al.* (2012), Zuo and Liu (2016), Lemos *et al.* (2018), Taheri-Ghahfarokhi *et al.* (2018), Gisler *et al.* (2019)].

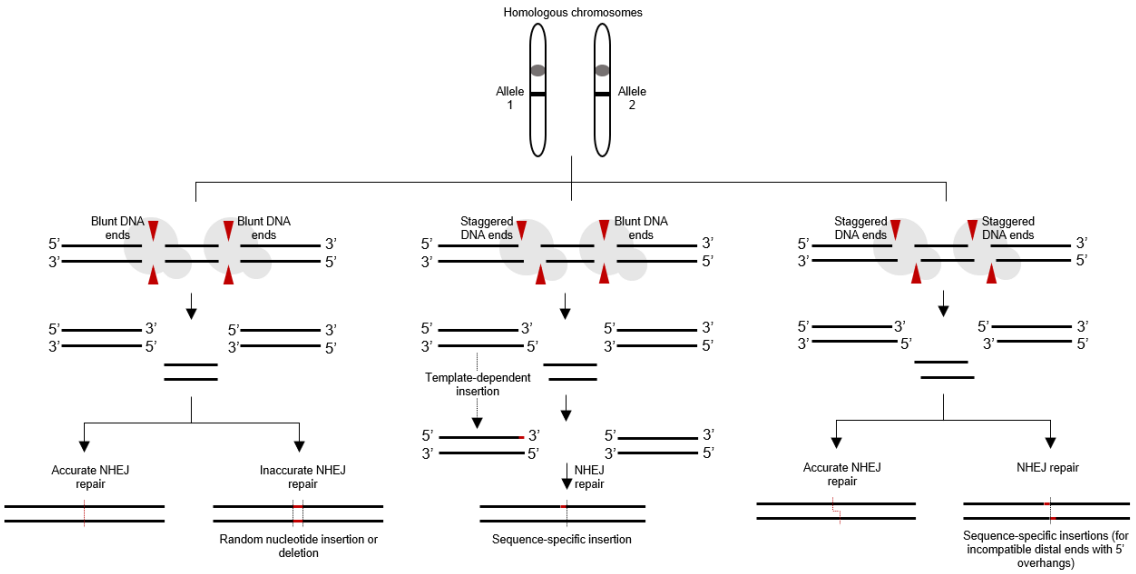

Figure 19. **Models depicting possible DNA repair outcomes after paired Cas9-induced DSBs**. Cas9 generates predominantly blunt DNA ends but occasionally staggered DNA ends (5' overhanging ends), particularly 1-nt and 2-nt 5' overhangs. In the repair of paired Cas9-induced DSBs, the distal blunt ends can be accurately rejoined (precise deletion) or result in random indels at the predicted deletion junction (through deletion by exonuclease activity prior to ligation or nucleotide insertion by a DNA polymerase). In the repair of paired Cas9-induced DSBs, the distal ends with 5' overhangs can be precisely re-ligated by the NHEJ repair pathway if the two 5' overhangs are compatible or may lead to templated insertions.

Although clones B9 and H7 were found as heterozygous for the CRISPR/Cas9-mediated deletion (i.e., clones have distinct alleles; **Figure 18**, **B**), part of the 5'-untranslated region (UTR) and the entire protein-coding region of *LRP1B* exon 1 was excised (except for one of the alleles of clone H7, downstream the start of the protein-coding

region of *LRP1B* exon 1). These CRISPR/Cas9-mediated deletions caused (i) the truncation of the 5' UTR (in which 10-nt to 12-nt at the 3' end is deleted) and (ii) the loss of the canonical AUG start codon on *LRP1B* mRNA. The translation of this mutant mRNA might be abrogated entirely (due to the canonical AUG start codon's removal) or may proceed if a downstream alternative start codon (usually the first downstream ATG) is available and the truncated 5' UTR is still functionally active (Marino *et al.*, 2009, Parsons *et al.*, 2015). On the assumption that the truncated 5' UTR is still functionally active, and intron 1 is correctly spliced out from the mutant *LRP1B* mRNA, the first downstream ATG present at exon 2 may encode an alternative translation start site. If this is the case, the translation initiated at the first alternative start codon can be shortly ceased due to the presence of an in-frame PTC [predicted using the ExPASy translate online tool; Gasteiger *et al.* (2003)]. Alternatively, the aberrant *LRP1B* mRNA (harboring a PTC) can be degraded through the NMD pathway. One of these events may also occur on the mutant *LRP1B* mRNA, with the first ATG (encoding the translation start site), due to the presence of another in-frame PTC. Hence, the biallelic deletion clones B9 and H7 were considered potential *LRP1B* knockout clones.

Since only one non-deletion clone (clone E6; **Figure 18**, **A**, *left side*) was found, its non-deletion amplicon was subjected to Sanger sequencing. Remarkably, this non-deletion clone revealed that it carried a 1-bp deletion in the sgRNA1 binding region and a 25-bp deletion in the sgRNA2 binding region. At first sight, this clone appeared to be homozygous for the individual deletion events (i.e., identical mutations at the individual sgRNA binding sites in both alleles; **Figure 20**, **A**). However, in contrast to the parental U87 human glioblastoma cell line, clone E6 did not show a single-nucleotide variant (SNV) at the nucleotide position 210 (C→G transversion; **Figure 20**, **B**, red arrowhead) in the 5'-UTR of the human *LRP1B* (which is upstream the target region within exon 1). Considering that (i) the biallelic deletion clones (B9 and H7) also showed the same SNV (data not shown) and (ii) the U87 human glioblastoma cell line is hypodiploid containing 43 to 45 chromosomes (Law *et al.*, 2005, Hu *et al.*, 2013), we hypothesized that this clone derived from a parental U87 cell containing only one copy of chromosome 2 (where the human *LRP1B* locus is located). This hypothesis can be proved (or disproved) by karyotyping clone E6. Interestingly, the 25-bp deletion in the sgRNA2 binding region caused the elimination of the last 7-bp of *LRP1B* exon 1 and the first 18-bp of *LRP1B* intron 1; therefore, disrupting exon 1 natural 5' splice site. This can result in either exon skipping, intron retention, or the introduction of a new splice site within an exon or intron (Baralle & Baralle, 2005). Since this 5' splice site disruption may affect the correct processivity (i.e., splicing) of the precursor mRNA [pre-mRNA; (Baralle & Baralle, 2005)],

clone E6 was also considered a potential *LRP1B* knockout clone.

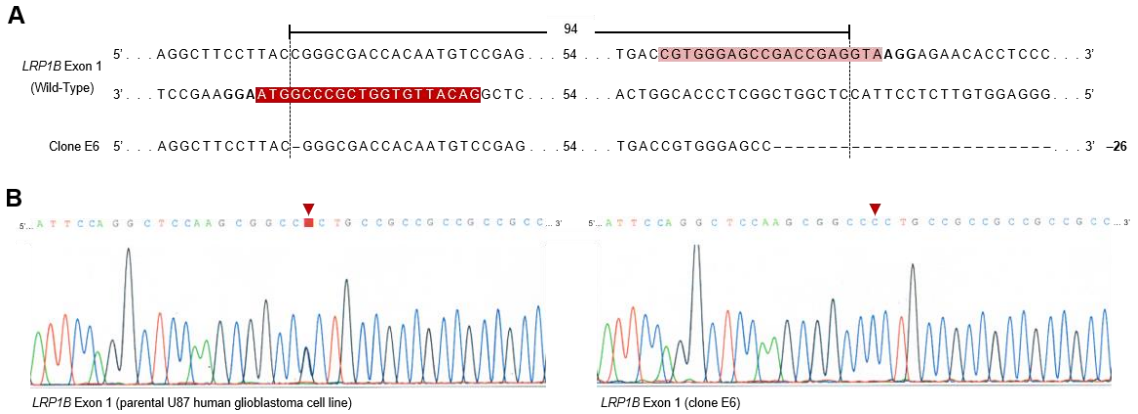

Figure 20. **Sequencing analysis of the non-deletion amplicon of clone E6. A**, The non-deleted amplicon sequence is aligned with the *LRP1B* wild-type sequence. The PAM (bold) and DNA target (highlighted in color) sequences within *LRP1B* exon 1 are depicted in the wild-type sequence. The number within the *LRP1B* alleles represents the number of nucleotides not shown. The vertical dashed lines indicate the predicted Cas9 cleavage site, 3-nt upstream (5') of the PAM sequence. The deleted nucleotides are indicated as dashes (–). The number of deleted nucleotides is indicated on the right side of the non-deleted amplicon sequence. **B**, Representative DNA-sequencing electropherograms are depicting the presence of an SNV at the nucleotide position 210 (C→G transversion; red arrowhead) in the 5'-UTR of the human *LRP1B* in the parental U87 human glioblastoma cell line and its absence in clone E6.

Regarding the analysis of exon 85, as expected, no deletion was detected through PCR (data not shown). Nevertheless, for the clones found to be potential *LRP1B* knockouts from the analysis of exon 1 (B9, E6, and H7), the non-deletion amplicons were subjected to Sanger sequencing. Interestingly, clones E6 and H7 showed small deletions (ranging from 1-bp to 2-bp) in the sgRNA4 binding region (light blue, **Figure 21**). These deletions were predicted to introduce an ORF-interrupting PTC. No mutation was found for clone B9. Although our results showed that the SpCas9, together with the pair sgRNA3 and sgRNA4, was unable to excise the targeted region of *LRP1B* exon 85, the sgRNA4/Cas9 complex was able to bind to the DNA target sequence and induce a DSB within the target DNA [3-nt upstream (5') of the PAM sequence; **Figure 21**]. These results were not a surprise since the on-target score of the sgRNA4 (44.2 out of 100) is higher than the on-target score of the sgRNA3 (32.1 out of 100).

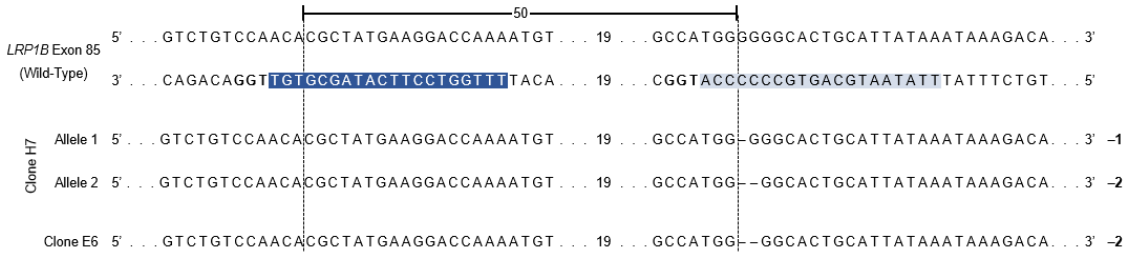

Figure 21. **Sequencing analysis of the non-deletion amplicons of potential knockout clones**. The non-deleted amplicon sequences are aligned with the *LRP1B* wild-type sequence. The PAM (bold) and DNA target (highlighted in color) sequences within *LRP1B* exon 85 are depicted in the wild-type sequence. The number within the *LRP1B* alleles represents the number of nucleotides not shown. The vertical dashed lines indicate the predicted Cas9 cleavage site, 3-nt upstream (5') of the PAM sequence (5'-NGG-3'). The deleted nucleotides are shown as dashes (–). The number of deleted nucleotides is indicated on the right side of the non-deleted amplicon sequences.

The summary of the genetic characteristics of the potential *LRP1B* knockout clones is depicted in **Table 10**.

Table 10. Summary of the characteristics of the potential *LRP1B* knockout clones.

Target exon	Clone name	Allelic status	CRISPR/Cas9-induced deletions	Deletion length (bp)	Effect of the deletion in *LRP1B* mRNA
1	B9	Biallelic-deleted	Heterozygous	94 (precise deletion)	Loss of the putative Kozak consensus sequence[a] and the canonical AUG start codon
				93 (1-bp insertion)	Loss of the putative Kozak consensus sequence[a] and the canonical AUG start codon
	H7	Biallelic-deleted	Heterozygous	92 (2-bp insertion)	Loss of the putative Kozak consensus sequence[a] and the canonical AUG start codon
				84 (20-bp insertion)	Preservation of the putative Kozak consensus sequence[a] and the canonical AUG start codon
	E6	NA	NA	26 (1-bp deletion in the sgRNA1 binding region and 25-bp deletion in the sgRNA2 binding region)	Loss of the exon 1 natural 5' splice site (5'-AG/GUAAGU-3' consensus sequence)
85	B9	NA	NA	No deletion	NA
	H7	NA	NA	1-bp deletion in the sgRNA4 binding region	Introduction of an ORF-interrupting PTC
				2-bp deletion in the sgRNA4 binding region	Introduction of an ORF-interrupting PTC
	E9	NA	NA	2-bp deletion in the sgRNA4 binding region	Introduction of an ORF-interrupting PTC

[a] The first AUG start codon occurs in the context of the so-called Kozak consensus sequence, which functions as the protein translation initiation site (TIS) in most eukaryotic mRNA transcripts (Kozak, 1989). TIS Miner (Liu & Wong, 2003) and NetStart 1.0 (Pedersen & Nielsen, 1997) were used to predict the putative TIS. Abbreviation: NA, non-applicable.

Interestingly, clones B9 and H7 exhibit similar phenotypes, whereas clone E6 shows a remarkably different phenotype (**Figure 22**). The question remains as to whether these phenotypic differences could (i) represent the heterogeneity of the parental U87 human glioblastoma cell line or (ii) reflect the consequences of the CRISPR/Cas9-induced alterations. To clarify this question, it would be essential to perform: (i) a short tandem repeat (STR) DNA profiling analysis, which enables the authentication of the identity of the cell line (Reid *et al.*, 2013), and (ii) a karyotyping analysis, which allows the identification of the numerical and structural chromosomal abnormalities (Tidball, 2019).

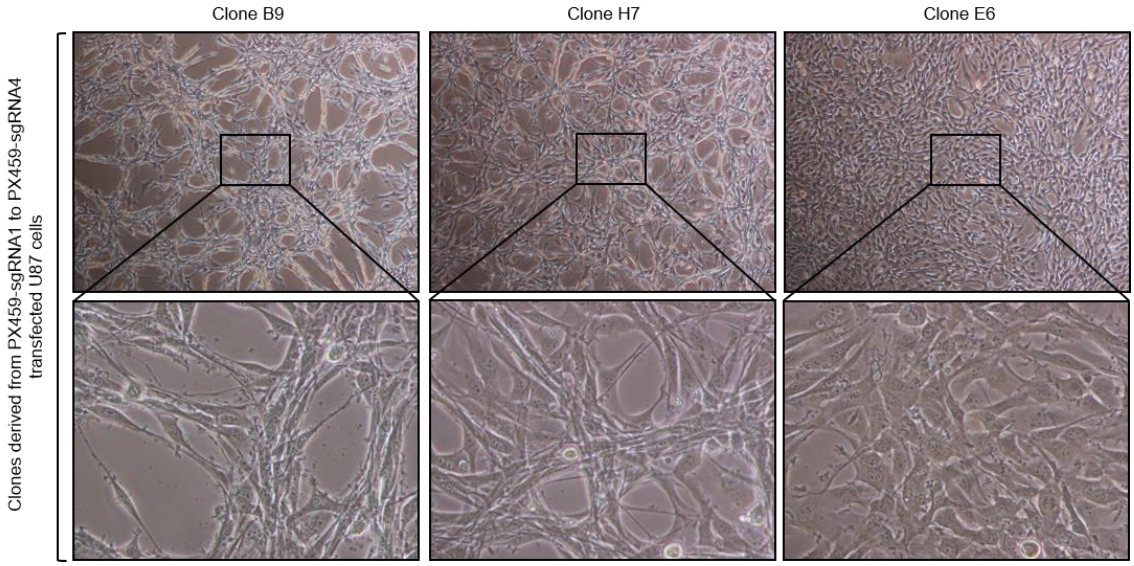

Figure 22. **Representative phase-contrast images of potential *LRP1B*-knockout clones**. Images were captured using 4× and 20× objectives (upper and lower panels, respectively) 3 days after seeding.

4.5 Assessing *LRP1B* mRNA Expression in Potential Knockout Clones

To evaluate *LRP1B* mRNA expression in the three potential knockout clones (B9, E6, and H7), two-step probe-based RT-qPCRs were carried out using three different gene expression assays targeting three distinct exon-exon junctions of *LRP1B* mRNA: assay A for the exon-exon junction 1-2, assay B for exon-exon junction 3-4, and assay C for exon-exon junction 85-86 (**Figure 23**). The human *TBP* was selected as the endogenous reference gene (i.e., housekeeping gene) for this study since it was previously described as suitable for the normalization of qPCR gene expression data in human glioblastoma tumors or cell lines (Valente *et al.*, 2009, Aithal & Rajeswari, 2015). As shown in **Figure 23**, no *LRP1B* mRNA expression was observed in the three potential knockout clones using assay A (target region, exon-exon junction 1-2). Using assay B (target region, exon-exon junction 3-4), no *LRP1B* mRNA expression was observed in clone E6. In contrast, clones B9 and H7 showed gene expression, although to a lesser extent than in the parental U87 human glioblastoma cell line. Using assay C (target region, exon-exon junction 85-86), in conformity with the results mentioned above, no expression of the human *LRP1B* was detected in clone E6. Interestingly, the expression level of *LRP1B* in clone B9 and clone H7 was similar to the parental U87 human glioblastoma cell line.

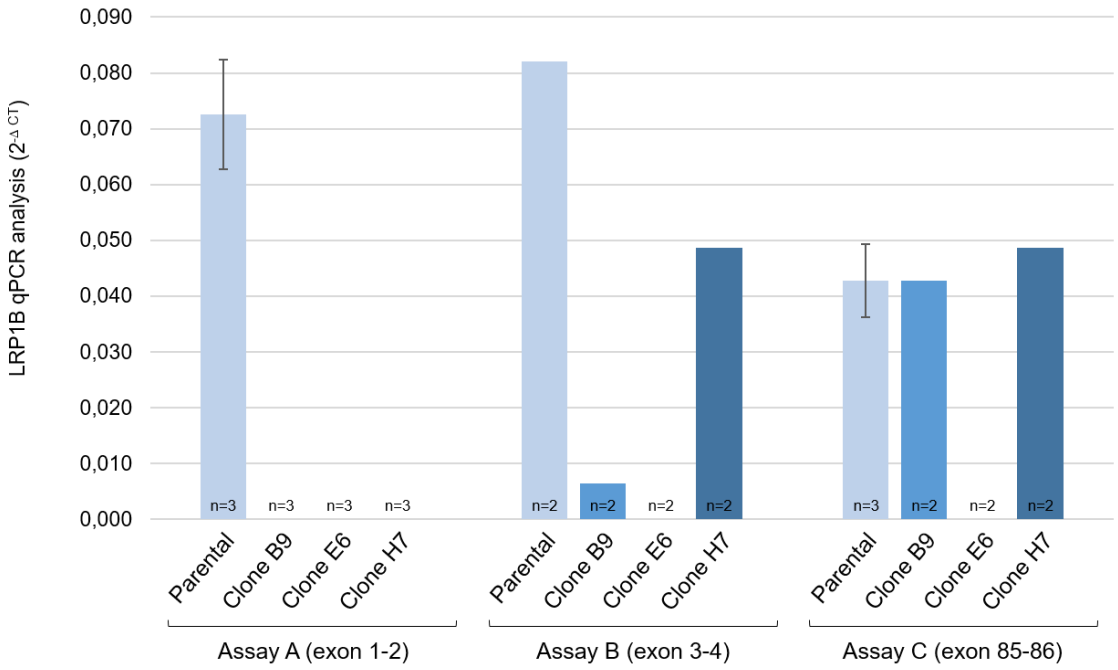

Figure 23. RT-qPCR analysis of the LRP1B mRNA levels in the potential knockout monoclonal cell lines. Data was normalized to the human TBP using the $2^{-\Delta CT}$ method. Data represent mean ± SEM from three independent experiments.

These results suggest that the 25-bp deletion of exon 1-intron 1 junction (disruption of exon 1 natural 5' splice site) in clone E6 resulted in the complete abrogation of the *LRP1B* mRNA. As previously mentioned, the disruption of a splice site can result in either exon skipping, intron retention, or the introduction of a new splice site within an exon or intron (Baralle & Baralle, 2005). However, considering the results obtained, we hypothesized that the complete ablation of the *LRP1B* mRNA might be attributed to intron 1 retention and the consequent establishment of a PTC that elicits nonsense-mediated decay of the mutant *LRP1B* mRNA. In fact, intron retention was already associated with down-regulation of gene expression via the NMD pathway (Ge & Porse, 2014) mainly because retained introns frequently interrupt the main ORF of the mRNA and often lead to the introduction of PTCs (Jacob & Smith, 2017). Clone E6 is therefore proposed to be an *LRP1B* knockout monoclonal cell line.

The absence of *LRP1B* mRNA expression in the clones B9 and H7 using assay A (target region, exon-exon junction 1-2) is explained by the probe binding site that is inside the region targeted by the sgRNA pair 1-2. Even though clones B9 and H7 showed RT-qPCR amplification of a specific targeted *LRP1B* mRNA sequence using the other assays (B and C; target region, exon-exon junction 3-4 and exon-exon junction 85-86, respectively), the expression levels of *LRP1B* in these clones were substantially lower compared to the parental U87 human glioblastoma cell line with assay B. The results suggest that aberrant *LRP1B* transcripts putatively harboring an in-frame PTC (of clones B9 and H7) are subjected to NMD. However, it seems that some aberrant *LRP1B*

transcripts escaped the NMD pathway. The mRNA resistance to NMD may result from the specific localization of the PTC in exon 2 of *LRP1B*. In fact, the UAG stop codon is localized to the position occupied by the exon junction complex (EJC; 20-nt to 24-nt upstream of the exon-exon junction), which serves to orient the NMD machinery and may be masked during the first (or pioneer) round of translation (Hwang & Kim, 2013, Popp & Maquat, 2016). Still, the presence of transcripts that have not escaped NMD does not imply that the aberrant *LRP1B* transcripts will be efficiently translated (Hwang & Kim, 2013). Moreover, on the assumption that the first alternative ATG (located in exon 2) encodes a translation start site, the translation initiated at the alternative AUG start codon would be shortly ceased (due to the existence of an ORF-interrupting PTC). In respect to the results obtained with assay C, no explanation was found. Although clones B9 and H7 seemed to be potential knockout clones, these were further tested for the presence of LRP1B through Western Blot. Unfortunately, we could not confirm their knockout status (using this technique) due to problems associated with the commercial anti-LRP1B antibodies (data not shown).

5 Conclusions

The aim of this study was to establish an *LRP1B*-knockout human cancer cell line using the CRISPR/Cas9 genome-editing tool. To achieve this, we decided to target the most upstream exons shared by the majority of the four predicted protein-coding transcripts of the human *LRP1B* gene. Thus, exon 1 and exon 85 were identified as targets for specific CRISPR/Cas9-mediated disrupting deletions. Four sgRNAs were designed and successfully cloned into the PX459 plasmid containing both the sgRNA scaffold and the SpCas9 nuclease. In total, four sgRNA/Cas9 expression vectors were generated: two designed to target *LRP1B* exon 1 (PX459-sgRNA1 and PX459-sgRNA2) and another two designed to target *LRP1B* exon 85 (PX459-sgRNA3 and PX459-sgRNA4). Combinations of these sgRNA/Cas9 expression vectors (two or all four) were effectively co-transfected into U87 glioblastoma cells using a cationic lipid-based transfection reagent. Transfected cells were selected, and single-cell clones were successfully isolated using limiting dilution. Our results showed that the SpCas9, together with the pair sgRNA1 and sgRNA2, can efficiently excise the targeted region of *LRP1B* exon 1. In contrast, the SpCas9, together with the pair sgRNA3 and sgRNA4, is unable to excise the targeted region of *LRP1B* exon 85 (at least efficiently). Overall, we were able to identify three potential knockout clones (B9, H7, E6) through PCR and sequencing analysis. In clones B9 and H7, the CRISPR/Cas9-mediated deletions resulted in the downregulation of *LRP1B* gene expression. Additional studies are needed to further evaluate the effect of CRISPR/Cas9-induced deletions in LRP1B protein expression and confirm their knockout status. In clone E6, the disruption of exon 1 natural 5' splice site (deletion of exon 1-intron 1 junction) resulted in the complete abrogation of the *LRP1B* mRNA; therefore, clone E6 is proposed to be an *LRP1B* knockout. In summary, we were able to establish an *LRP1B*-knockout human cancer monoclonal cell line using the CRISPR/Cas9 genome-editing tool. The now developed *LRP1B*-knockout model can be extremely useful for deciphering the LRP1B associated cancer mechanisms.

6 References

Aisina, R.B., and Mukhametova, L.I. (2014). Structure And Function Of Plasminogen/Plasmin System. *Russian Journal of Bioorganic Chemistry* **40**(6): 590-605. DOI: 10.1134/S1068162014060028.

Aithal, M.G.S., and Rajeswari, N. (2015). Validation Of Housekeeping Genes For Gene Expression Analysis In Glioblastoma Using Quantitative Real-Time Polymerase Chain Reaction. *Brain Tumor Res Treat* **3**(1): 24-29. DOI: 10.14791/btrt.2015.3.1.24.

Alkhnbashi, O.S., Shah, S.A., Garrett, R.A., Saunders, S.J., Costa, F., and Backofen, R. (2016). Characterizing Leader Sequences Of CRISPR Loci. *Bioinformatics* **32**(17): i576-i585. DOI: 10.1093/bioinformatics/btw454.

Altschul, S.F., Madden, T.L., Schäffer, A.A., Zhang, J., Zhang, Z., Miller, W., and Lipman, D.J. (1997). Gapped BLAST And PSI-BLAST: A New Generation Of Protein Database Search Programs. *Nucleic Acids Research* **25**(17): 3389-3402. DOI: 10.1093/nar/25.17.3389.

Amitai, G., and Sorek, R. (2016). CRISPR–Cas Adaptation: Insights Into The Mechanism Of Action. *Nature Reviews Microbiology* **14**(2): 67-76. DOI: 10.1038/nrmicro.2015.14.

Aparicio-Prat, E., Arnan, C., Sala, I., Bosch, N., Guigó, R., and Johnson, R. (2015). DECKO: Single-Oligo, Dual-Crispr Deletion Of Genomic Elements Including Long Non-Coding RNAs. *BMC genomics* **16**(1): 846. DOI: 10.1186/s12864-015-2086-z.

Baralle, D., and Baralle, M. (2005). Splicing In Action: Assessing Disease Causing Sequence Changes. *Journal of Medical Genetics* **42**(10): 737-748. DOI: 10.1136/jmg.2004.029538.

Barrangou, R., Fremaux, C., Deveau, H., Richards, M., Boyaval, P., Moineau, S., Romero, D.A., and Horvath, P. (2007). CRISPR Provides Acquired Resistance Against Viruses In Prokaryotes. *Science* **315**(5819): 1709-1712. DOI: 10.1126/science.1138140.

Battle, M.A., Maher, V.M., and McCormick, J.J. (2003). ST7 Is A Novel Low-Density Lipoprotein Receptor-Related Protein (LRP) With A Cytoplasmic Tail That Interacts With Proteins Related To Signal Transduction Pathways. *Biochemistry* **42**(24): 7270-7282. DOI: 10.1021/bi034081y.

Beer, A.G., Zenzmaier, C., Schreinlechner, M., Haas, J., Dietrich, M.F., Herz, J., and Marschang, P. (2016). Expression Of A Recombinant Full-Length LRP1B Receptor In Human Non-Small Cell Lung Cancer Cells Confirms The Postulated

Growth-Suppressing Function Of This Large LDL Receptor Family Member. *Oncotarget* **7**(42): 68721-68733. DOI: 10.18632/oncotarget.11897.

Benchling [Biology Software]. CRISPR Guide RNA Design Tool. Retrieved from https://benchling.com (accessed on September 2019).

Bhat, S.S., Ali, R., and Khanday, F.A. (2019). Syntrophins Entangled In Cytoskeletal Meshwork: Helping To Hold It All Together. *Cell Proliferation* **52**(2): e12562. DOI: 10.1111/cpr.12562.

Bieri, S., Djordjevic, J.T., Daly, N.L., Smith, R., and Kroon, P.A. (1995). Disulfide Bridges Of A Cysteine-Rich Repeat Of The LDL Receptor Ligand-Binding Domain. *Biochemistry* **34**(40): 13059-13065. DOI: 10.1021/bi00040a017.

Bolotin, A., Quinquis, B., Sorokin, A., and Ehrlich, S.D. (2005). Clustered Regularly Interspaced Short Palindrome Repeats (CRISPRs) Have Spacers Of Extrachromosomal Origin. *Microbiology (Reading)* **151**(Pt 8): 2551-2561. DOI: 10.1099/mic.0.28048-0.

Brandl, C., Ortiz, O., Röttig, B., Wefers, B., Wurst, W., and Kühn, R. (2015). Creation Of Targeted Genomic Deletions Using TALEN Or CRISPR/Cas Nuclease Pairs In One-Cell Mouse Embryos. *FEBS Open Bio* **5**: 26-35. DOI: 10.1016/j.fob.2014.11.009.

Brouns, S.J.J., Jore, M.M., Lundgren, M., Westra, E.R., Slijkhuis, R.J.H., Snijders, A.P.L., Dickman, M.J., Makarova, K.S., Koonin, E.V., and van der Oost, J. (2008). Small CRISPR RNAs Guide Antiviral Defense In Prokaryotes. *Science* **321**(5891): 960. DOI: 10.1126/science.1159689.

Brown, J., Bothma, H., Veale, R., and Willem, P. (2011). Genomic Imbalances In Esophageal Carcinoma Cell Lines Involve Wnt Pathway Genes. *World Journal of Gastroenterology* **17**(24): 2909-2923. DOI: 10.3748/wjg.v17.i24.2909.

Brown, M.S., Ye, J., Rawson, R.B., and Goldstein, J.L. (2000). Regulated Intramembrane Proteolysis: A Control Mechanism Conserved From Bacteria To Humans. *Cell* **100**(4): 391-398. DOI: 10.1016/s0092-8674(00)80675-3.

Brown, S.D., Twells, R.C., Hey, P.J., Cox, R.D., Levy, E.R., Soderman, A.R., Metzker, M.L., Caskey, C.T., Todd, J.A., and Hess, J.F. (1998). Isolation And Characterization Of LRP6, A Novel Member Of The Low Density Lipoprotein Receptor Gene Family. *Biochemical and Biophysical Research Communications* **248**(3): 879-888. DOI: 10.1006/bbrc.1998.9061.

Bu, G. (1998). Receptor-Associated Protein: A Specialized Chaperone And Antagonist For Members Of The LDL Receptor Gene Family. *Current Opinion in Lipidology* **9**(2): 149-155. DOI: 10.1097/00041433-199804000-00012.

Bult, C.J., White, O., Olsen, G.J., Zhou, L., Fleischmann, R.D., Sutton, G.G., Blake, J.A., FitzGerald, L.M., Clayton, R.A., Gocayne, J.D., Kerlavage, A.R., Dougherty, B.A., Tomb, J.F., Adams, M.D., Reich, C.I., Overbeek, R., Kirkness, E.F., Weinstock, K.G., Merrick, J.M., Glodek, A., Scott, J.L., Geoghagen, N.S., and Venter, J.C. (1996). Complete Genome Sequence Of The Methanogenic Archaeon, Methanococcus jannaschii. *Science* **273**(5278): 1058-1073. DOI: 10.1126/science.273.5278.1058.

Burstein, D., Harrington, L.B., Strutt, S.C., Probst, A.J., Anantharaman, K., Thomas, B.C., Doudna, J.A., and Banfield, J.F. (2017). New CRISPR–Cas Systems From Uncultivated Microbes. *Nature* **542**(7640): 237-241. DOI: 10.1038/nature21059.

Cam, J.A., Zerbinatti, C.V., Knisely, J.M., Hecimovic, S., Li, Y.H., and Bu, G.J. (2004). The Low Density Lipoprotein Receptor-Related Protein 1B Retains Beta-Amyloid Precursor Protein At The Cell Surface And Reduces Amyloid-Beta Peptide Production. *Journal of Biological Chemistry* **279**(28): 29639-29646. DOI: 10.1074/jbc.M313893200.

Campenhout, C.V., Cabochette, P., Veillard, A.C., Laczik, M., Zelisko-Schmidt, A., Sabatel, C., Dhainaut, M., Vanhollebeke, B., Gueydan, C., and Kruys, V. (2019). Guidelines For Optimized Gene Knockout Using CRISPR/Cas9. *BioTechniques* **66**(6): 295-302. DOI: 10.2144/btn-2018-0187.

Canver, M.C., Bauer, D.E., Dass, A., Yien, Y.Y., Chung, J., Masuda, T., Maeda, T., Paw, B.H., and Orkin, S.H. (2014). Characterization Of Genomic Deletion Efficiency Mediated By Clustered Regularly Interspaced Short Palindromic Repeats (CRISPR)/Cas9 Nuclease System In Mammalian Cells. *Journal of Biological Chemistry* **289**(31): 21312-21324. DOI: 10.1074/jbc.M114.564625.

Ceccaldi, R., Rondinelli, B., and D'Andrea, A.D. (2016). Repair Pathway Choices and Consequences at the Double-Strand Break. *Trends in cell biology* **26**(1): 52-64. DOI: 10.1016/j.tcb.2015.07.009.

Cengiz, B., Gunduz, M., Nagatsuka, H., Beder, L., Gunduz, E., Tarnarnura, R., Mahmut, N., Fukushirna, K., Ali, M.A.S., NaoMoto, Y., Shimizu, K., and Nagai, N. (2007). Fine Deletion Mapping Of Chromosome 2q21-37 Shows Three Preferentially Deleted Regions In Oral Cancer. *Oral Oncology* **43**(3): 241-247. DOI: 10.1016/j.oraloncology.2006.03.004.

Chen, H., Chong, W., Wu, Q., Yao, Y., Mao, M., and Wang, X. (2019). Association Of LRP1B Mutation With Tumor Mutation Burden And Outcomes In Melanoma And Non-Small Cell Lung Cancer Patients Treated With Immune Check-Point Blockades. *Front Immunol* **10**: 1113-1113. DOI: 10.3389/fimmu.2019.01113.

Chen, W.J., Goldstein, J.L., and Brown, M.S. (1990). NPXY, A Sequence Often Found In Cytoplasmic Tails, Is Required For Coated Pit-Mediated Internalization Of The Low Density Lipoprotein Receptor. *Journal of Biological Chemistry* **265**(6): 3116-3123.

Chen, X., Xu, F., Zhu, C., Ji, J., Zhou, X., Feng, X., and Guang, S. (2014). Dual sgRNA-Directed Gene Knockout Using CRISPR/Cas9 Technology In Caenorhabditis elegans. *Sci Rep-Uk* **4**: 7581-7581. DOI: 10.1038/srep07581.

Choi, Y.W., Bae, S.M., Kim, Y.W., Lee, H.N., Kim, Y.W., Park, T.C., Ro, D.Y., Shin, J.C., Shin, S.J., Seo, J.S., and Ahn, W.S. (2007). Gene Expression Profiles In Squamous Cell Cervical Carcinoma Using Array-Based Comparative Genomic Hybridization Analysis. *International Journal of Gynecological Cancer* **17**(3): 687-696. DOI: 10.1111/j.1525-1438.2007.00834.x.

Chu, P.Y., Li, T.K., Ding, S.T., Lai, I.R., and Shen, T.L. (2010). EGF-Induced Grb7 Recruits And Promotes Ras Activity Essential For The Tumorigenicity Of Sk-Br3 Breast Cancer Cells. *Journal of Biological Chemistry* **285**(38): 29279-29285. DOI: 10.1074/jbc.C110.114124.

Coley, A.A., and Gao, W. (2019). PSD-95 Deficiency Disrupts PFC-Associated Function And Behavior During Neurodevelopment. *Sci Rep-Uk* **9**(1): 9486. DOI: 10.1038/s41598-019-45971-w.

Conese, M., Nykjaer, A., Petersen, C.M., Cremona, O., Pardi, R., Andreasen, P.A., Gliemann, J., Christensen, E.I., and Blasi, F. (1995). Alpha-2 Macroglobulin Receptor/LDL Receptor-Related Protein(LRP)-Dependent Internalization Of The Urokinase Receptor. *The Journal of cell biology* **131**(6 Pt 1): 1609-1622. DOI: 10.1083/jcb.131.6.1609.

Cong, L., Ran, F.A., Cox, D., Lin, S., Barretto, R., Habib, N., Hsu, P.D., Wu, X., Jiang, W., Marraffini, L.A., and Zhang, F. (2013). Multiplex Genome Engineering Using CRISPR/Cas Systems. *Science* **339**(6121): 819-823. DOI: 10.1126/science.1231143.

Corre, J., Cleynen, A., du Pont, S.R., Buisson, L., Bolli, N., Attal, M., Munshi, N., and Avet-Loiseau, H. (2018). Multiple Myeloma Clonal Evolution In Homogeneously Treated Patients. *Leukemia* **32**(12): 2636-2647. DOI: 10.1038/s41375-018-0153-6.

Cowin, P.A., George, J., Fereday, S., Loehrer, E., Van Loo, P., Cullinane, C., Etemadmoghadam, D., Ftouni, S., Galletta, L., Anglesio, M.S., Hendley, J., Bowes, L., Sheppard, K.E., Christie, E.L., Pearson, R.B., Harnett, P.R., Heinzelmann-Schwarz, V., Friedlander, M., McNally, O., Quinn, M., Campbell, P., deFazio, A., and Bowtell, D.D. (2012). LRP1B Deletion In High-Grade Serous

Ovarian Cancers Is Associated With Acquired Chemotherapy Resistance To Liposomal Doxorubicin. *Cancer research* **72**(16): 4060-4073. DOI: 10.1158/0008-5472.Can-12-0203.

Czekay, R.P., Kuemmel, T.A., Orlando, R.A., and Farquhar, M.G. (2001). Direct Binding Of Occupied Urokinase Receptor (uPAR) To LDL Receptor-Related Protein Is Required For Endocytosis Of uPAR And Regulation Of Cell Surface Urokinase Activity. *Molecular biology of the cell* **12**(5): 1467-1479. DOI: 10.1091/mbc.12.5.1467.

Daly, N.L., Scanlon, M.J., Djordjevic, J.T., Kroon, P.A., and Smith, R. (1995). Three-Dimensional Structure Of A Cysteine-Rich Repeat From The Low-Density Lipoprotein Receptor. *Proceedings of the National Academy of Sciences* **92**(14): 6334-6338. DOI: 10.1073/pnas.92.14.6334.

de Haas, C.J.C. (1999). New Insights Into The Role Of Serum Amyloid P Component, A Novel Lipopolysaccharide-Binding Protein. *FEMS Immunology & Medical Microbiology* **26**(3-4): 197-202. DOI: 10.1111/j.1574-695X.1999.tb01390.x.

Dehairs, J., Talebi, A., Cherifi, Y., and Swinnen, J.V. (2016). CRISP-ID: Decoding CRISPR Mediated Indels By Sanger Sequencing. *Sci Rep-Uk* **6**(1): 28973. DOI: 10.1038/srep28973.

Deltcheva, E., Chylinski, K., Sharma, C.M., Gonzales, K., Chao, Y., Pirzada, Z.A., Eckert, M.R., Vogel, J., and Charpentier, E. (2011). CRISPR RNA Maturation By Trans-Encoded Small RNA And Host Factor RNase III. *Nature* **471**(7340): 602-607. DOI: 10.1038/nature09886.

Deriano, L., and Roth, D.B. (2013). Modernizing The Nonhomologous End-Joining Repertoire: Alternative And Classical NHEJ Share The Stage. *Annual Review of Genetics* **47**: 433-455. DOI: 10.1146/annurev-genet-110711-155540.

Deveau, H., Barrangou, R., Garneau, J.E., Labonté, J., Fremaux, C., Boyaval, P., Romero, D.A., Horvath, P., and Moineau, S. (2008). Phage Response To CRISPR-Encoded Resistance In Streptococcus thermophilus. *Journal of Bacteriology* **190**(4): 1390. DOI: 10.1128/JB.01412-07.

Dieckmann, M., Dietrich, M.F., and Herz, J. (2010). Lipoprotein Receptors - An Evolutionarily Ancient Multifunctional Receptor Family. *Biological chemistry* **391**(11): 1341-1363. DOI: 10.1515/BC.2010.129.

DiGiacomo, V., and Meruelo, D. (2016). Looking Into Laminin Receptor: Critical Discussion Regarding The Non-Integrin 37/67-kDa Laminin Receptor/RPSA Protein. *Biological reviews of the Cambridge Philosophical Society* **91**(2): 288-310. DOI: 10.1111/brv.12170.

Ding, D., Lou, X., Hua, D., Yu, W., Li, L., Wang, J., Gao, F., Zhao, N., Ren, G., Li, L., and Lin, B. (2012). Recurrent Targeted Genes Of Hepatitis B Virus In The Liver Cancer Genomes Identified By A Next-Generation Sequencing-Based Approach. *PLoS genetics* **8**(12): e1003065. DOI: 10.1371/journal.pgen.1003065.

Ding, L., Getz, G., Wheeler, D.A., Mardis, E.R., McLellan, M.D., Cibulskis, K., Sougnez, C., Greulich, H., Muzny, D.M., Morgan, M.B., Fulton, L., Fulton, R.S., Zhang, Q.Y., Wendl, M.C., Lawrence, M.S., Larson, D.E., Chen, K., Dooling, D.J., Sabo, A., Hawes, A.C., Shen, H., Jhangiani, S.N., Lewis, L.R., Hall, O., Zhu, Y.M., Mathew, T., Ren, Y.R., Yao, J.Q., Scherer, S.E., Clerc, K., Metcalf, G.A., Ng, B., Milosavljevic, A., Gonzalez-Garay, M.L., Osborne, J.R., Meyer, R., Shi, X.Q., Tang, Y.Z., Koboldt, D.C., Lin, L., Abbott, R., Miner, T.L., Pohl, C., Fewell, G., Haipek, C., Schmidt, H., Dunford-Shore, B.H., Kraja, A., Crosby, S.D., Sawyer, C.S., Vickery, T., Sander, S., Robinson, J., Winckler, W., Baldwin, J., Chirieac, L.R., Dutt, A., Fennell, T., Hanna, M., Johnson, B.E., Onofrio, R.C., Thomas, R.K., Tonon, G., Weir, B.A., Zhao, X.J., Ziaugra, L., Zody, M.C., Giordano, T., Orringer, M.B., Roth, J.A., Spitz, M.R., Wistuba, II, Ozenberger, B., Good, P.J., Chang, A.C., Beer, D.G., Watson, M.A., Ladanyi, M., Broderick, S., Yoshizawa, A., Travis, W.D., Pao, W., Province, M.A., Weinstock, G.M., Varmus, H.E., Gabriel, S.B., Lander, E.S., Gibbs, R.A., Meyerson, M., and Wilson, R.K. (2008). Somatic Mutations Affect Key Pathways In Lung Adenocarcinoma. *Nature* **455**(7216): 1069-1075. DOI: 10.1038/nature07423.

Doench, J.G., Fusi, N., Sullender, M., Hegde, M., Vaimberg, E.W., Donovan, K.F., Smith, I., Tothova, Z., Wilen, C., Orchard, R., Virgin, H.W., Listgarten, J., and Root, D.E. (2016). Optimized sgRNA Design To Maximize Activity And Minimize Off-Target Effects Of CRISPR-Cas9. *Nature Biotechnology* **34**(2): 184-191. DOI: 10.1038/nbt.3437.

Dong, Y., Lathrop, W., Weaver, D., Qiu, Q., Cini, J., Bertolini, D., and Chen, D. (1998). Molecular Cloning And Characterization Of LR3, A Novel LDL Receptor Family Protein With Mitogenic Activity. *Biochemical and Biophysical Research Communications* **251**(3): 784-790. DOI: 10.1006/bbrc.1998.9545.

East-Seletsky, A., O'Connell, M.R., Knight, S.C., Burstein, D., Cate, J.H.D., Tjian, R., and Doudna, J.A. (2016). Two Distinct RNase Activities Of CRISPR-C2c2 Enable Guide-RNA Processing And RNA detection. *Nature* **538**(7624): 270-273. DOI: 10.1038/nature19802.

Elgendy, M., Fusco, J.P., Segura, V., Lozano, M.D., Minucci, S., Echeveste, J.I., Gurpide, A., Andueza, M., Melero, I., Sanmamed, M.F., Ruiz, M.R., Calvo, A., Pascual, J.I., Velis, J.M., Minana, B., Valle, R.D., Pio, R., Agorreta, J.,

Abengozar, M., Colecchia, M., Brich, S., Renne, S.L., Guruceaga, E., Patino-Garcia, A., and Perez-Gracia, J.L. (2019). Identification Of Mutations Associated With Acquired Resistance To Sunitinib In Renal Cell Cancer. *International journal of cancer* **145**(7): 1991-2001. DOI: 10.1002/ijc.32256.

Fjorback, A.W., Seaman, M., Gustafsen, C., Mehmedbasic, A., Gokool, S., Wu, C., Militz, D., Schmidt, V., Madsen, P., Nyengaard, J.R., Willnow, T.E., Christensen, E.I., Mobley, W.B., Nykjær, A., and Andersen, O.M. (2012). Retromer Binds The FANSHY Sorting Motif In SorLA To Regulate Amyloid Precursor Protein Sorting And Processing. *Journal of Neuroscience* **32**(4): 1467-1480. DOI: 10.1523/jneurosci.2272-11.2012.

Fonfara, I., Richter, H., Bratovič, M., Le Rhun, A., and Charpentier, E. (2016). The CRISPR-Associated DNA-Cleaving Enzyme Cpf1 Also Processes Precursor CRISPR RNA. *Nature* **532**(7600): 517-521. DOI: 10.1038/nature17945.

Frankish, A., Diekhans, M., Ferreira, A., Johnson, R., Jungreis, I., Loveland, J., Mudge, J.M., Sisu, C., Wright, J., Armstrong, J., Barnes, I., Berry, A., Bignell, A., Sala, S.C., Chrast, J., Cunningham, F., Di Domenico, T., Donaldson, S., Fiddes, I.T., García Girón, C., Gonzalez, J.M., Grego, T., Hardy, M., Hourlier, T., Hunt, T., Izuogu, O.G., Lagarde, J., Martin, F.J., Martínez, L., Mohanan, S., Muir, P., Navarro, F.C.P., Parker, A., Pei, B., Pozo, F., Ruffier, M., Schmitt, B.M., Stapleton, E., Suner, M., Sycheva, I., Uszczynska-Ratajczak, B., Xu, J., Yates, A., Zerbino, D., Zhang, Y., Aken, B., Choudhary, J.S., Gerstein, M., Guigó, R., Hubbard, T.J.P., Kellis, M., Paten, B., Reymond, A., Tress, M.L., and Flicek, P. (2018). GENCODE Reference Annotation For The Human And Mouse Genomes. *Nucleic Acids Research* **47**(D1): D766-D773. DOI: 10.1093/nar/gky955.

Garneau, J.E., Dupuis, M., Villion, M., Romero, D.A., Barrangou, R., Boyaval, P., Fremaux, C., Horvath, P., Magadán, A.H., and Moineau, S. (2010). The CRISPR/Cas Bacterial Immune System Cleaves Bacteriophage And Plasmid DNA. *Nature* **468**(7320): 67-71. DOI: 10.1038/nature09523.

Gasiunas, G., Barrangou, R., Horvath, P., and Siksnys, V. (2012). Cas9-crRNA Ribonucleoprotein Complex Mediates Specific DNA Cleavage For Adaptive Immunity In Bacteria. *Proceedings of the National Academy of Sciences* **109**(39): E2579-2586. DOI: 10.1073/pnas.1208507109.

Gasteiger, E., Gattiker, A., Hoogland, C., Ivanyi, I., Appel, R.D., and Bairoch, A. (2003). ExPASy: The Proteomics Server For In-Depth Protein Knowledge And Analysis. *Nucleic Acids Research* **31**(13): 3784-3788. DOI: 10.1093/nar/gkg563.

Ge, W.T., Hu, H.G., Cai, W., Xu, J.H., Hu, W.X., Weng, X.Y., Qin, X., Huang, Y.Q., Han, W.D., Hu, Y.T., Yu, J.K., Zhang, W.F., Ye, S.S., Qi, L.N., Huang, P.J., Chen, L.R.,

Ding, K.F., Wang, L., and Zheng, S. (2020). High-Risk Stage III Colon Cancer Patients Identified By A Novel Five-Gene Mutational Signature Are Characterized By Upregulation Of IL-23A And Gut Bacterial Translocation Of The Tumor Microenvironment. *International journal of cancer* **146**(7): 2027-2035. DOI: 10.1002/ijc.32775.

Ge, Y., and Porse, B.T. (2014). The Functional Consequences Of Intron Retention: Alternative Splicing Coupled To NMD As A Regulator Of Gene Expression. *Bioessays* **36**(3): 236-243. DOI: 10.1002/bies.201300156.

Geisinger, J.M., Turan, S., Hernandez, S., Spector, L.P., and Calos, M.P. (2016). In Vivo Blunt-End Cloning Through CRISPR/Cas9-Facilitated Non-Homologous End-Joining. *Nucleic Acids Research* **44**(8): e76. DOI: 10.1093/nar/gkv1542.

Gisler, S., Gonçalves, J.P., Akhtar, W., de Jong, J., Pindyurin, A.V., Wessels, L.F.A., and van Lohuizen, M. (2019). Multiplexed Cas9 Targeting Reveals Genomic Location Effects And gRNA-Based Staggered Breaks Influencing Mutation Efficiency. *Nature communications* **10**(1): 1598. DOI: 10.1038/s41467-019-09551-w.

Gotthardt, M., Trommsdorff, M., Nevitt, M.F., Shelton, J., Richardson, J.A., Stockinger, W., Nimpf, J., and Herz, J. (2000). Interactions Of The Low Density Lipoprotein Receptor Gene Family With Cytosolic Adaptor And Scaffold Proteins Suggest Diverse Biological Functions In Cellular Communication And Signal Transduction. *Journal of Biological Chemistry* **275**(33): 25616-25624. DOI: 10.1074/jbc.M000955200.

Grotz, A.K., Abaitua, F., Navarro-Guerrero, E., Hastoy, B., Ebner, D., and Gloyn, A.L. (2019). A CRISPR/Cas9 Genome Editing Pipeline In The EndoC-betaH1 Cell Line To Study Genes Implicated In Beta Cell Function. *Wellcome Open Research* **4**: 150. DOI: 10.12688/wellcomeopenres.15447.1.

Guo, T., Feng, Y., Xiao, J., Liu, Q., Sun, X., Xiang, J., Kong, N., Liu, S., Chen, G., Wang, Y., Dong, M., Cai, Z., Lin, H., Cai, X., and Xie, A. (2018). Harnessing Accurate Non-Homologous End Joining For Efficient Precise Deletion In CRISPR/Cas9-Mediated Genome Editing. *Genome biology* **19**(1): 170. DOI: 10.1186/s13059-018-1518-x.

Guschin, D.Y., Waite, A.J., Katibah, G.E., Miller, J.C., Holmes, M.C., and Rebar, E.J. (2010). A Rapid And General Assay For Monitoring Endogenous Gene Modification. *Methods in Molecular Biology* **649**: 247-256. DOI: 10.1007/978-1-60761-753-2_15.

Haas, J., Beer, A.G., Widschwendter, P., Oberdanner, J., Salzmann, K., Sarg, B., Lindner, H., Herz, J., Patsch, J.R., and Marschang, P. (2011). LRP1B Shows Restricted Expression In Human Tissues And Binds To Several Extracellular

Ligands, Including Fibrinogen And ApoE - Carrying Lipoproteins. *Atherosclerosis* **216**(2): 342-347. DOI: 10.1016/j.atherosclerosis.2011.02.030.

Haft, D.H., Selengut, J., Mongodin, E.F., and Nelson, K.E. (2005). A Guild Of 45 CRISPR-Associated (Cas) Protein Families And Multiple CRISPR/Cas Subtypes Exist In Prokaryotic Genomes. *PLoS computational biology* **1**(6): e60. DOI: 10.1371/journal.pcbi.0010060.

Hale, C., Kleppe, K., Terns, R.M., and Terns, M.P. (2008). Prokaryotic Silencing (psi)RNAs In Pyrococcus furiosus. *RNA* **14**(12): 2572-2579. DOI: 10.1261/rna.1246808.

Hale, C.R., Zhao, P., Olson, S., Duff, M.O., Graveley, B.R., Wells, L., Terns, R.M., and Terns, M.P. (2009). RNA-Guided RNA Cleavage By A CRISPR RNA-Cas Protein Complex. *Cell* **139**(5): 945-956. DOI: 10.1016/j.cell.2009.07.040.

Han, D.C., Shen, T.L., Miao, H., Wang, B., and Guan, J.L. (2002). EphB1 Associates With Grb7 And Regulates Cell Migration. *Journal of Biological Chemistry* **277**(47): 45655-45661. DOI: 10.1074/jbc.M203165200.

Han, J., Zhang, J., Chen, L., Shen, B., Zhou, J., Hu, B., Du, Y., Tate, P.H., Huang, X., and Zhang, W. (2014). Efficient In Vivo Deletion Of A Large Imprinted lncRNA By CRISPR/Cas9. *RNA Biology* **11**(7): 829-835. DOI: 10.4161/rna.29624.

Hannafon, B.N., Cai, A., Calloway, C.L., Xu, Y.F., Zhang, R., Fung, K.M., and Ding, W.Q. (2019). miR-23b And miR-27b Are Oncogenic microRNAs In Breast Cancer: Evidence From A CRISPR/Cas9 Deletion Study. *BMC Cancer* **19**. DOI: 10.1186/s12885-019-5839-2.

Hermans, P.W., van Soolingen, D., Bik, E.M., de Haas, P.E., Dale, J.W., and van Embden, J.D. (1991). Insertion Element IS987 From Mycobacterium bovis BCG Is Located In A Hot-Spot Integration Region For Insertion Elements In Mycobacterium tuberculosis Complex Strains. *Infect Immun* **59**(8): 2695-2705. DOI: 10.1128/IAI.59.8.2695-2705.1991.

Herz, J. (2001). The LDL Receptor Gene Family: (Un)Expected Signal Transducers In The Brain. *Neuron* **29**(3): 571-581. DOI: 10.1016/S0896-6273(01)00234-3.

Herz, J., and Bock, H.H. (2002). Lipoprotein Receptors In The Nervous System. *Annual review of biochemistry* **71**: 405-434. DOI: 10.1146/annurev.biochem.71.110601.135342.

Herz, J., Chen, Y., Masiulis, I., and Zhou, L. (2009). Expanding Functions Of Lipoprotein Receptors. *J Lipid Res* **50 Suppl**: S287-292. DOI: 10.1194/jlr.R800077-JLR200.

Herz, J., Hamann, U., Rogne, S., Myklebost, O., Gausepohl, H., and Stanley, K.K. (1988). Surface Location And High Affinity For Calcium Of A 500-kd Liver Membrane Protein Closely Related To The LDL-Receptor Suggest A

Physiological Role As Lipoprotein Receptor. *EMBO Journal* **7**(13): 4119-4127. DOI: 10.1002/j.1460-2075.1988.tb03306.x.

Herz, J., Kowal, R.C., Goldstein, J.L., and Brown, M.S. (1990). Proteolytic Processing Of The 600 Kd Low Density Lipoprotein Receptor-Related Protein (LRP) Occurs In A Trans-Golgi Compartment. *EMBO Journal* **9**(6): 1769-1776.

Herz, J., and Strickland, D.K. (2001). LRP: A Multifunctional Scavenger And Signaling Receptor. *Journal of Clinical Investigation* **108**(6): 779-784. DOI: 10.1172/jci13992.

Hey, P.J., Twells, R.C., Phillips, M.S., Yusuke, N., Brown, S.D., Kawaguchi, Y., Cox, R., Guochun, X., Dugan, V., Hammond, H., Metzker, M.L., Todd, J.A., and Hess, J.F. (1998). Cloning Of A Novel Member Of The Low-Density Lipoprotein Receptor Family. *Gene* **216**(1): 103-111. DOI: 10.1016/s0378-1119(98)00311-4.

Hille, F., Richter, H., Wong, S.P., Bratovič, M., Ressel, S., and Charpentier, E. (2018). The Biology Of CRISPR-Cas: Backward And Forward. *Cell* **172**(6): 1239-1259. DOI: 10.1016/j.cell.2017.11.032.

Hirai, Y., Utsugi, K., Takeshima, N., Kawamata, Y., Furuta, R., Kitagawa, T., Kawaguchi, T., Hasumi, K., and Noda, S.T. (2004). Putative Gene Loci Associated With Carcinogenesis And Metastasis Of Endocervical Adenocarcinomas Of Uterus Determined By Conventional And Array-Based CGH. *American Journal of Obstetrics and Gynecology* **191**(4): 1173-1182. DOI: 10.1016/j.ajog.2004.04.015.

Ho, T., Zhou, N., Huang, J., Koirala, P., Xu, M., Fung, R., Wu, F., and Mo, Y. (2015). Targeting Non-Coding RNAs With The CRISPR/Cas9 System In Human Cell Lines. *Nucleic Acids Research* **43**(3): e17-e17. DOI: 10.1093/nar/gku1198.

Hockemeyer, D., Wang, H., Kiani, S., Lai, C.S., Gao, Q., Cassady, J.P., Cost, G.J., Zhang, L., Santiago, Y., Miller, J.C., Zeitler, B., Cherone, J.M., Meng, X., Hinkley, S.J., Rebar, E.J., Gregory, P.D., Urnov, F.D., and Jaenisch, R. (2011). Genetic Engineering Of Human Pluripotent Cells Using TALE Nucleases. *Nature Biotechnology* **29**(8): 731-734. DOI: 10.1038/nbt.1927.

Hou, Z., Zhang, Y., Propson, N.E., Howden, S.E., Chu, L., Sontheimer, E.J., and Thomson, J.A. (2013). Efficient Genome Engineering In Human Pluripotent Stem Cells Using Cas9 From Neisseria meningitidis. *Proceedings of the National Academy of Sciences* **110**(39): 15644. DOI: 10.1073/pnas.1313587110.

Hsu, P.D., Lander, E.S., and Zhang, F. (2014). Development And Applications Of CRISPR-Cas9 For Genome Engineering. *Cell* **157**(6): 1262-1278. DOI: 10.1016/j.cell.2014.05.010.

Hsu, P.D., Scott, D.A., Weinstein, J.A., Ran, F.A., Konermann, S., Agarwala, V., Li, Y., Fine, E.J., Wu, X., Shalem, O., Cradick, T.J., Marraffini, L.A., Bao, G., and Zhang, F. (2013a). DNA Targeting Specificity Of RNA-Guided Cas9 Nucleases. *Nature Biotechnology* **31**(9): 827-832. DOI: 10.1038/nbt.2647.

Hsu, P.D., Scott, D.A., Weinstein, J.A., Ran, F.A., Konermann, S., Agarwala, V., Li, Y., Fine, E.J., Wu, X., Shalem, O., Cradick, T.J., Marraffini, L.A., Bao, G., and Zhang, F. (2013b). DNA Targeting Specificity Of RNA-Guided Cas9 Nucleases. *Nature Biotechnology* **31**(9): 827-832. DOI: 10.1038/nbt.2647.

Hu, J., Wang, Y., Zhang, Y., Yu, Y.F., Chen, H., Liu, K., Yao, M., Wang, K., Gu, W.G., and Shou, T. (2019). Comprehensive Genomic Profiling Of Small Cell Lung Cancer In Chinese Patients And The Implications For Therapeutic Potential. *Cancer Medicine* **8**(9): 4338-4347. DOI: 10.1002/cam4.2199.

Hu, Y., Ru, N., Xiao, H., Chaturbedi, A., Hoa, N.T., Tian, X., Zhang, H., Ke, C., Yan, F., Nelson, J., Li, Z., Gramer, R., Yu, L., Siegel, E., Zhang, X., Jia, Z., Jadus, M.R., Limoli, C.L., Linskey, M.E., Xing, J., and Zhou, Y. (2013). Tumor-Specific Chromosome Mis-Segregation Controls Cancer Plasticity by Maintaining Tumor Heterogeneity. *PloS one* **8**(11): e80898. DOI: 10.1371/journal.pone.0080898.

Hu, Z., Zhu, D., Wang, W., Li, W., Jia, W., Zeng, X., Ding, W., Yu, L., Wang, X., Wang, L., Shen, H., Zhang, C., Liu, H., Liu, X., Zhao, Y., Fang, X., Li, S., Chen, W., Tang, T., Fu, A., Wang, Z., Chen, G., Gao, Q., Li, S., Xi, L., Wang, C., Liao, S., Ma, X., Wu, P., Li, K., Wang, S., Zhou, J., Wang, J., Xu, X., Wang, H., and Ma, D. (2015). Genome-Wide Profiling Of HPV Integration In Cervical Cancer Identifies Clustered Genomic Hot Spots And A Potential Microhomology-Mediated Integration Mechanism. *Nature genetics* **47**(2): 158-163. DOI: 10.1038/ng.3178.

Hwang, J., and Kim, Y.K. (2013). When A Ribosome Encounters A Premature Termination Codon. *BMB Rep* **46**(1): 9-16. DOI: 10.5483/bmbrep.2013.46.1.002.

Ishii, H., Kim, D.H., Fujita, T., Endo, Y., Saeki, S., and Yamamoto, T.T. (1998). cDNA Cloning Of A New Low-Density Lipoprotein Receptor-Related Protein And Mapping Of Its Gene (LRP3) To Chromosome Bands 19q12-q13. 2. *Genomics* **51**(1): 132-135. DOI: 10.1006/geno.1998.5339.

Ishino, Y., Shinagawa, H., Makino, K., Amemura, M., and Nakata, A. (1987). Nucleotide Sequence Of The iap Gene, Responsible For Alkaline Phosphatase Isozyme Conversion In Escherichia coli, And Identification Of The Gene Product. *Journal of Bacteriology* **169**(12): 5429-5433. DOI: 10.1128/jb.169.12.5429-5433.1987.

Jackson, S.P. (2002). Sensing And Repairing DNA Double-Strand Breaks. *Carcinogenesis* **23**(5): 687-696. DOI: 10.1093/carcin/23.5.687.

Jacob, A.G., and Smith, C.W.J. (2017). Intron Retention As A Component Of Regulated Gene Expression Programs. *Hum Genet* **136**(9): 1043-1057. DOI: 10.1007/s00439-017-1791-x.

Jacobsen, L., Madsen, P., Moestrup, S.K., Lund, A.H., Tommerup, N., Nykjaer, A., Sottrup-Jensen, L., Gliemann, J., and Petersen, C.M. (1996). Molecular Characterization Of A Novel Human Hybrid-Type Receptor That Binds The Alpha2-Macroglobulin Receptor-Associated Protein. *Journal of Biological Chemistry* **271**(49): 31379-31383. DOI: 10.1074/jbc.271.49.31379.

Jansen, R., Embden, J.D., Gaastra, W., and Schouls, L.M. (2002). Identification Of Genes That Are Associated With DNA Repeats In Prokaryotes. *Molecular microbiology* **43**(6): 1565-1575. DOI: 10.1046/j.1365-2958.2002.02839.x.

Jeon, H., Meng, W., Takagi, J., Eck, M.J., Springer, T.A., and Blacklow, S.C. (2001). Implications For Familial Hypercholesterolemia From The Structure Of The LDL Receptor YWTD-EGF Domain Pair. *Nature Structural Biology* **8**(6): 499-504. DOI: 10.1038/88556.

Jiang, Y.H., Zhu, C.Y., He, D., Gao, Q.L., Tian, X., Ma, X., Wu, J., Das, B.C., Severinov, K., Hitzeroth, II, Debata, P.R., Liu, R., Zou, L., Shi, L., Xu, H., Wang, K.X., Bao, Y.X., Ka-Kit, L.R., You, Z.S., Cui, Z.F., and Hu, Z. (2019). Cytological Immunostaining Of HMGA2, LRP1B, And TP63 As Potential Biomarkers For Triaging Human Papillomavirus-Positive Women. *Translational Oncology* **12**(7): 959-967. DOI: 10.1016/j.tranon.2019.04.012.

Jinek, M., Chylinski, K., Fonfara, I., Hauer, M., Doudna, J.A., and Charpentier, E. (2012). A Programmable Dual-RNA-Guided DNA Endonuclease In Adaptive Bacterial Immunity. *Science* **337**(6096): 816-821. DOI: 10.1126/science.1225829.

Kadota, M., Yang, H.H., Gomez, B., Sato, M., Clifford, R.J., Meerzaman, D., Dunn, B.K., Wakefield, L.M., and Lee, M.P. (2010). Delineating Genetic Alterations For Tumor Progression In The MCF10A Series Of Breast Cancer Cell Lines. *PloS one* **5**(2). DOI: 10.1371/journal.pone.0009201.

Karlsson, J., Mengelbier, L.H., Elfving, P., and Nord, D.G. (2011). High-Resolution Genomic Profiling Of An Adult Wilms' Tumor: Evidence For A Pathogenesis Distinct From Corresponding Pediatric Tumors. *Virchows Archiv* **459**(5): 547-553. DOI: 10.1007/s00428-011-1148-0.

Kawarabayasi, Y., Hino, Y., Horikawa, H., Yamazaki, S., Haikawa, Y., Jin-no, K., Takahashi, M., Sekine, M., Baba, S., Ankai, A., Kosugi, H., Hosoyama, A., Fukui, S., Nagai, Y., Nishijima, K., Nakazawa, H., Takamiya, M., Masuda, S., Funahashi, T., Tanaka, T., Kudoh, Y., Yamazaki, J., Kushida, N., Oguchi, A., Aoki, K., Kubota, K., Nakamura, Y., Nomura, N., Sako, Y., and Kikuchi, H. (1999).

Complete Genome Sequence Of An Aerobic Hyper-Thermophilic Crenarchaeon, Aeropyrum pernix K1. *DNA Research* **6**(2): 83-101. DOI: 10.1093/dnares/6.2.83.

Kawarabayasi, Y., Sawada, M., Horikawa, H., Haikawa, Y., Hino, Y., Yamamoto, S., Sekine, M., Baba, S., Kosugi, H., Hosoyama, A., Nagai, Y., Sakai, M., Ogura, K., Otsuka, R., Nakazawa, H., Takamiya, M., Ohfuku, Y., Funahashi, T., Tanaka, T., Kudoh, Y., Yamazaki, J., Kushida, N., Oguchi, A., Aoki, K., and Kikuchi, H. (1998). Complete Sequence And Gene Organization Of The Genome Of A Hyper-Thermophilic Archaebacterium, Pyrococcus horikoshii OT3. *DNA Research* **5**(2): 55-76. DOI: 10.1093/dnares/5.2.55.

Kim, D.H., Iijima, H., Goto, K., Sakai, J., Ishii, H., Kim, H.J., Suzuki, H., Kondo, H., Saeki, S., and Yamamoto, T. (1996). Human Apolipoprotein E Receptor 2: A Novel Lipoprotein Receptor Of The Low Density Lipoprotein Receptor Family Predominantly Expressed In Brain. *Journal of Biological Chemistry* **271**(14): 8373-8380. DOI: 10.1074/jbc.271.14.8373.

Kim, D.H., Inagaki, Y., Suzuki, T., Ioka, R.X., Yoshioka, S.Z., Magoori, K., Kang, M.J., Cho, Y., Nakano, A.Z., Liu, Q., Fujino, T., Suzuki, H., Sasano, H., and Yamamoto, T.T. (1998). A New Low Density Lipoprotein Receptor Related Protein, LRP5, Is Expressed In Hepatocytes And Adrenal Cortex, And Recognizes Apolipoprotein E. *Journal of Biochemistry* **124**(6): 1072-1076. DOI: 10.1093/oxfordjournals.jbchem.a022223.

Knisely, J.M., Li, Y., Grifflith, J.M., Geuze, H.J., Schwartz, A.L., and Bu, G.J. (2007). Slow Endocytosis Of The LDL Receptor-Related Protein 1B: Implications For A Novel Cytoplasmic Tail Conformation. *Experimental cell research* **313**(15): 3298-3307. DOI: 10.1016/j.yexcr.2007.05.026.

Kohno, T., Otsuka, A., Girard, L., Sato, M., Iwakawa, R., Ogiwara, H., Sanchez-Cespedes, M., Minna, J.D., and Yokota, J. (2010). A Catalog of Genes Homozygously Deleted in Human Lung Cancer and the Candidacy of PTPRD as a Tumor Suppressor Gene. *Genes Chromosomes & Cancer* **49**(4): 342-352. DOI: 10.1002/gcc.20746.

Konukiewitz, B., Jesinghaus, M., Steiger, K., Schlitter, A.M., Kasajima, A., Sipos, B., Zamboni, G., Welchert, W., Pfarr, N., and Kloppel, G. (2018). Pancreatic Neuroendocrine Carcinomas Reveal A Closer Relationship To Ductal Adenocarcinomas Than To Neuroendocrine Tumors G3. *Human Pathology* **77**: 70-79. DOI: 10.1016/j.humpath.2018.03.018.

Koonin, E.V., and Makarova, K.S. (2019). Origins And Evolution Of CRISPR-Cas Systems. *Philosophical Transactions of the Royal Society of London* **374**(1772): 20180087. DOI: 10.1098/rstb.2018.0087.

Koonin, E.V., Makarova, K.S., and Zhang, F. (2017). Diversity, Classification And Evolution Of CRISPR-Cas Systems. *Current opinion in microbiology* **37**: 67-78. DOI: 10.1016/j.mib.2017.05.008.

Kozak, M. (1989). The Scanning Model For Translation: An Update. *Journal of Cell Biology* **108**(2): 229-241. DOI: 10.1083/jcb.108.2.229.

Kühnle, N., Dederer, V., and Lemberg, M. (2019). Intramembrane Proteolysis At A Glance: From Signalling To Protein Degradation. *Journal of cell science* **132**: jcs217745. DOI: 10.1242/jcs.217745.

Lal, M., and Caplan, M. (2011). Regulated Intramembrane Proteolysis: Signaling Pathways And Biological Functions. *Physiology (Bethesda)* **26**(1): 34-44. DOI: 10.1152/physiol.00028.2010.

Lan, S.W., Li, H., Liu, Y., Ma, L.X., Liu, X.H., Liu, Y., Yan, S., and Cheng, Y. (2019). Somatic Mutation Of LRP1B Is Associated With Tumor Mutational Burden In Patients With Lung Cancer. *Lung Cancer* **132**: 154-156. DOI: 10.1016/j.lungcan.2019.04.025.

Langbein, S., Szakacs, O., Wilhelm, M., Sukosd, F., Weber, S., Jauch, A., Beltran, A.L., Alken, P., Kalble, T., and Kovacs, G. (2002). Alteration Of The LRP1B Gene Region Is Associated With High Grade Of Urothelial Cancer. *Laboratory Investigation* **82**(5): 639-643. DOI: 10.1038/labinvest.3780458.

Law, M.E., Templeton, K.L., Kitange, G., Smith, J., Misra, A., Feuerstein, B.G., and Jenkins, R.B. (2005). Molecular Cytogenetic Analysis Of Chromosomes 1 And 19 In Glioma Cell Lines. *Cancer Genetics and Cytogenetics* **160**(1): 1-14. DOI: 10.1016/j.cancergencyto.2004.11.012.

Lee, S., Lee, J., Sim, S.H., Lee, Y., Moon, K.C., Lee, C., Park, W.Y., Kim, N.K., Lee, S.H., and Lee, H. (2017). Comprehensive Somatic Genome Alterations Of Urachal Carcinoma. *Journal of Medical Genetics* **54**(8): 572-578. DOI: 10.1136/jmedgenet-2016-104390.

Lemos, B.R., Kaplan, A.C., Bae, J.E., Ferrazzoli, A.E., Kuo, J., Anand, R.P., Waterman, D.P., and Haber, J.E. (2018). CRISPR/Cas9 Cleavages In Budding Yeast Reveal Templated Insertions And Strand-Specific Insertion/Deletion Profiles. *Proceedings of the National Academy of Sciences* **115**(9): E2040-e2047. DOI: 10.1073/pnas.1716855115.

Leung, E.Y., Askarian-Amiri, M.E., Singleton, D.C., Ferraro-Peyret, C., Joseph, W.R., Finlay, G.J., Brooms, R.J., Kakadia, P.M., Bohlander, S.K., Marshall, E., and Baguley, B.C. (2018). Derivation Of Breast Cancer Cell Lines Under Physiological (5%) Oxygen Concentrations. *Frontiers in Oncology* **8**. DOI: 10.3389/fonc.2018.00425.

Li, B.J., Liu, C.X., Cheng, G.X., Peng, M.L., Qin, X.S., Liu, Y., Li, Y.Z., and Qin, D.C. (2019). LRP1B Polymorphisms Are Associated with Multiple Myeloma Risk in a Chinese Han Population. *Journal of Cancer* **10**(3): 577-582. DOI: 10.7150/jca.28905.

Li, Y., Marzolo, M.P., van Kerkhof, P., Strous, G.J., and Bu, G. (2000). The YXXL Motif, But Not The Two NPXY Motifs, Serves As The Dominant Endocytosis Signal For Low Density Lipoprotein Receptor-Related Protein. *Journal of Biological Chemistry* **275**(22): 17187-17194. DOI: 10.1074/jbc.M000490200.

Li, Y., Rivera, C.M., Ishii, H., Jin, F., Selvaraj, S., Lee, A.Y., Dixon, J.R., and Ren, B. (2014). CRISPR Reveals A Distal Super-Enhancer Required For Sox2 Expression In Mouse Embryonic Stem Cells. *PloS one* **9**(12): e114485. DOI: 10.1371/journal.pone.0114485.

Li, Y.H., Knisely, J.M., Lu, W.Y., McCormick, L.M., Wang, J.Y., Henkin, J., Schwartz, A.L., and Bu, G.J. (2002). Low Density Lipoprotein (LDL) Receptor-Related Protein 1B Impairs Urokinase Receptor Regeneration On The Cell Surface And Inhibits Cell Migration. *Journal of Biological Chemistry* **277**(44): 42366-42371. DOI: 10.1074/jbc.M207705200.

Li, Y.H., Lu, W.Y., and Bu, G.J. (2005). Striking Differences Of LDL Receptor-Related Protein 1B Expression In Mouse And Human. *Biochemical and Biophysical Research Communications* **333**(3): 868-873. DOI: 10.1016/j.bbrc.2005.05.170.

Lieber, M.R. (2010). The Mechanism Of Double-Strand DNA Break Repair By The Nonhomologous DNA End-Joining Pathway. *Annual review of biochemistry* **79**: 181-211. DOI: 10.1146/annurev.biochem.052308.093131.

Liu, C.X., Li, Y., Obermoeller-McCormick, L.M., Schwartz, A.L., and Bu, G. (2001). The Putative Tumor Suppressor LRP1B, A Novel Member Of The Low Density Lipoprotein (LDL) Receptor Family, Exhibits Both Overlapping And Distinct Properties With The LDL Receptor-Related Protein. *Journal of Biological Chemistry* **276**(31): 28889-28896. DOI: 10.1074/jbc.M102727200.

Liu, C.X., Musco, S., Lisitsina, N.M., Forgacs, E., Minna, J.D., and Lisitsyn, N.A. (2000a). LRP-DIT, A Putative Endocytic Receptor Gene, Is Frequently Inactivated In Non-Small Cell Lung Cancer Cell Lines. *Cancer research* **60**(7): 1961-1967.

Liu, C.X., Musco, S., Lisitsina, N.M., Yaklichkin, S.Y., and Lisitsyn, N.A. (2000b). Genomic Organization Of A New Candidate Tumor Suppressor Gene, LRP1B. *Genomics* **69**(2): 271-274. DOI: 10.1006/geno.2000.6331.

Liu, C.X., Ranganathan, S., Robinson, S., and Strickland, D.K. (2007). Gamma-Secretase-Mediated Release Of The Low Density Lipoprotein Receptor-Related Protein 1B Intracellular Domain Suppresses Anchorage-Independent Growth Of

Neuroglioma Cells. *Journal of Biological Chemistry* **282**(10): 7504-7511. DOI: 10.1074/jbc.M608088200.

Liu, H., and Wong, L. (2003). Data Mining Tools For Biological Sequences. *Journal of Bioinformatics and Computational Biology* **01**(01): 139-167. DOI: 10.1142/S0219720003000216.

Liu, L., Ren, M.Y., Han, S.Y., Sun, L., and Zhu, L. (2018). Expression Level And Clinical Significance Of Low-Density Lipoprotein Receptor-Related Protein 1B Gene In Cervical Squamous Cell Carcinoma. *International Journal of Clinical and Experimental Pathology* **11**(3): 1701-1706.

Lu, Y.J., Wu, C.S., Li, H.P., Liu, H.P., Lu, C.Y., Leu, Y.W., Wang, C.S., Chen, L.C., Lin, K.H., and Chang, Y.S. (2010). Aberrant Methylation Impairs Low Density Lipoprotein Receptor-Related Protein 1B Tumor Suppressor Function In Gastric Cancer. *Genes Chromosomes & Cancer* **49**(5): 412-424. DOI: 10.1002/gcc.20752.

Makarova, K.S., Aravind, L., Grishin, N.V., Rogozin, I.B., and Koonin, E.V. (2002). A DNA Repair System Specific For Thermophilic Archaea and Bacteria Predicted By Genomic Context Analysis. *Nucleic Acids Research* **30**(2): 482-496. DOI: 10.1093/nar/30.2.482.

Makarova, K.S., Grishin, N.V., Shabalina, S.A., Wolf, Y.I., and Koonin, E.V. (2006). A Putative RNA-Interference-Based Immune System In Prokaryotes: Computational Analysis Of The Predicted Enzymatic Machinery, Functional Analogies With Eukaryotic RNAi, And Hypothetical Mechanisms Of Action. *Biology direct* **1**: 7. DOI: 10.1186/1745-6150-1-7.

Makarova, K.S., Wolf, Y.I., Iranzo, J., Shmakov, S.A., Alkhnbashi, O.S., Brouns, S.J.J., Charpentier, E., Cheng, D., Haft, D.H., Horvath, P., Moineau, S., Mojica, F.J.M., Scott, D., Shah, S.A., Siksnys, V., Terns, M.P., Venclovas, Č., White, M.F., Yakunin, A.F., Yan, W., Zhang, F., Garrett, R.A., Backofen, R., van der Oost, J., Barrangou, R., and Koonin, E.V. (2020). Evolutionary Classification Of CRISPR–Cas Systems: A Burst Of Class 2 And Derived Variants. *Nature Reviews Microbiology* **18**(2): 67-83. DOI: 10.1038/s41579-019-0299-x.

Mali, P., Yang, L., Esvelt, K.M., Aach, J., Guell, M., DiCarlo, J.E., Norville, J.E., and Church, G.M. (2013). RNA-Guided Human Genome Engineering Via Cas9. *Science* **339**(6121): 823-826. DOI: 10.1126/science.1232033.

Marino, M., Rabacchi, C., Simone, M.L., Medici, V., Cortesi, L., and Calandra, S. (2009). A Novel Deletion Of BRCA1 Gene That Eliminates The ATG Initiation Codon Without Affecting The Promoter Region. *Clinica Chimica Acta* **403**(1): 249-253. DOI: 10.1016/j.cca.2009.02.020.

Marraffini, L.A. (2015). CRISPR-Cas Immunity In Prokaryotes. *Nature* **526**(7571): 55-61. DOI: 10.1038/nature15386.

Marraffini, L.A., and Sontheimer, E.J. (2008). CRISPR Interference Limits Horizontal Gene Transfer In Staphylococci By Targeting DNA. *Science* **322**(5909): 1843-1845. DOI: 10.1126/science.1165771.

Marschang, P., Brich, J., Weeber, E.J., Sweatt, J.D., Shelton, J.M., Richardson, J.A., Hammer, R.E., and Herz, J. (2004). Normal Development And Fertility Of Knockout Mice Lacking The Tumor Suppressor Gene LRP1B Suggest Functional Compensation By LRP1. *Molecular and Cellular Biology* **24**(9): 3782-3793. DOI: 10.1128/mcb.24.9.3782-3793.2004.

Maru, Y., Tanaka, N., Ohira, M., Itami, M., Hippo, Y., and Nagase, H. (2017). Identification Of Novel Mutations In Japanese Ovarian Clear Cell Carcinoma Patients Using Optimized Targeted NGS For Clinical Diagnosis. *Gynecol Oncol* **144**(2): 377-383. DOI: 10.1016/j.ygyno.2016.11.045.

Marzec, M., Eletto, D., and Argon, Y. (2012). GRP94: An HSP90-Like Protein Specialized For Protein Folding And Quality Control In The Endoplasmic Reticulum. *Biochimica et Biophysica Acta - Molecular Cell Research* **1823**(3): 774-787. DOI: 10.1016/j.bbamcr.2011.10.013.

Marzolo, M.P., and Bu, G.J. (2009). Lipoprotein Receptors And Cholesterol In App Trafficking And Proteolytic Processing, Implications For Alzheimer's Disease. *Seminars in cell & developmental biology* **20**(2): 191-200. DOI: 10.1016/j.semcdb.2008.10.005.

Masepohl, B., Görlitz, K., and Böhme, H. (1996). Long Tandemly Repeated Repetitive (LTRR) Sequences In The Filamentous Cyanobacterium Anabaena sp. PCC 7120. *Biochimica et biophysica acta* **1307**(1): 26-30. DOI: 10.1016/0167-4781(96)00040-1.

Matukumalli, S.R., Tangirala, R., and Rao, C.M. (2017). Clusterin: Full-Length Protein And One Of Its Chains Show Opposing Effects On Cellular Lipid Accumulation. *Sci Rep-Uk* **7**(1): 41235. DOI: 10.1038/srep41235.

May, P., Bock, H.H., and Herz, J. (2003). Integration Of Endocytosis And Signal Transduction By Lipoprotein Receptors. *Science Signaling* **2003**(176): Pe12. DOI: 10.1126/stke.2003.176.pe12.

May, P., Woldt, E., Matz, R.L., and Boucher, P. (2007). The LDL Receptor-Related Protein (LRP) Family: An Old Family Of Proteins With New Physiological Functions. *Annals of medicine* **39**(3): 219-228. DOI: 10.1080/07853890701214881.

McCarthy, A.J., Coleman-Vaughan, C., and McCarthy, J.V. (2017). Regulated Intramembrane Proteolysis: Emergent Role In Cell Signalling Pathways. *Biochemical Society Transactions* **45**(6): 1185-1202. DOI: 10.1042/bst20170002.

Miller, J.C., Holmes, M.C., Wang, J., Guschin, D.Y., Lee, Y., Rupniewski, I., Beausejour, C.M., Waite, A.J., Wang, N.S., Kim, K.A., Gregory, P.D., Pabo, C.O., and Rebar, E.J. (2007). An Improved Zinc-Finger Nuclease Architecture For Highly Specific Genome Editing. *Nature Biotechnology* **25**(7): 778-785. DOI: 10.1038/nbt1319.

Mojica, F.J., Díez-Villaseñor, C., García-Martínez, J., and Soria, E. (2005). Intervening Sequences Of Regularly Spaced Prokaryotic Repeats Derive From Foreign Genetic Elements. *Journal of Molecular Evolution* **60**(2): 174-182. DOI: 10.1007/s00239-004-0046-3.

Mojica, F.J., Díez-Villaseñor, C., Soria, E., and Juez, G. (2000). Biological Significance Of A Family Of Regularly Spaced Repeats In The Genomes Of Archaea, Bacteria And Mitochondria. *Molecular microbiology* **36**(1): 244-246. DOI: 10.1046/j.1365-2958.2000.01838.x.

Mojica, F.J., Ferrer, C., Juez, G., and Rodríguez-Valera, F. (1995). Long Stretches Of Short Tandem Repeats Are Present In The Largest Replicons Of The Archaea Haloferax Mediterranei And Haloferax Volcanii And Could Be Involved In Replicon Partitioning. *Molecular microbiology* **17**(1): 85-93. DOI: 10.1111/j.1365-2958.1995.mmi_17010085.x.

Mojica, F.J., Juez, G., and Rodríguez-Valera, F. (1993). Transcription At Different Salinities Of Haloferax mediterranei Sequences Adjacent To Partially Modified PstI Sites. *Molecular microbiology* **9**(3): 613-621. DOI: 10.1111/j.1365-2958.1993.tb01721.x.

Morwald, S., Yamazaki, H., Bujo, H., Kusunoki, J., Kanaki, T., Seimiya, K., Morisaki, N., Nimpf, J., Schneider, W.J., and Saito, Y. (1997). A Novel Mosaic Protein Containing LDL Receptor Elements Is Highly Conserved In Humans And Chickens. *Arteriosclerosis, Thrombosis, and Vascular Biology* **17**(5): 996-1002. DOI: 10.1161/01.atv.17.5.996.

Mosesson, M.W. (2005). Fibrinogen And Fibrin Structure And Functions. *Journal of Thrombosis and Haemostasis* **3**(8): 1894-1904. DOI: 10.1111/j.1538-7836.2005.01365.x.

Nakagawa, T., Pimkhaokham, A., Suzuki, E., Omura, K., Inazawa, J., and Imoto, I. (2006). Genetic Or Epigenetic Silencing Of Low Density Lipoprotein Receptor-Related Protein 1B Expression In Oral Squamous Cell Carcinoma. *Cancer Science* **97**(10): 1070-1074. DOI: 10.1111/j.1349-7006.2006.00283.x.

Nakata, A., Amemura, M., and Makino, K. (1989). Unusual Nucleotide Arrangement With Repeated Sequences In The Escherichia coli K-12 Chromosome. *Journal of Bacteriology* **171**(6): 3553-3556. DOI: 10.1128/jb.171.6.3553-3556.1989.

Nakayama, M., Nakajima, D., Nagase, T., Nomura, N., Seki, N., and Ohara, O. (1998). Identification Of High-Molecular-Weight Proteins With Multiple EGF-Like Motifs By Motif-Trap Screening. *Genomics* **51**(1): 27-34. DOI: 10.1006/geno.1998.5341.

NCBI Genome Page Decoration. Human Chromosome 2 Idiogram (Human Genome Assembly GRCh38.p12; Resolution 850 bphs). Retrieved from https://www.ncbi.nlm.nih.gov/genome/tools/gdp (accessed on March 2020).

Nelson, K.E., Clayton, R.A., Gill, S.R., Gwinn, M.L., Dodson, R.J., Haft, D.H., Hickey, E.K., Peterson, J.D., Nelson, W.C., Ketchum, K.A., McDonald, L., Utterback, T.R., Malek, J.A., Linher, K.D., Garrett, M.M., Stewart, A.M., Cotton, M.D., Pratt, M.S., Phillips, C.A., Richardson, D., Heidelberg, J., Sutton, G.G., Fleischmann, R.D., Eisen, J.A., White, O., Salzberg, S.L., Smith, H.O., Venter, J.C., and Fraser, C.M. (1999). Evidence For Lateral Gene Transfer Between Archaea And Bacteria From Genome Sequence Of Thermotoga maritima. *Nature* **399**(6734): 323-329. DOI: 10.1038/20601.

Ni, S.B., Hu, J.R., Duan, Y.S., Shi, S.L., Li, R., Wu, H.J., Qu, Y.P., and Li, Y. (2013). Down Expression Of LRP1B Promotes Cell Migration Via RhoA/Cdc42 Pathway And Actin Cytoskeleton Remodeling In Renal Cell Cancer. *Cancer Science* **104**(7): 817-825. DOI: 10.1111/cas.12157.

Nikolaev, S.I., Rimoldi, D., Iseli, C., Valsesia, A., Robyr, D., Gehrig, C., Harshman, K., Guipponi, M., Bukach, O., Zoete, V., Michielin, O., Muehlethaler, K., Speiser, D., Beckmann, J.S., Xenarios, I., Halazonetis, T.D., Jongeneel, C.V., Stevenson, B.J., and Antonarakis, S.E. (2011). Exome Sequencing Identifies Recurrent Somatic MAP2K1 and MAP2K2 Mutations In Melanoma. *Nature genetics* **44**(2): 133-139. DOI: 10.1038/ng.1026.

Nishimasu, H., and Nureki, O. (2017). Structures And Mechanisms Of CRISPR RNA-Guided Effector Nucleases. *Current Opinion in Structural Biology* **43**: 68-78. DOI: 10.1016/j.sbi.2016.11.013.

Novak, S., Hiesberger, T., Schneider, W.J., and Nimpf, J. (1996). A New Low Density Lipoprotein Receptor Homologue With 8 Ligand Binding Repeats In Brain Of Chicken And Mouse. *Journal of Biological Chemistry* **271**(20): 11732-11736. DOI: 10.1074/jbc.271.20.11732.

Nykjaer, A., Conese, M., Christensen, E.I., Olson, D., Cremona, O., Gliemann, J., and Blasi, F. (1997). Recycling Of The Urokinase Receptor Upon Internalization Of

The uPA:Serpin Complexes. *The EMBO journal* **16**(10): 2610-2620. DOI: 10.1093/emboj/16.10.2610.

Nykjaer, A., Petersen, C.M., Møller, B., Jensen, P.H., Moestrup, S.K., Holtet, T.L., Etzerodt, M., Thøgersen, H.C., Munch, M., Andreasen, P.A., and et al. (1992). Purified Alpha 2-Macroglobulin Receptor/LDL Receptor-Related Protein Binds Urokinase/Plasminogen Activator Inhibitor Type-1 Complex. Evidence That The Alpha 2-Macroglobulin Receptor Mediates Cellular Degradation Of Urokinase Receptor-Bound Complexes. *Journal of Biological Chemistry* **267**(21): 14543-14546.

O'Leary, N.A., Wright, M.W., Brister, J.R., Ciufo, S., Haddad, D., McVeigh, R., Rajput, B., Robbertse, B., Smith-White, B., Ako-Adjei, D., Astashyn, A., Badretdin, A., Bao, Y., Blinkova, O., Brover, V., Chetvernin, V., Choi, J., Cox, E., Ermolaeva, O., Farrell, C.M., Goldfarb, T., Gupta, T., Haft, D., Hatcher, E., Hlavina, W., Joardar, V.S., Kodali, V.K., Li, W., Maglott, D., Masterson, P., McGarvey, K.M., Murphy, M.R., O'Neill, K., Pujar, S., Rangwala, S.H., Rausch, D., Riddick, L.D., Schoch, C., Shkeda, A., Storz, S.S., Sun, H., Thibaud-Nissen, F., Tolstoy, I., Tully, R.E., Vatsan, A.R., Wallin, C., Webb, D., Wu, W., Landrum, M.J., Kimchi, A., Tatusova, T., DiCuccio, M., Kitts, P., Murphy, T.D., and Pruitt, K.D. (2016). Reference Sequence (RefSeq) Database At NCBI: Current Status, Taxonomic Expansion, And Functional Annotation. *Nucleic Acids Research* **44**(D1): D733-745. DOI: 10.1093/nar/gkv1189.

Palmieri, D., Scarpa, M., Tessari, A., Uka, R., Amari, F., Lee, C., Richmond, T., Foray, C., Sheetz, T., Braddom, A., Burd, C.E., Parvin, J.D., Ludwig, T., Croce, C.M., and Coppola, V. (2016). Ran Binding Protein 9 (RanBP9) Is A Novel Mediator Of Cellular DNA Damage Response In Lung Cancer Cells. *Oncotarget* **7**(14): 18371-18383. DOI: 10.18632/oncotarget.7813.

Parsons, M.T., Whiley, P.J., Beesley, J., Drost, M., de Wind, N., Thompson, B.A., Marquart, L., Hopper, J.L., Jenkins, M.A., Australasian Colorectal Cancer Family, R., Brown, M.A., Tucker, K., Warwick, L., Buchanan, D.D., and Spurdle, A.B. (2015). Consequences Of Germline Variation Disrupting The Constitutional Translational Initiation Codon Start Sites Of MLH1 and BRCA2: Use Of Potential Alternative Start Sites And Implications For Predicting Variant Pathogenicity. *Mol Carcinog* **54**(7): 513-522. DOI: 10.1002/mc.22116.

Pastrana, D.V., Hanson, A.J., Knisely, J., Bu, G.J., and Fitzgerald, D.J. (2005). LRP1B Functions As A Receptor For Pseudomonas Exotoxin. *Biochimica et Biophysica Acta - Molecular Basis of Disease* **1741**(3): 234-239. DOI: 10.1016/j.bbadis.2005.06.007.

Pedersen, A.G., and Nielsen, H. (1997). Neural Network Prediction Of Translation Initiation Sites In Eukaryotes: Perspectives For EST And Genome Analysis. *Proceedings of the International Conference on Intelligent Systems for Molecular Biology* **5**: 226-233.

Pineau, P., Marchio, A., Nagamori, S., Seki, S., Tiollais, P., and Dejean, A. (2003). Homozygous Deletion Scanning In Hepatobiliary Tumor Cell Lines Reveals Alternative Pathways For Liver Carcinogenesis. *Hepatology (Baltimore, Md.)* **37**(4): 852-861. DOI: 10.1053/jhep.2003.50138.

Plagens, A., Richter, H., Charpentier, E., and Randau, L. (2015). DNA And RNA Interference Mechanisms By CRISPR-Cas Surveillance Complexes. *FEMS Microbiology Reviews* **39**(3): 442-463. DOI: 10.1093/femsre/fuv019.

Poon, I.K., Patel, K.K., Davis, D.S., Parish, C.R., and Hulett, M.D. (2011). Histidine-Rich Glycoprotein: The Swiss Army Knife Of Mammalian Plasma. *Blood* **117**(7): 2093-2101. DOI: 10.1182/blood-2010-09-303842.

Popp, M.W., and Maquat, L.E. (2016). Leveraging Rules Of Nonsense-Mediated mRNA Decay For Genome Engineering And Personalized Medicine. *Cell* **165**(6): 1319-1322. DOI: 10.1016/j.cell.2016.05.053.

Porteus, M.H., and Baltimore, D. (2003). Chimeric Nucleases Stimulate Gene Targeting In Human Cells. *Science* **300**(5620): 763. DOI: 10.1126/science.1078395.

Pourcel, C., Salvignol, G., and Vergnaud, G. (2005). CRISPR Elements In Yersinia pestis Acquire New Repeats By Preferential Uptake Of Bacteriophage DNA, And Provide Additional Tools For Evolutionary Studies. *Microbiology (Reading)* **151**(Pt 3): 653-663. DOI: 10.1099/mic.0.27437-0.

Prazeres, H., Torres, J., Rodrigues, F., Pinto, M., Pastoriza, M.C., Gomes, D., Cameselle-Teijeiro, J., Vidal, A., Martins, T.C., Sobrinho-Simoes, M., and Soares, P. (2011). Chromosomal, Epigenetic And MicroRNA-Mediated Inactivation Of LRP1B, A Modulator Of The Extracellular Environment Of Thyroid Cancer Cells. *Oncogene* **36**(1): 146. DOI: 10.1038/onc.2016.143.

Qing, J., Wei, D., Maher, V.M., and McCormick, J.J. (1999). Cloning And Characterization Of A Novel Gene Encoding A Putative Transmembrane Protein With Altered Expression In Some Human Transformed And Tumor-Derived Cell Lines. *Oncogene* **18**(2): 335-342. DOI: 10.1038/sj.onc.1202290.

Rahmatpanah, F.B., Carstens, S., Guo, J., Sjahputera, O., Taylor, K.H., Duff, D., Shi, H., Davis, J.W., Hooshmand, S.I., Chitma-Matsiga, R., and Caldwell, C.W. (2006). Differential DNA Methylation Patterns Of Small B-Cell Lymphoma Subclasses With Different Clinical Behavior. *Leukemia* **20**(10): 1855-1862. DOI: 10.1038/sj.leu.2404345.

Ran, F.A., Cong, L., Yan, W.X., Scott, D.A., Gootenberg, J.S., Kriz, A.J., Zetsche, B., Shalem, O., Wu, X., Makarova, K.S., Koonin, E.V., Sharp, P.A., and Zhang, F. (2015). In Vivo Genome Editing Using Staphylococcus aureus Cas9. *Nature* **520**(7546): 186-191. DOI: 10.1038/nature14299.

Ran, F.A., Hsu, P.D., Wright, J., Agarwala, V., Scott, D.A., and Zhang, F. (2013). Genome Engineering Using The CRISPR-Cas9 System. *Nature protocols* **8**(11): 2281-2308. DOI: 10.1038/nprot.2013.143.

Ranganathan, S., Liu, C.X., Migliorini, M.M., Von Arnim, C.A., Peltan, I.D., Mikhailenko, I., Hyman, B.T., and Strickland, D.K. (2004). Serine And Threonine Phosphorylation Of The Low Density Lipoprotein Receptor-Related Protein By Protein Kinase Calpha Regulates Endocytosis And Association With Adaptor Molecules. *Journal of Biological Chemistry* **279**(39): 40536-40544. DOI: 10.1074/jbc.M407592200.

Reid, Y., Storts, D., Riss, T., and Minor, L., (2013) Authentication of Human Cell Lines by STR DNA Profiling Analysis. In: Assay Guidance Manual S. Markossian, G.S. Sittampalam, A. Grossman, K. Brimacombe, M. Arkin, D. Auld, C.P. Austin, J. Baell, J.M.M. Caaveiro, T.D.Y. Chung, N.P. Coussens, J.L. Dahlin, V. Devanaryan, T.L. Foley, M. Glicksman, M.D. Hall, J.V. Haas, S.R.J. Hoare, J. Inglese, P.W. Iversen, S.D. Kahl, S.C. Kales, S. Kirshner, M. Lal-Nag, Z. Li, J. McGee, O. McManus, T. Riss, P. Saradjian, O.J. Trask, J.R. Weidner, M.J. Wildey, M. Xia & X. Xu (eds). Bethesda (MD): Eli Lilly & Company and the National Center for Advancing Translational Sciences, pp.

Roversi, G., Pfundt, R., Moroni, R.F., Magnani, I., van Reijmersdal, S., Pollo, B., Straatman, H., Larizza, L., and Schoenmakers, E.F.P.M. (2005). Identification Of Novel Genomic Markers Related To Progression To Glioblastoma Through Genomic Profiling Of 25 Primary Glioma Cell Lines. *Oncogene* **25**(10): 1571-1583. DOI: 10.1038/sj.onc.1209177.

Saito, A., Pietromonaco, S., Loo, A.K., and Farquhar, M.G. (1994). Complete Cloning And Sequencing Of Rat gp330/"megalin," A Distinctive Member Of The Low Density Lipoprotein Receptor Gene Family. *Proceedings of the National Academy of Sciences* **91**(21): 9725-9729. DOI: 10.1073/pnas.91.21.9725.

Santiago, Y., Chan, E., Liu, P., Orlando, S., Zhang, L., Urnov, F.D., Holmes, M.C., Guschin, D., Waite, A., Miller, J.C., Rebar, E.J., Gregory, P.D., Klug, A., and Collingwood, T.N. (2008). Targeted Gene Knockout In Mammalian Cells By Using Engineered Zinc-Finger Nucleases. *Proceedings of the National Academy of Sciences* **105**(15): 5809. DOI: 10.1073/pnas.0800940105.

Sapranauskas, R., Gasiunas, G., Fremaux, C., Barrangou, R., Horvath, P., and Siksnys, V. (2011). The Streptococcus thermophilus CRISPR/Cas System Provides Immunity In Escherichia coli. *Nucleic Acids Research* **39**(21): 9275-9282. DOI: 10.1093/nar/gkr606.

Scheiman, J., Tseng, J.C., Zheng, Y., and Meruelo, D. (2010). Multiple Functions Of The 37/67-kd Laminin Receptor Make It A Suitable Target For Novel Cancer Gene Therapy. *Molecular Therapy* **18**(1): 63-74. DOI: 10.1038/mt.2009.199.

Schneider, V.A., Graves-Lindsay, T., Howe, K., Bouk, N., Chen, H.C., Kitts, P.A., Murphy, T.D., Pruitt, K.D., Thibaud-Nissen, F., Albracht, D., Fulton, R.S., Kremitzki, M., Magrini, V., Markovic, C., McGrath, S., Steinberg, K.M., Auger, K., Chow, W., Collins, J., Harden, G., Hubbard, T., Pelan, S., Simpson, J.T., Threadgold, G., Torrance, J., Wood, J.M., Clarke, L., Koren, S., Boitano, M., Peluso, P., Li, H., Chin, C.S., Phillippy, A.M., Durbin, R., Wilson, R.K., Flicek, P., Eichler, E.E., and Church, D.M. (2017). Evaluation Of GRCh38 And De Novo Haploid Genome Assemblies Demonstrates The Enduring Quality Of The Reference Assembly. *Genome research* **27**(5): 849-864. DOI: 10.1101/gr.213611.116.

Schneider, W., J., (2016) Lipoprotein Receptors. In: *Biochemistry Of Lipids, Lipoproteins And Membranes.* N.D. Ridgway & R.S. McLeod (eds). Boston: Elsevier, pp. 489-518.

Schneider, W.J., and Nimpf, J. (2003). LDL Receptor Relatives At The Crossroad Of Endocytosis And Signaling. *Cellular and Molecular Life Sciences* **60**(5): 892-903. DOI: 10.1007/s00018-003-2183-Z.

Schroeder, H.W., and Cavacini, L. (2010). Structure And Function Of Immunoglobulins. *J Allergy Clin Immunol* **125**(2 Suppl 2): S41-S52. DOI: 10.1016/j.jaci.2009.09.046.

Schvartz, I., Seger, D., and Shaltiel, S. (1999). Vitronectin. *International Journal of Biochemistry & Cell Biology* **31**(5): 539-544. DOI: 10.1016/s1357-2725(99)00005-9.

Sensen, C.W., Charlebois, R.L., Chow, C., Clausen, I.G., Curtis, B., Doolittle, W.F., Duguet, M., Erauso, G., Gaasterland, T., Garrett, R.A., Gordon, P., de Jong, I.H., Jeffries, A.C., Kozera, C., Medina, N., De Moors, A., van der Oost, J., Phan, H., Ragan, M.A., Schenk, M.E., She, Q., Singh, R.K., and Tolstrup, N. (1998). Completing The Sequence Of The Sulfolobus solfataricus P2 Genome. *Extremophiles* **2**(3): 305-312. DOI: 10.1007/s007920050073.

She, Q., Phan, H., Garrett, R.A., Albers, S., Stedman, K.M., and Zillig, W. (1998). Genetic Profile Of pNOB8 From Sulfolobus: The First Conjugative Plasmid From An Archaeon. *Extremophiles* **2**(4): 417-425. DOI: 10.1007/s007920050087.

Shiroshima, T., Oka, C., and Kawaichi, M. (2009). Identification Of LRP1B-Interacting Proteins And Inhibition Of Protein Kinase C Alpha-Phosphorylation Of LRP1B By Association With PICK1. *FEBS Letters* **583**(1): 43-48. DOI: 10.1016/j.febslet.2008.11.045.

Shmakov, S., Smargon, A., Scott, D., Cox, D., Pyzocha, N., Yan, W., Abudayyeh, O.O., Gootenberg, J.S., Makarova, K.S., Wolf, Y.I., Severinov, K., Zhang, F., and Koonin, E.V. (2017). Diversity And Evolution Of Class 2 CRISPR–Cas Systems. *Nature Reviews Microbiology* **15**(3): 169-182. DOI: 10.1038/nrmicro.2016.184.

Smith, D.R., Doucette-Stamm, L.A., Deloughery, C., Lee, H., Dubois, J., Aldredge, T., Bashirzadeh, R., Blakely, D., Cook, R., Gilbert, K., Harrison, D., Hoang, L., Keagle, P., Lumm, W., Pothier, B., Qiu, D., Spadafora, R., Vicaire, R., Wang, Y., Wierzbowski, J., Gibson, R., Jiwani, N., Caruso, A., Bush, D., Reeve, J.N., and et al. (1997). Complete Genome Sequence Of Methanobacterium thermoautotrophicum DeltaH: Functional Analysis And Comparative Genomics. *Journal of Bacteriology* **179**(22): 7135-7155. DOI: 10.1128/jb.179.22.7135-7155.1997.

Solimene, A.C.C., Carneiro, C.R.W., Melati, I., and Lopes, J. (2001). Functional Differences Between Two Morphologically Distinct Cell Subpopulations Within A Human Colorectal Carcinoma Cell Line. *Brazilian Journal of Medical and Biological Research* **34**: 653-661. DOI: 10.1590/S0100-879X2001000500014.

Sonoda, I., Imoto, I., Inoue, J., Shibata, T., Shimada, Y., Chin, K., Imamura, M., Amagasa, T., Gray, J.W., Hirohashi, S., and Inazawa, J. (2004). Frequent Silencing Of Low Density Lipoprotein Receptor-Related Protein 1B (LRP1B) Expression By Genetic And Epigenetic Mechanisms In Esophageal Squamous Cell Carcinoma. *Cancer research* **64**(11): 3741-3747. DOI: 10.1158/0008-5472.Can-04-0172.

Sorek, R., Lawrence, C.M., and Wiedenheft, B. (2013). CRISPR-Mediated Adaptive Immune Systems In Bacteria And Archaea. *Annual review of biochemistry* **82**: 237-266. DOI: 10.1146/annurev-biochem-072911-172315.

Spiegel, A., Bachmann, M., Jiménez, G.J., and Sarov, M. (2019). CRISPR/Cas9-Based Knockout Pipeline For Reverse Genetics In Mammalian Cell Culture. *Methods* **164-165**: 49-58. DOI: 10.1016/j.ymeth.2019.04.016.

Springer, T.A. (1998). An Extracellular Beta-Propeller Module Predicted In Lipoprotein And Scavenger Receptors, Tyrosine Kinases, Epidermal Growth Factor

Precursor, And Extracellular Matrix Components. *Journal of molecular biology* **283**(4): 837-862. DOI: 10.1006/jmbi.1998.2115.

Sternberg, S.H., Richter, H., Charpentier, E., and Qimron, U. (2016). Adaptation In CRISPR-Cas Systems. *Molecular cell* **61**(6): 797-808. DOI: 10.1016/j.molcel.2016.01.030.

Strickland, D.K., Gonias, S.L., and Argraves, W.S. (2002). Diverse Roles For The LDL Receptor Family. *Trends in Endocrinology & Metabolism* **13**(2): 66-74. DOI: 10.1016/s1043-2760(01)00526-4.

Südhof, T.C., Goldstein, J.L., Brown, M.S., and Russell, D.W. (1985). The LDL Receptor Gene: A Mosaic Of Exons Shared With Different Proteins. *Science* **228**(4701): 815-822. DOI: 10.1126/science.2988123.

Sugiyama, T., Kumagai, H., Morikawa, Y., Wada, Y., Sugiyama, A., Yasuda, K., Yokoi, N., Tamura, S., Kojima, T., Nosaka, T., Senba, E., Kimura, S., Kadowaki, T., Kodama, T., and Kitamura, T. (2000). A Novel Low-Density Lipoprotein Receptor-Related Protein Mediating Cellular Uptake Of Apolipoprotein E-Enriched Beta-VLDL In Vitro. *Biochemistry* **39**(51): 15817-15825. DOI: 10.1021/bi001583s.

Tabouret, E., Labussiere, M., Alentorn, A., Schmitt, Y., Marie, Y., and Sanson, M. (2015). LRP1B Deletion Is Associated With Poor Outcome For Glioblastoma Patients. *Journal of the Neurological Sciences* **358**(1-2): 440-443. DOI: 10.1016/j.jns.2015.09.345.

Taheri-Ghahfarokhi, A., Taylor, B.J.M., Nitsch, R., Lundin, A., Cavallo, A., Madeyski-Bengtson, K., Karlsson, F., Clausen, M., Hicks, R., Mayr, L.M., Bohlooly-Y, M., and Maresca, M. (2018). Decoding Non-Random Mutational Signatures At Cas9 Targeted Sites. *Nucleic Acids Research* **46**(16): 8417-8434. DOI: 10.1093/nar/gky653.

Takahashi, S., Kawarabayasi, Y., Nakai, T., Sakai, J., and Yamamoto, T. (1992). Rabbit Very Low Density Lipoprotein Receptor: A Low Density Lipoprotein Receptor-Like Protein With Distinct Ligand Specificity. *Proceedings of the National Academy of Sciences* **89**(19): 9252-9256. DOI: 10.1073/pnas.89.19.9252.

Tanaga, K., Bujo, H., Zhu, Y.J., Kanaki, T., Hirayama, S., Takahashi, K., Inoue, M., Mikami, K., Schneider, W.J., and Saito, Y. (2004). LRP1B Attenuates The Migration Of Smooth Muscle Cells By Reducing Membrane Localization Of Urokinase And PDGF Receptors. *Arteriosclerosis Thrombosis and Vascular Biology* **24**(8): 1422-1428. DOI: 10.1161/01.Atv.0000133607.80554.09.

Tang, T.H., Bachellerie, J.P., Rozhdestvensky, T., Bortolin, M.L., Huber, H., Drungowski, M., Elge, T., Brosius, J., and Hüttenhofer, A. (2002). Identification Of 86 Candidates For Small Non-Messenger RNAs From The Archaeon

Archaeoglobus fulgidus. *Proceedings of the National Academy of Sciences* **99**(11): 7536-7541. DOI: 10.1073/pnas.112047299.

Taylor, K.H., Kramer, R.S., Davis, J.W., Guo, J., Duff, D.J., Xu, D., Caldwell, C.W., and Shi, H. (2007a). Ultradeep Bisulfite Sequencing Analysis Of DNA Methylation Patterns In Multiple Gene Promoters By 454 Sequencing. *Cancer research* **67**(18): 8511-8518. DOI: 10.1158/0008-5472.Can-07-1016.

Taylor, K.H., Pena-Hernandez, K.E., Davis, J.W., Arthur, G.L., Duff, D.J., Shi, H.D., Rahmatpanah, F.B., Sjahputera, O., and Caldwell, C.W. (2007b). Large-Scale CpG Methylation Analysis Identifies Novel Candidate Genes And Reveals Methylation Hotspots In Acute Lymphoblastic Leukemia. *Cancer research* **67**(6): 2617-2625. DOI: 10.1158/0008-5472.Can-06-3993.

Terashima, A., Pelkey, K.A., Rah, J., Suh, Y.H., Roche, K.W., Collingridge, G.L., McBain, C.J., and Isaac, J.T.R. (2008). An Essential Role For PICK1 In NMDA Receptor-Dependent Bidirectional Synaptic Plasticity. *Neuron* **57**(6): 872-882. DOI: 10.1016/j.neuron.2008.01.028.

The Human Protein Atlas. Low density lipoprotein receptor related protein 1B (LRP1B). Retrieved from https://www.proteinatlas.org/ENSG00000168702-LRP1B (accessed on September 2019).

Tidball, A.M., (2019) Disease in a Dish: Cellular Models to Understand Human Conditions. In: *Cellular and Animal Models in Human Genomics Research.* K. Walz & J.I. Young (eds). Academic Press, pp. 19-47.

Treuren, T.V., and Vishwanatha, J.K. (2018). CRISPR Deletion Of MIEN1 in Breast Cancer Cells. *PloS one* **13**(10): e0204976-e0204976. DOI: 10.1371/journal.pone.0204976.

Tucker, M.D., Zhu, J.S., Marin, D., Gupta, R.T., Gupta, S., Berry, W.R., Ramalingam, S., Zhang, T., Harrison, M., Wu, Y., Healy, P., Lisi, S., George, D.J., and Armstrong, A.J. (2019). Pembrolizumab In Men With Heavily Treated Metastatic Castrate-Resistant Prostate Cancer. *Cancer Medicine* **8**(10): 4644-4655. DOI: 10.1002/cam4.2375.

Uhlén, M., Fagerberg, L., Hallström, B.M., Lindskog, C., Oksvold, P., Mardinoglu, A., Sivertsson, Å., Kampf, C., Sjöstedt, E., Asplund, A., Olsson, I., Edlund, K., Lundberg, E., Navani, S., Szigyarto, C.A., Odeberg, J., Djureinovic, D., Takanen, J.O., Hober, S., Alm, T., Edqvist, P.H., Berling, H., Tegel, H., Mulder, J., Rockberg, J., Nilsson, P., Schwenk, J.M., Hamsten, M., von Feilitzen, K., Forsberg, M., Persson, L., Johansson, F., Zwahlen, M., von Heijne, G., Nielsen, J., and Pontén, F. (2015). Tissue-Based Map Of The Human Proteome. *Science* **347**(6220): 1260419. DOI: 10.1126/science.1260419.

Uhlen, M., Zhang, C., Lee, S., Sjöstedt, E., Fagerberg, L., Bidkhori, G., Benfeitas, R., Arif, M., Liu, Z., Edfors, F., Sanli, K., von Feilitzen, K., Oksvold, P., Lundberg, E., Hober, S., Nilsson, P., Mattsson, J., Schwenk, J.M., Brunnström, H., Glimelius, B., Sjöblom, T., Edqvist, P., Djureinovic, D., Micke, P., Lindskog, C., Mardinoglu, A., and Ponten, F. (2017). A Pathology Atlas Of The Human Cancer Transcriptome. *Science* **357**(6352): eaan2507. DOI: 10.1126/science.aan2507.

Valente, V., Teixeira, S.A., Neder, L., Okamoto, O.K., Oba-Shinjo, S.M., Marie, S.K.N., Scrideli, C.A., Paçó-Larson, M.L., and Carlotti, C.G. (2009). Selection Of Suitable Housekeeping Genes For Expression Analysis In Glioblastoma Using Quantitative RT-PCR. *BMC Mol Biol* **10**: 17-17. DOI: 10.1186/1471-2199-10-17.

van der Oost, J., Westra, E.R., Jackson, R.N., and Wiedenheft, B. (2014). Unravelling The Structural And Mechanistic Basis Of CRISPR–Cas Systems. *Nature Reviews Microbiology* **12**(7): 479-492. DOI: 10.1038/nrmicro3279.

Volk, L., Kim, C., Takamiya, K., Yu, Y., and Huganir, R. (2010). Developmental Regulation Of Protein Interacting With C Kinase 1 (PICK1) Function In Hippocampal Synaptic Plasticity And Learning. *Proceedings of the National Academy of Sciences* **107**: 21784-21789. DOI: 10.1073/pnas.1016103107.

Wang, L.R., Yan, K., Zhou, J.M., Zhang, N., Wang, M., Song, J., Zhao, J., Zhang, Y.Z., Cai, S.L., Zhao, Y.M., and Wang, L. (2019). Relationship Of Liver Cancer With LRP1B Or TP53 Mutation And Tumor Mutation Burden And Survival. *Journal of Clinical Oncology* **37**(15). DOI: 10.1200/JCO.2019.37.15_suppl.1573.

Wang, Z., Sun, P., Gao, C., Chen, J., Li, J., Chen, Z., Xu, M., Shao, J., Zhang, Y., and Xie, J. (2017). Down-Regulation Of LRP1B In Colon Cancer Promoted The Growth And Migration Of Cancer Cells. *Experimental cell research* **357**(1): 1-8. DOI: 10.1016/j.yexcr.2017.04.010.

Wangsa, D., Braun, R., Schiefer, M., Gertz, E.M., Bronder, D., Quintanilla, I., Padilla-Nash, H.M., Torres, I., Hunn, C., Warner, L., Buishand, F.O., Hu, Y., Hirsch, D., Gaiser, T., Camps, J., Schwartz, R., Schäffer, A.A., Heselmeyer-Haddad, K., and Ried, T. (2018). The Evolution Of Single Cell-Derived Colorectal Cancer Cell Lines Is Dominated By The Continued Selection Of Tumor-Specific Genomic Imbalances, Despite Random Chromosomal Instability. *Carcinogenesis* **39**(8): 993-1005. DOI: 10.1093/carcin/bgy068.

Willnow, T.E., Christ, A., and Hammes, A. (2012). Endocytic Receptor-Mediated Control Of Morphogen Signaling. *Development (Cambridge, England)* **139**(23): 4311-4319. DOI: 10.1242/dev.084467.

Willnow, T.E., Hammes, A., and Eaton, S. (2007). Lipoproteins And Their Receptors In Embryonic Development: More Than Cholesterol Clearance. *Development (Cambridge, England)* **134**(18): 3239-3249. DOI: 10.1242/dev.004408.

Willnow, T.E., Nykjaer, A., and Herz, J. (1999). Lipoprotein Receptors: New Roles For Ancient Proteins. *Nature cell biology* **1**(6): E157-162. DOI: 10.1038/14109.

Wolff, R.K., Hoffman, M.D., Wolff, E.C., Herrick, J.S., Sakoda, L.C., Samowitz, W.S., and Slattery, M.L. (2018). Mutation Analysis Of Adenomas And Carcinomas Of The Colon: Early And Late Drivers. *Genes Chromosomes & Cancer* **57**(7): 366-376. DOI: 10.1002/gcc.22539.

Wood, A.J., Lo, T.W., Zeitler, B., Pickle, C.S., Ralston, E.J., Lee, A.H., Amora, R., Miller, J.C., Leung, E., Meng, X., Zhang, L., Rebar, E.J., Gregory, P.D., Urnov, F.D., and Meyer, B.J. (2011). Targeted Genome Editing Across Species Using ZFNs And TALENs. *Science* **333**(6040): 307. DOI: 10.1126/science.1207773.

Wu, P., Gilkes, D.M., Phillip, J.M., Narkar, A., Cheng, T.W., Marchand, J., Lee, M., Li, R., and Wirtz, D. (2020). Single-Cell Morphology Encodes Metastatic Potential. *Science Advances* **6**(4): eaaw6938. DOI: 10.1126/sciadv.aaw6938.

Xiao, D.K., Li, F.Q., Pan, H., Liang, H., Wu, K., and He, J.X. (2017). Integrative Analysis Of Genomic Sequencing Data Reveals Higher Prevalence Of LRP1B Mutations In Lung Adenocarcinoma Patients With COPD. *Sci Rep-Uk* **7**. DOI: 10.1038/s41598-017-02405-9.

Xu, J., Pang, Z.P., Shin, O., and Südhof, T.C. (2009). Synaptotagmin-1 Functions As A Ca2+ Sensor For Spontaneous Release. *Nature Neuroscience* **12**(6): 759-766. DOI: 10.1038/nn.2320.

Yamamoto, T., Davis, C.G., Brown, M.S., Schneider, W.J., Casey, M.L., Goldstein, J.L., and Russell, D.W. (1984). The Human LDL Receptor: A Cysteine-Rich Protein With Multiple Alu Sequences In Its mRNA. *Cell* **39**(1): 27-38. DOI: 10.1016/0092-8674(84)90188-0.

Yamazaki, H., Bujo, H., Kusunoki, J., Seimiya, K., Kanaki, T., Morisaki, N., Schneider, W.J., and Saito, Y. (1996). Elements Of Neural Adhesion Molecules And A Yeast Vacuolar Protein Sorting Receptor Are Present In A Novel Mammalian Low Density Lipoprotein Receptor Family Member. *Journal of Biological Chemistry* **271**(40): 24761-24768. DOI: 10.1074/jbc.271.40.24761.

Yasuda, J., Whitmarsh, A.J., Cavanagh, J., Sharma, M., and Davis, R.J. (1999). The JIP Group Of Mitogen-Activated Protein Kinase Scaffold Proteins. *Molecular and Cellular Biology* **19**(10): 7245. DOI: 10.1128/MCB.19.10.7245.

Yates, A.D., Achuthan, P., Akanni, W., Allen, J., Allen, J., Alvarez-Jarreta, J., Amode, M.R., Armean, I.M., Azov, A.G., Bennett, R., Bhai, J., Billis, K., Boddu, S.,

Marugán, J.C., Cummins, C., Davidson, C., Dodiya, K., Fatima, R., Gall, A., Giron, C.G., Gil, L., Grego, T., Haggerty, L., Haskell, E., Hourlier, T., Izuogu, O.G., Janacek, S.H., Juettemann, T., Kay, M., Lavidas, I., Le, T., Lemos, D., Martinez, J.G., Maurel, T., McDowall, M., McMahon, A., Mohanan, S., Moore, B., Nuhn, M., Oheh, D.N., Parker, A., Parton, A., Patricio, M., Sakthivel, M.P., Abdul Salam, A.I., Schmitt, B.M., Schuilenburg, H., Sheppard, D., Sycheva, M., Szuba, M., Taylor, K., Thormann, A., Threadgold, G., Vullo, A., Walts, B., Winterbottom, A., Zadissa, A., Chakiachvili, M., Flint, B., Frankish, A., Hunt, S.E., Iisley, G., Kostadima, M., Langridge, N., Loveland, J.E., Martin, F.J., Morales, J., Mudge, J.M., Muffato, M., Perry, E., Ruffier, M., Trevanion, S.J., Cunningham, F., Howe, K.L., Zerbino, D.R., and Flicek, P. (2019). Ensembl 2020. *Nucleic Acids Research* **48**(D1): D682-D688. DOI: 10.1093/nar/gkz966.

Ye, J., Coulouris, G., Zaretskaya, I., Cutcutache, I., Rozen, S., and Madden, T.L. (2012). Primer-BLAST: A Tool To Design Target-Specific Primers For Polymerase Chain Reaction. *BMC bioinformatics* **13**: 134-134. DOI: 10.1186/1471-2105-13-134.

Yin, D., Ogawa, S., Kawamata, N., Tunici, P., Finocchiaro, G., Eoli, M., Ruckert, C., Huynh, T., Liu, G.T., Kato, M., Sanada, M., Jauch, A., Dugas, M., Black, K.L., and Koeffler, H.P. (2009). High-Resolution Genomic Copy Number Profiling of Glioblastoma Multiforme by Single Nucleotide Polymorphism DNA Microarray. *Molecular Cancer Research* **7**(5): 665-677. DOI: 10.1158/1541-7786.Mcr-08-0270.

Zare, K., Shademan, M., Ghahramani Seno, M.M., and Dehghani, H. (2018). CRISPR/Cas9 Knockout Strategies to Ablate CCAT1 lncRNA Gene in Cancer Cells. *Biological Procedures Online* **20**(1): 21. DOI: 10.1186/s12575-018-0086-5.

Zhang, Z.L., Cui, R., Li, H., and Li, J.L. (2019). miR-500 Promotes Cell Proliferation By Directly Targetting LRP1B In Prostate Cancer. *Bioscience Reports* **39**. DOI: 10.1042/bsr20181854.

Zhao, X., Lei, Y., Li, G., Cheng, Y., Yang, H., Xie, L., Long, H., and Jiang, R. (2019). Integrative Analysis Of Cancer Driver Genes In Prostate Adenocarcinoma. *Mol Med Rep* **19**(4): 2707-2715. DOI: 10.3892/mmr.2019.9902.

Zheng, H., and Koo, E.H. (2011). Biology And Pathophysiology Of The Amyloid Precursor Protein. *Molecular Neurodegeneration* **6**(1): 27. DOI: 10.1186/1750-1326-6-27.

Zheng, H.Y., and Bai, L.G. (2019). Hypoxia Induced microRNA-301b-3p Overexpression Promotes Proliferation, Migration And Invasion Of Prostate Cancer Cells By

Targeting LRP1B. *Experimental and Molecular Pathology* **111**. DOI: 10.1016/j.yexmp.2019.104301.

Zheng, Q., Cai, X., Tan, M.H., Schaffert, S., Arnold, C.P., Gong, X., Chen, C.Z., and Huang, S. (2014). Precise Gene Deletion And Replacement Using The CRISPR/Cas9 System In Human Cells. *BioTechniques* **57**(3): 115-124. DOI: 10.2144/000114196.

Zhu, H., Yang, B., Liu, J., Wu, W., and Ling, Y. (2020). Case Report Of Acute Myeloid Leukemia With "WT1, ATRX, CEBPA, CSMD1, IKZF1, And LRP1B Mutation And Translocation Between Chromosome 1 And 19" Developing From Philadelphia-Negative Chronic Myeloid Leukemia After TKI Therapy. *Medicine* **99**(3): e18888. DOI: 10.1097/md.0000000000018888.

Zuo, Z., and Liu, J. (2016). Cas9-Catalyzed DNA Cleavage Generates Staggered Ends: Evidence From Molecular Dynamics Simulations. *Sci Rep-Uk* **6**(1): 37584. DOI: 10.1038/srep37584.

7 Appendix

Generation of an *LRP1B*-Knockout Glioblastoma Cell Line Model via CRISPR/Cas9

Catarina Príncipe [1, 2, 3]; Ana Pestana [1, 2, 4]; Paula Soares[1, 2, 4]; Raquel T. Lima[1, 2, 4]

[1] i3S - Institute for Research and Innovation in Health, University of Porto, 4200-135 Porto, Portugal; [2] IPATIMUP- Institute of Molecular Pathology and Immunology of the University of Porto, 4200-135 Porto, Portugal; [3] Faculty of Sciences of the University of Porto, 4150-179 Porto, Portugal; [4] Faculty of Medicine of the University of Porto, 4200-319 Porto, Portugal

Introduction

The low-density lipoprotein (LDL) receptor-related protein 1B (LRP1B) is a member of the LDL Receptor (LDLR) protein family which includes several structurally related cell-surface receptors with highly diverse biological functions, ranging from cargo transport to cellular signaling[1,2]. *LRP1B* inactivation by either chromosomal, epigenetic or microRNA-mediated mechanisms has been reported in multiple cancer types; being proposed as a tumor suppressor gene[3]. LRP1B binds to a myriad of ligands, activating extracellular proteolytic cascades and modulating ligand internalization and trafficking[4–6]. Therefore, LRP1B can influence several cellular functions such as growth, migration, and invasion[7–9]. Furthermore, LRP1B endocytic activity may contribute to resistance to liposomal therapies and have clinical impact[10,11]. Nevertheless, its role in cancer remains elusive. The accumulated knowledge on LRP1B has largely arisen from studies based on the expression of LRP1B minireceptors (comprising only part of the protein), or LRP1B known soluble ectodomains. Additionally, LRP1B downregulation using RNA interference-based strategies has also been used to validate specific results[3–10]. Regardless of being extremely useful, these approaches may underestimate the full potential of LRP1B.

CRISPR/Cas9 system has become an unprecedented powerful genome-editing tool[12]. The current system relies on programmable short single guide RNAs (sgRNAs) that drive DNA targeting and cleavage by Cas9 to introduce, delete or replace a genomic region of interest[13,14].

Aim

The aim of the ongoing project is to establish and characterize CRISPR/Cas9-induced LRP1B-knockout glioblastoma cell line model.

Acknowledgements

This work was financed by FEEI (Fundos Europeus Estruturais e de Investimento) and FEDER (Fundo Europeu de Desenvolvimento Regional) funds through the COMPETE 2020 - Operacional Programme for Competitiveness and Internationalisation (POCI); project NORTE-01-0145-FEDER-000029 - Advancing Cancer Research: from Basic Knowledge to Application, supported by Norte Portugal Regional Operational Programme (NORTE 2020), under the PORTUGAL 2020 Partnership Agreement; and by Portuguese funds through FCT - Fundação para a Ciência e a Tecnologia / Ministério da Ciência, Tecnologia e Ensino Superior in the framework of the project - Predicting Patients' Response to Liposomal Anticancer Drugs: Focusing on LRP1B Endocytic Activity (PTDC/MEC-ONC/31520/2017).

CRISPR/Cas9 Knockout Strategy

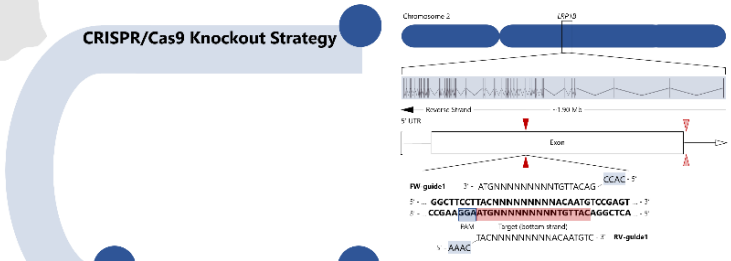

Vector Construction

Transfection and Antibiotic Selection

- Human Glioblastoma Cell Line: U87

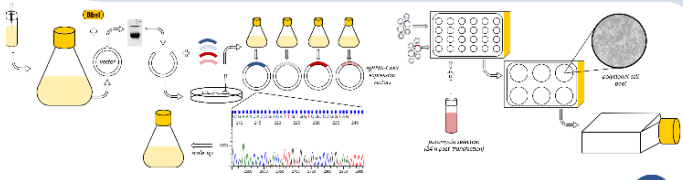

Single-Cell Isolation and Clonal Expansion

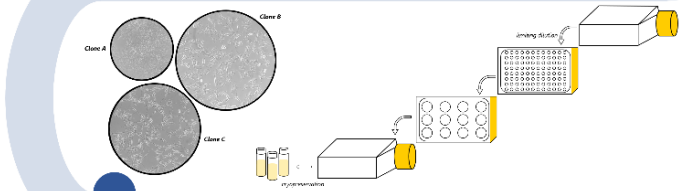

CRISPR/Cas9 Genome-Edited Clones Screening

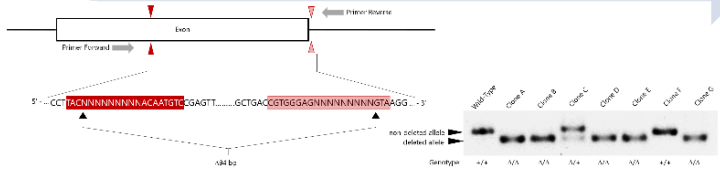

What's Next?

- Characterization of CRISPR/Cas9-induced mutations by Sanger sequencing.
- Validation of biallelic knockout clones at mRNA and protein level.
- Characterization of LRP1B-knockout clones in terms of cell viability, proliferation, motility and invasion.

This project will allow the development of an LRP1B-knockout model of upmost importance for the study of the LRP1B role in cancer.

References

1. Gent, J. and I. Braakman. (2004). Cellular and Molecular Life Sciences. 61(19): p. 2461-2470.
2. May, P., et al. (2007). Annals of Medicine.39(3): p. 219-28.
3. Prazeres, H., et al. (2011). Oncogene. 36(1): p. 146.
4. Cam, J.A., et al. (2004). Journal of Biological Chemistry. 279(28): p. 29639-29646.
5. Haas, J., et al. (2011). Atherosclerosis. 216(2): p. 342-347.
6. Marschang, P., et al. (2004). Molecular and Cellular Biology. 24(9): p. 3782-3793.
7. Beer, A.G., et al. (2016). Oncotarget. 7(42): p.68721-68733.
8. Liu, C.X., et al. (2007). Journal of Biological Chemistry. 282(10): p. 7504-7511.
9. Ni, S.B., et al. (2013). Cancer Science. 104(7): p. 817-825.
10. Cowin, P.A., et al. (2012). Cancer Research. 72(16): p. 4060-73.
11. Sousa I. *et al.* (2018). Cancer Chemotherapy and Pharmacology. 82(5):741-5512.
12. Martínez-Lage, M., et al. Biomedicines, 2018. 6(4): p. 105.
13. Adli, M. Nature Communications, 2018. 9(1): p. 1911.
14. Chakrabarti, A.M., et al. Molecular Cell, 2019. 73(4): p. 699-713.